
Electronic Thesis and Dissertation Repository

10-18-2019 2:00 PM

Bioremediation of Refinery Desalter Effluent using *Debaryomyces hansenii* and *Parachlorella kessleri*

Leila Azimian, *The University of Western Ontario*

Supervisor: Amarjeet Bassi, *University of Western University*

A thesis submitted in partial fulfillment of the requirements for the Doctor of Philosophy degree in Chemical and Biochemical Engineering

© Leila Azimian 2019

Follow this and additional works at: <https://ir.lib.uwo.ca/etd>

 Part of the [Apiculture Commons](#), [Biochemical and Biomolecular Engineering Commons](#), [Biology Commons](#), [Biotechnology Commons](#), [Environmental Engineering Commons](#), and the [Petroleum Engineering Commons](#)

Recommended Citation

Azimian, Leila, "Bioremediation of Refinery Desalter Effluent using *Debaryomyces hansenii* and *Parachlorella kessleri*" (2019). *Electronic Thesis and Dissertation Repository*. 6592.
<https://ir.lib.uwo.ca/etd/6592>

This Dissertation/Thesis is brought to you for free and open access by Scholarship@Western. It has been accepted for inclusion in Electronic Thesis and Dissertation Repository by an authorized administrator of Scholarship@Western. For more information, please contact wlsadmin@uwo.ca.

Abstract

Crude oil desalting operations produce an effluent stream which is challenging to treat due to its salt, heavy metal and hydrocarbon content. Consequently, desalter effluent (DE) is usually diluted into other effluent streams and sent to conventional wastewater treatment plants which may lead to upsets the plant operation.

In this study, a novel microbial approach was applied which investigated DE treatment using halotolerant yeast *Debaryomyces hansenii* (LAF-3 10 U) or the environmentally robust microalgae *Parachlorella kessleri* strain CPCC 266. The effect of these two different approaches on both synthetic and actual DE was investigated in both batch and/or continuous mode.

In the first stage, effect of phenol substrate inhibition in simulated desalter effluent (SDE) on *D.hansenii* was evaluated. The Edward inhibition model describes the yeast growth in SDE as follows: μ_{\max} 0.21 h⁻¹, K_S 633.9 mgL⁻¹ and K_I 1263.61 mg.L⁻¹. Next a response surface methodology was applied in SDE containing dodecane as a substrate under different growth conditions. A quadratic model based on central composite design was formulated and dodecane utilization by *D.hansenii* in various salt concentrations was confirmed to be efficient and rapid. A maximum chemical oxygen demand (COD) of 61.6% was obtained at a pH of 9, a dodecane concentration of 750 mgL⁻¹, and a temperature of 20°C. Using dodecane as a model substrate, the continuous cultivation of *D.hansenii* was next investigated in a continuous stirred bioreactor (CSTR) at high salt concentration and different dilution rates to determine Monod kinetic model parameters with μ_{\max} 0.085 h⁻¹, and K_S 1575.2 mgL⁻¹. COD removal of 95.7% was obtained at a dilution rate of 0.007 h⁻¹. Finally, the growth of *P. kessleri* was investigated for cultivation in batch mode for actual and SDE treatment containing benzene and phenol. These microalgae grew on both types of DE and reduced COD and benzene up to 82.9% and 51% respectively. In addition, it produced lipids with a maximum of 71.5% of dry weight.

Overall, this work demonstrated the feasibility of utilizing two different microorganisms to achieve high COD removal and biomass production on a challenging wastewater stream. The microalgae and yeast can both serve as a source of value stream for lipids for biofuel production or nutraceutical industry.

Keywords

Halotolerant Microorganism, Desalting, Microalgae. Petroleum wastewater, Benzene, Phenol, Dodecane, Ammonia, Lipid, *Debaryomyces hansenii* and *Parachlorella kessleri*

Summary for Lay Audience

Effluent from the desalination unit from petroleum refinery wastewater (desalter effluent) contains different inorganic and organic impurities, such as nitrogen, phosphorus, heavy metals, and hydrocarbon, which can significantly impact the environment if they are discharged in soil, surface water or groundwater. Current approaches utilize mixed cultures of microorganisms in conventional wastewater treatment systems. However, the presence of salt makes desalter effluent very challenging to treat in a conventional way.

In this study, an alternative approach is investigated where a single yeast which is resistant in salt or a strain of biofuel producing green microalgae is utilized for desalter effluent treatment.

The halophilic yeast has been shown to degrade hydrocarbons in saline solutions. The microalgae use light, nutrients, and CO₂ to grow, and their biomass is used for many applications, such as the production of chemicals, biodiesel, and bioenergy. These characteristics make both the yeast and the microalgae an excellent choice for investigating desalter effluent treatment. The studies were carried out in batch and continuous mode. Simulated solutions of desalter effluent were prepared using specific substrates such as phenol, Benzene, dodecane and actual samples of desalter effluent were also investigated. The results showed that both the yeast and the microalgae can be applied to effectively degrade the desalter effluent and provide biomass for further applications such as lipid production.

Co-Authorship Statement

Chapter 2 has been submitted to *Desalination journal* (Azimian and Bassi)

Chapter 3 was published in *Canadian Journal of Chemical Engineering* (L.Azimian, S. Mercer and A. Bassi)

Chapter 4 has been submitted in *Chemosphere Journal* (L.Azimian, and A. Bassi)

Chapter 5 is being prepared for submission to in *Bioresource Technology Journal* (L.Azimian, and A. Bassi)

Chapter 6 is being prepared for submission to *Biotechnology & Bioengineering Journal* (L.Azimian, and A. Bassi)

Leila Azimian carried out all experimental studies, planned all experiments and wrote all the manuscripts. Dr Amarjeet Bassi was the main supervisor who guided the research project and assisted in the editing, and the correction of the manuscripts. Dr. Sean Mercer reviewed Chapter 3.

Acknowledgments

I would like to express my sincere gratitude to my supervisor, Dr. Amarjeet Bassi, for admitting me in his research group, and for his guidance, assistance and support throughout my PhD study and research. I am indebted to his outstanding and invaluable advice. This work was supported by Imperial Oil University Research Grant (URG) to Professor Bassi.

I also wish to gracefully acknowledge Dr. Rehmann for the permission to use the instruments in his lab, and Dr. Erin Jonson, Dr. Yi-Kai (Ethan) Su, Dr. Karamanev, Dr. Rohani, Dr. Barghi, for advising, sharing their knowledge, and experience.

I owe much to my parents and my sister and brothers for their unconditional love and continued support throughout my PhD studies.

Table of Contents

Abstract.....	i
Summary for Lay Audience.....	iii
Table of Contents.....	vi
List of Tables.....	ix
List of Figures.....	xii
Chapter 1.....	1
1.1 Introduction.....	1
1.2 Objectives.....	3
1.3 Thesis organization.....	4
1.4 Novelty and Major Contributions.....	6
Chapter 2.....	9
2 A review of treatment technology for desalter effluent.....	9
2.1 Introduction.....	9
2.2 Desalting Unit Operations- Current State-of-The-Art.....	11
2.2.1 Types of desalter units.....	13
2.2.2 Neutral desalter.....	13
2.2.3 Chemical desalter.....	14
2.2.4 Electrostatic desalter.....	14
2.3 Desalter Effluent Characteristics.....	16
2.3.1 Typical desalter effluent characteristics and components.....	17
2.4 Current Technologies Of Desalter Effluent Treatment Introduction.....	19
2.4.1 Pre-treatment approaches.....	20
2.4.2 New directions in desalter effluent treatment.....	29

2.4.3	Economy and energy requirement	35
2.5	Review of microorganism for desalter effluent treatment	40
2.5.1	Biotechnology of halotolerant yeast <i>Debaryomyces hansenii</i>	41
2.5.2	Biotechnology of <i>Parachlorella kessleri</i>	42
2.6	Conclusion	44
Chapter 3	46
3	Investigation of Growth Kinetics of <i>Debaryomyces hansenii</i> (LAF-3 10 u) in Petroleum Refinery Desalter Effluent	46
3.1	Introduction.....	46
3.2	Materials and methods	48
3.2.1	Materials	48
3.2.2	Analytical methods	50
3.3	Results and discussion	51
	Growth kinetics of <i>D.hansenii</i> on simulated desalter effluent.....	51
3.3.1	Investigation of kinetic models.....	53
3.3.2	COD removal rates in simulated desalter media.....	56
3.3.3	Investigation of growth kinetics in real desalter effluent media.....	57
3.4	Conclusions.....	59
Chapter 4	61
4	Investigation of Degradation of N-Dodecane By <i>Debaryomyces Hansenii</i> In Simulated Desalter Effluent	61
4.1	Introduction.....	61
4.2	Materials and methods	63
4.2.1	Materials	63
4.2.2	Analytical methods	65
4.3	Results and Discussion	69
4.3.1	COD analysis	69

4.3.2	Kinetics of <i>D. hansenii</i> n-dodecane biodegradation in simulated desalter effluent	70
4.3.3	Optimization of n-dodecane removal and response surface model validation.....	77
4.3.4	Combined effects of pH, temperature, sodium chloride, and n-dodecane concentration on dodecane removal.....	79
4.3.5	Single factor effects on dodecane removal	82
4.3.6	Response optimization and model validation	85
4.4	Conclusion	86
Chapter 5.....		88
5	Investigation of <i>Parachlorella Kessleri</i> strain CPCC 266 on refinery desalter effluent for lipid production	88
5.1	Introduction.....	88
5.2	Materials and methods	90
5.2.1	Materials	90
5.2.2	Analytical Methods.....	95
5.3	Result and Discussion.....	100
5.3.1	Growth of <i>Parachlorella kessleri</i> in desalter effluent	100
5.3.2	Biomass production	105
5.3.3	COD removal and desalter effluent treatment quality	107
5.3.4	Investigation of ammonia removal	109
5.3.5	Total Phosphorous removal	111
5.3.6	Analysis of Phenol and Benzene removal	115
5.3.7	Lipid content	118
5.3.8	Effect of salt in Biomass and lipid production of <i>Parachlorella kessleri</i>	120
5.3.9	Possibility of Lipid production, harvesting and extraction Industrial scale	122
5.4	Conclusion	124

Chapter 6.....	127
6 Continuous cultivation of <i>Debaryomyces hansenii</i> (Laf-3 10 U) at Varying Dilution Rates on Dodecane.....	127
6.1 Introduction.....	127
6.1.1 Growth kinetic modeling in CSTR.....	128
6.2 Materials and methods	133
6.2.1 Materials	133
6.2.2 Analytical methods	136
6.3 Results and Discussion	140
6.3.1 Effect of dilution rate (DR).....	140
6.3.2 Growth kinetic modeling	144
6.3.3 Design of CSTR.....	149
6.4 Conclusions.....	151
Chapter 7.....	152
7 Conclusions and Recommendations	152
7.1 Recommendation	154
References.....	157
Appendices.....	191
Curriculum Vitae	197

List of Tables

Table 2-1: Characteristics of water discharged after the desalination-dehydration operation 18

Table 2-2: Petroleum refining effluent treatment technology performance data identified from data source meeting data quality criteria in pilot and full scale.....	26
Table 2-3: Equivalent electrical energy consumption for major desalination processes.....	36
Table 2-4: Total specific costs of the major desalination processes.....	37
Table 2-5: Comparison of water costs for conventional and transported desalination water supply options.....	38
Table 2-6: Desalination costs for different desalination processes based on capacities.....	40
Table 3-1: Best-fit biokinetic constants using non-linear regression with three different unstructured models applied to <i>Debaryomyces hansenii</i> cultivation on synthetic desalter effluent degradation compared to reported literature values.	56
Table 4-1: Synthetic desalter effluent (SDE) components without hydrocarbon.....	64
Table 4-2. Experiment dodecane concentrations.....	65
Table 4-3. COD of dodecane in synthetic desalter effluent at NaCl concentrations of zero and 5gL ⁻¹ , pH = 6.4.....	67
Table 4-4: Experimental design with four factors and three levels.....	68
Table 4-5: Chemical oxygen demand percentage (average of triplicates ± standard deviation) under conditions determined for CCD.....	78
Table 4-6: Analysis of variance of fitted model.....	80
Table 4-7: Specific growth rate of yeast <i>D. hansenii</i> in different experimental conditions of the four main factors (SD of factors ± 0.005).....	85
Table 4-8: Predicted and measured dodecane removal yields according to maximum model parameters.....	86
Table 5-1: Analyses of Desalter effluent from two sources Coker Brine (CB), AV Brine (AVB).....	92

Table 5-2: The abbreviation of different conditions in experimental protocol in Table 5-3 ..	93
Table 5-3: Experimental protocol with two sources of desalter effluent.....	93
Table 5-4: Specific growth rate and doubling time of <i>P. kessleri</i> growth under different modes as described in table 5.3.....	106
Table 5-5: ANOVA for quality parameters of wastewater treatment and lipid content of <i>P.kessleri</i> biomass in desalter effluent in different types, nutrient concentration and light .	112
Table 6-1: Phase 1 of synthetic desalter effluent components with Dodecane.....	134
Table 6-2 : Operational parameters and steady state data and COD removal in CSTR with yeast <i>D.hansenii</i>	141
Table 6-3: Summary of the kinetic parameters used in the modeling of <i>D.hansenii</i> dilution rate using Monod, Aiba, Edwards and Haldane models	148

List of Figures

Figure 1-1 Micrographs of <i>Parachlorella kessleri</i> . Scale bar = 500 nm. ²	2
Figure 1-2 : <i>Debaryomyces hansenii</i> cells with microscope (4500× magnification). ³	2
Figure 2-1: Process flow diagram of a typical crude oil refining unit ⁴⁰	12
Figure 2-2: Cross-sectional diagram of a crude oil desalter ⁴⁰	12
Figure 2-3: (a) Description of a Neutral Desalter Unit; (b) Simplified diagram of the Neutral Desalter operation ⁴¹	14
Figure 2-4: Cross section diagram of an electrostatic desalter ⁴²	15
Figure 2-5: Desalting process flow diagrams (a) one-step and (b) two-step. ⁴	16
Figure 3-1: Growth kinetics of <i>D.hansenii</i> in high-salt media in simulated desalter effluent at various COD values (120-4000 mg L ⁻¹).	53
Figure 3-2: Average specific growth rate as a function of COD for a range of COD values in simulated desalter effluent containing 1g L ⁻¹ sodium chloride solution.....	54
Figure 3-3 : Experimental and model simulations for specific growth rate of <i>D.hansenii</i> growth in 1 g L ⁻¹ salt as a function of initial COD using Andrews, Aiba and Edward models (Equations 3-1).....	55
Figure 3-4: Various Phenol COD removal by using <i>D.hansenii</i> cultivation in simulated desalter effluent in 1g L ⁻¹ NaCl.	57
Figure 3-5: Growth of <i>D.hansenii</i> in actual desalter effluent with dilution of initial COD to 300,600,900 and 1200 mgL ⁻¹	58
Figure 3-6: Desalter effluent COD removal by using <i>D.hansenii</i> at different initial CODs in actual desalter effluent media.	59
Figure 4-1. Degradation of <i>n</i> -dodecane with Tween 20 over 50 hours with control Error bars indicate standard deviations of triplicate measurements.	71

Figure 4-2: Growth of <i>D. hansenii</i> in different dodecane concentrations of 3.75, 11.25, 18.75 and 30 gL ⁻¹ in the presence of Tween 20 Error bars indicate standard deviations of triplicate measurements	72
Figure 4-3. Dodecane removal as a function of initial dodecane concentration after five days. Error bars indicate standard deviations of triplicate measurements.	74
Figure 4-4: Experimental data and Aiba model simulations for the specific growth rate of <i>D. hansenii</i> growth as a function of initial <i>n</i> -dodecane concentration of 0.3 to 30 gL ⁻¹	76
Figure 4-5: Surface plots of combined effect of process variables temperature and dodecane concentration on dodecane removal.....	81
Figure 5-1: Cultivation of <i>P.Kessleri</i> cells in AV media under different modes as described in Table 5.3	103
Figure 5-2: Cultivation of <i>P.Kessleri</i> cells in CK media under different modes as described in Table 5.3	104
Figure 5-3: Cultivation of <i>P.Kessleri</i> cells in CB+AV under different modes as described in Table 5.3	105
Figure 5-4: Mean of <i>P. kessleri</i> dry weight under different modes as described in Table 5.3	107
Figure 5-5: Percent removal of a. COD removal, b. Phosphorous removal, c. Ammonium removal in two different desalter effluents in 12 days culture.....	115
Figure 5-6: ●, Mixotrophic growth of <i>Parachlorella kessleri</i> (<i>P. kessleri</i>) in simulated desalter effluent containing Benzene	116
Figure 5-7: Lipid content biomass <i>P. kessleri</i> after 12 days growth in desalter effluent in different conditions	120
Figure 6-1: Schematic of continuous bioreactor	129
Figure 6-2: Schematic of continuous reactor for dodecane removal from SDE.....	136

Figure 6-3: A Lineweaver-Burk plot of $1/\mu$ against $1/s^{298}$	140
Figure 6-4: Steady-state values of the concentrations of dodecane (■), and CO	142
Figure 6-5: The change of cell concentration in SDE at different dilution rates during the continuous operation.....	143
Figure 6-6: Dodecane concentration equivalent with COD in SDE as function of time during biodegradation in aerobic bioreactor CSTR	144
Figure 6-7: (a) Relationship between substrate concentration and the rate of growth rate reaction (b) Lineweaver–Burk plot of the same kinetic data.....	145
<i>Figure 6-8: The effect of COD (Dodecane load) using <i>D.hansenii</i> on different dilution rates. The curves refer to the simulated data using the Monod, Aiba, Edwards and Haldane models, equations 6-13,14 and 15,</i>	148

Nomenclature

Symbol	Description	Unit
μ	Specific growth rate day or hours	$\text{h}^{-1}, \text{day}^{-1}$
μ_{max}	Maximum Specific growth rate	$\text{h}^{-1}, \text{day}^{-1}$
OD	Optical Density	% Abs
K_S	Saturated Constant	mgL^{-1}
K_I	inhibitor constant	mgL^{-1}
S	substrate	mgL^{-1}
COD	Chemical Oxygen Demand	mgL^{-1}
BOD	Biological Oxygen Demand	mgL^{-1}
C	Concentration	mgL^{-1}
T	Temperature	$^{\circ}\text{C}$
D	Dilution rate	h^{-1}
D_{max}	Maximum dilution rate	h^{-1}
t	Time (minutes)	min
t	Time (hour)	h
t	Time(day)	d
V	Reactor volume	m^3, ml
X	Cell concentration	$\text{g}_{\text{cell DW}} \text{L}^{-1}$
$Y_{x/s}$	Cell yield coefficient g cell DW per gram substrate consumed	
ΔG	Gibbs free energy	Energy
S_0	Initial Substrate	mgL^{-1}
SP	the solubilization power (SP)	Molar solubility/surfactant
CMC	critical micelle concentration	gL^{-1}

Nomenclature

Design of Experiment	DOE
Dimethyl sulfoxide	DMSO
Full factorial design	FFD
Central composite design	CCD
Central composite face centered design	CCF
Coefficient of determination	R^2
Bold's Basal Medium	BBM
Bligh & Dyer	B & D
Adjusted regression coefficients	adj- R^2
University of Texas	UTEX
High-performance liquid chromatography	HPLC
Ratio of weight to volume	%(w/v)
Response surface method	RSM
R^2 Regression coefficients	R^2
Standard deviation	STDEV
Fraction of the solute extracted in fast stage	f1
Fraction of the solute extracted in slow stage	f2
Continuous stirred-tank reactor	CSTR
Gas chromatography	GC
Tween 20	T
Dodecane	D

Chapter 1

1.1 Introduction

Desalting is the first step in a petroleum refining operation. The addition of water to crude oil removes salt but also produces an emulsion of water and oil. Emulsified salt-water is the major impurity extracted from crude oil and discharged into wastewater treatment plants. Desalter effluent also contains heavy metals, amines, BTEX (benzene toluene, ethyl benzene and xylenes), phenols and other aliphatic and aromatic hydrocarbons, hydrogen sulfide (H₂S), and dissolved inorganic compounds¹ during the water emulsification phase, which are then processed with the brine in a conventional wastewater treatment. This approach can create high COD and ammonia loads in the plant because desalters are the predominant source of such wastewater in a refinery, which can lead to upsets in the conventional wastewater treatment and put that system at risk of not meeting discharge requirements. Most current methods for the removal of salt and metal ions from desalter effluent have a significant cost. In order to overcome these challenges, more efficient and economical alternative procedures are needed.

Several fungi (yeasts and molds) and also some microalgae (in mixotrophic mode) can be applied to address the treatment of hydrocarbons in waste water streams. The halotolerant yeast *Debaryomyces hansenii*, is a blue cheese yeast which can grow in media containing 25 % NaCl and also in a wide range of pH values and temperatures. *Parachlorella kessleri* is a robust microalga which has been shown to be able to adapt to harsh environments. Figure 1.1 shows the structure of microalgae *Parachlorella kessleri* and yeast *Debaryomyces hansenii* is depicted in Figure 1.2.

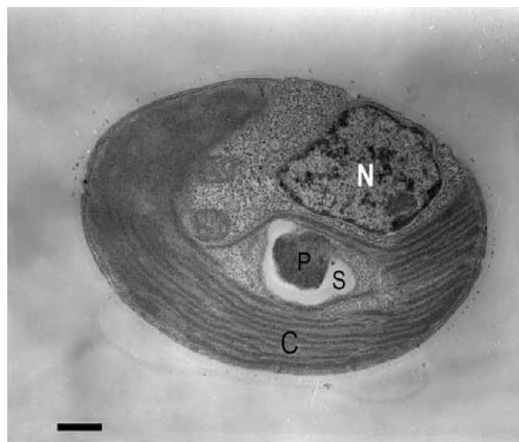


Figure 2-1 Micrographs of *Parachlorella kessleri*. Scale bar = 500 nm.²

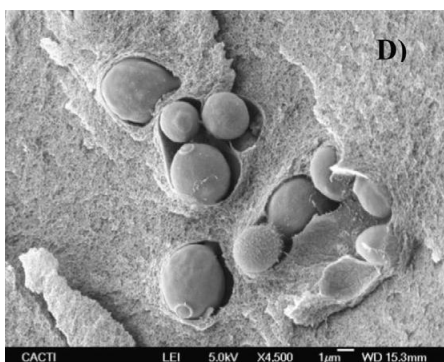


Figure 2-2 : *Debaryomyces hansenii* cells with microscope (4500× magnification).³

While both the halophilic and robust microorganisms *Debaryomycys hansenii* and *Parachlorella kessleri* have been investigated in environmental applications in the presence of salt, they have not been previously evaluated for desalter effluent treatment. Therefore, this study focused on the novel application of these two microorganisms for desalter effluent treatment.

1.2 Objectives

The overall objective of this research was to investigate the bioremediation of desalter effluent using halotolerant yeast *Debaryomyces hansenii* (LAF-3 10 U) or the environmentally robust micro-algae *Parachlorella kessleri* strain CPCC 266. The effect of these two different approaches on both synthetic and actual desalter effluent was investigated in both batch and/or continuous mode.

Several sub-objectives in this study were as follows:

- Investigate the bioremediation of real desalter effluent and simulated desalter effluent with *Debaryomyces hansenii*
- Study and model the inhibition kinetics of *Debaryomyces hansenii* with phenol in simulated desalter effluent in a batch reactor (shake flasks)
- Using response surface methodology, estimate and predict the effects of some environmental parameters on biodegradation and removal of dodecane in simulated desalter effluent using *D.hansenii*
- Investigate growth of *Parachlorella kessleri* in two types of desalter effluent
- Investigate benzene degradation in simulated and real wastewater treatment using *Parachlorella kessleri*
- Investigate growth of *Parachlorella kessleri* in real desalter effluent with additional phenol supplementation
- Investigate the lipid production in *Parachlorella kessleri* cultivated in real desalter effluent
- Investigate and model the CSTR kinetic model of *D.hansenii* when dodecane is the carbon source in simulated desalter effluent to predict yield (Dodecane removal) at different dilution rates.

1.3 Thesis organization

The present thesis encompasses seven chapters in the “Integrated Article” format as outlined in the Thesis Regulations Guided by the School of Graduate and Postdoctoral Studies (SGPS) of The University of Western Ontario. The chapters are structured as follows.

Chapter 1: Introduction

The introduction previews the thesis structure, including the problem definition, current approaches and methodology to desalter effluent treatment, objectives, thesis organization and novelty and contributions.

Chapter 2: Treatment Technology of Desalter Effluent: a review

This chapter presents a state of the art on current approaches to desalter effluent, the biotechnology of *Debaryomyces hansenii* and *Parachlorella kessleri*.

Chapter 3: Investigation of Growth Kinetics of *Debaryomyces hansenii* (Laf-3 10 U) in Petroleum Refinery Desalter Effluent

In third chapter, the feasibility of growth of the yeast in desalter effluent with phenol as the only carbon source. The effects of growth kinetics of *D.hansenii* in simulated desalter effluent at different phenol concentrations was also modelled. Different inhibition mathematical models were compared with experimental data

This chapter is published as: Azimian, L., Bassi, A.S., 2019, Investigation of Growth Kinetics of *Debaryomyces Hansenii* in Petroleum Refinery Desalter Effluent, *Canadian Journal of Chemical Engineering* 97 (1), 27-31, <https://doi.org/10.1002/cjce.23297>

Chapter 4: Investigation of Degradation of N-Dodecane by *Debaryomyces hansenii* In Simulated Desalter Effluent

In this chapter, the growth of halotolerant yeast in Synthetic desalter effluent containing dodecane as a substrate was carried out. Various operating parameters including pH, Salt concentration, substrate concentrations and temperature were examined.

A version of this chapter has been submitted to *Chemosphere Journal*

Chapter 5: Investigation of *Parachlorella Kessleri* strain CPCC 266 on refinery desalter effluent for lipid production

This chapter explores the feasibility of treatment of actual Desalter Effluent using robust microalgae with lipid production. The effects of light/dark, supplement media, additional hydrocarbon in two sources of desalter effluents on growth and cultivation of microalgae were studied.

This phase of the research is being prepared for submission to *Bioresource Technology Journal*

Chapter 6: Bioremediation of Synthetic Desalter Effluent Using *Debaryomyces Hansenii* (Laf-3 10 U) in Continuously Stirred Tank Bioreactor (CSTR)

It reports treatment of synthetic Desalter effluent using a halophilic yeast in continuously Stirred tank Bioreactor (CSTR) in the lab scale to find optimum kinetics model based on two variables of substrate concentration and dilution rate.

This chapter is being prepared for submission to *Biotechnology & Bioengineering Journal*

Chapter 7 Conclusion and Recommendation

This chapter has summarized the main output from the present study and recommends suggestions for future directions of research.

1.4 Novelty and Major Contributions

The research in this thesis resulted in the following contributions:

The literature review conducted for the project contributed to:

- Identifying and describing challenging aspects of desalter effluent treatment

The study of removal of phenol using *D.hansenii* in simulated desalter effluent contributed to:

- Identification of substrate inhibition by phenol on the yeast
- Development of the mathematical model for the growth of *D.hansenii* when phenol is the only carbon source in simulated desalter effluent. By changing the substrate concentration, specific growth rate can be predicted for biodegradation of phenol under a mathematical inhibition model
- Identifying the suitability of *D.hansenii* growth in actual and synthetic desalter effluent at the typical salt concentration range
- This yeast is, therefore, suggested to serve as an appropriate system for biological treatment of phenolic wastes in difficult to treat effluents such as desalter effluent.

The study of dodecane removal in simulated desalter effluent resulted in

- Understanding the effects of various operational factors including temperature, pH, substrate (dodecane), and NaCl concentration in removal of COD
- Understanding the effect of varying desalter effluent load and predicting dodecane removal rate by having kinetic constants and the inhibition mathematical model.
- Finding optimal points to maximize COD removal using *D.hansenii* by changing the environmental factors through the empirical models obtained.

Investigation of growth of *P.kessleri* in treatment of desalter effluent and lipid production

- Development of an alternative biological treatment approach for desalter effluent using microalgae *Parachlorella kessleri*.
- Establishment of a dual purpose process in petroleum refinery industry: treatment of desalter effluent, growth and harvesting *P.kessleri* for lipid production as a source of biofuel
- Demonstration the effect of desalter effluent characteristics in COD removal, ammonia removal, biomass production and lipid production using response surface method
- Indication of *P.kessleri* growth in desalter effluent is an excellent feedstock for lipid production
- Identification of *P.kessleri* growth in actual desalter effluent based on media composition.

The study of different dilution rate in COD removal (dodecane removal) in CSTR system at SDE

- Understanding the effects of various dilution rates in dodecane removal (COD removal) in SDE which plays a crucial role in the industrial scale regarding the fluctuation in desalter effluent loading rate in constant volume of bioreactor.
- Identifying growth of *D.hansenii* profile based on different dilution rates in constant initial dodecane, NaCl concentration and finding a kinetics model to fit experimental data for prediction and adjusting of substrate concentration to have optimum dilution rate

The main novelties of this research are summarized as follows:

- In this study, an osmotolerant and halotolerant yeast, *Debaryomyces hansenii*, was investigated for the first time for phenol removal from simulated and actual desalter

effluent. The results in this study confirmed that *D.hansenii* has a high tolerance toward phenols and other organic compounds and salt found in desalter effluent.

- The yeast *D. hansenii* rapidly reduced high concentrations of n-dodecane in shorter time periods compared to previous findings for biodegradation of this effluent, suggesting *D. hansenii* could be useful for bioremediation and enhanced microbial oil recovery in high salinity environments.
- *P. kessleri* is able to grow in desalter effluent suggests that selected microalgae possess certain traits that allow them to be good candidates for cultivation in wastewater with high salt concentration and toxic hydrocarbons.
- Phenol and Benzene were degraded by *P.kessleri* in actual and synthetic desalter effluent.
- Robust and halotolerant microalgal, *P.kessleri*, was grown in harsh desalter effluent and produced high content of lipid.
- A completely novel approach based on single types of micrororganisms can be applied for treatment of challenging desalter effluents.

Chapter 2

2 A review of treatment technology for desalter effluent

2.1 Introduction

Crude oils entering a refinery may include dilute dispersions of water droplets containing a variety of dissolved salts, suspended solids, and metals. These can also include emulsions in oil such as asphaltenes, resins, naphthenic acids, and fine solids stabilized by the presence of natural surfactants in oil. Salts of sodium, calcium and magnesium chlorides (NaCl , CaCl_2 , and MgCl_2) are frequently found in crude oil. The presence of these compounds in crude oil can cause several problems in the petroleum refining operations due to scaling, and corrosion in the refining processes^{4,5}. Desalters are installed in crude oil production units to remove the dissolved salts from oil streams in order to prevent corrosion, plugging, and fouling of equipment, or poisoning of the catalysts in the processing units (leading to a shortened unit life span and reduced equipment reliability)⁶. The process of desalting involves water washing and de-emulsification operations for cleaning up crude oil and to remove inorganic contaminants^{4,7}. The salt content of crude can be as high as 2000 pounds per thousand barrels (PTB) (5.7 Kg m^{-3}). Desalting of crude oil is an essential part of the refinery operation. The salt content should be lowered in the range of 5.7 and $14.3 \text{ kg}/1000 \text{ m}^3$ ^{8,9}.

The effluent from the desalting operation is a major source of contaminated wastewater and contains phenols, BTEX, hydrocarbons such as dodecane, and dissolved inorganic compounds¹. Phenol is toxic to aquatic life, liver, lungs, and kidneys¹ and is a potential environmental concerns in the desalting operation due to carry-over into the brine stream.

Amines present with the water phase and leaving with brine are also a concern due to high COD and nitrification loads. Moreover, amines cause an increase of pH in desalters and can affect desalter operation ¹⁰.

With the process of desalting of the crude oil with water, the washed water, demulsifier and inorganic contaminants ^{4,7} with high salt are removed ⁶. This discharged effluent disturbs the conventional treatments process in the wastewater treatment plant (WWP) ^{4,5}. In addition, toxic hydrocarbon and other contaminants in the current process do not meet new regulations of emission ^{1,11}.

There is limited research to date on desalting unit effluent treatment in petroleum refinery. Pak and Mohammadi in 2008 described the use of membrane distillation (MD) and a polymeric teflon microfiltration (MF) that fulfill high flow rate irrigation water standard⁵. Recently, ultrasonic-electric installing before desalter with the salt reduction rate of 94% ¹² and Reverse Osmosis membranes have been reported. Results showed that this approach reduces high salinity from 143,054 mgL⁻¹ to 842.8 mgL⁻¹ and metals were removed from desalter effluent up to 99%¹³ Other approaches investigated the improvement of desalination process to prevent a “rag layer“ (separation of emulsified oil from water) by adjusting temperature, fresh water injection, emulsifier, electric field and gravity settelin¹⁴ or withdrawing sample electrically until the result of sampling demonstrate acceptable water-oil separation ¹⁵. Mathematical modeling and statistical analysis have been applied for adjusting parameters for better desalination approaches¹⁶⁻¹⁹.

The majority of research in desalination of salt that is focused on seawater, brackish water, and mineral wastewater. Hydrocyclones, membrane distillation, ultrafiltration, reverse osmosis, and Nano filtration, physicochemical separators, centrifuge, dehydration, electrochemical oxidation have been proposed for removal of salt from effluent and preparation for reuse or treatment ^{1,5,9,20-27}. But these techniques are used infrequently in industrial production because of the complexity of the equipment and low reliability ²⁸ and also high consumption of energy and material. Several studies have been reported on the biodegradation of crude oil wastewater by different microorganisms such as bacteria and yeast²⁹⁻³⁷. However, there are limited reports on the remediation of petroleum desalter

effluent. In this review typical characteristics of desalter effluent are presented and various approaches of treatment for development of desalting and desalter effluent treatment are discussed.

2.2 Desalting Unit Operations- Current State-of-The-Art

Desalting units remove contaminants from crude oil by washing with water at a ratio of 2-6% of the crude oil feed⁵. Another report applied wash water to dissolve salt in desalter at about 6 to 8% v/v of crude oil³⁸. The optimum wash water rate depends on the American Petroleum Institute (API) gravity of the crude oil and the desalter temperature³⁹. The wash water applied may be fresh supplied water, or recycled water from other unit operations in the refinery including vacuum tower overhead, recycled crude tower overhead or stripped sour water³⁸. Desalter effluent is a mixture of many components, including brine wash water, sand, grit, mud, demulsifier and hydrocarbons⁵.

Figure 2.1 is an example of a process flow diagram of a typical distillation unit, illustrating the location of the desalter. First, as seen in Figure 2-1, the desalter (colored red) is installed next to the heat exchanger that heats the incoming crude oil, to about 100 to 150°C before it flows through a fired heater and the distillation tower. At that point, wash water is injected and mixed into the continuous flow of crude oil and the resulting oil-water emulsion then continuously enters the electrostatic desalter. Wash water pH should be maintained between 6 to 8.²⁸ Figure 2-2 is a cross-sectional diagram of a crude oil desalter. The desalter is horizontal and cylindrical. The wash water is continuously added to the desalter, and dissolves salt and exits from the lower part of the desalter. The discharged brine water contains the inorganic salts that originally are extracted from crude oil in the desalter. The settled sediment sludge at the bottom of desalter is removed and may contain components such as asphaltenes, and other sediment contaminants that are not soluble in water⁴.

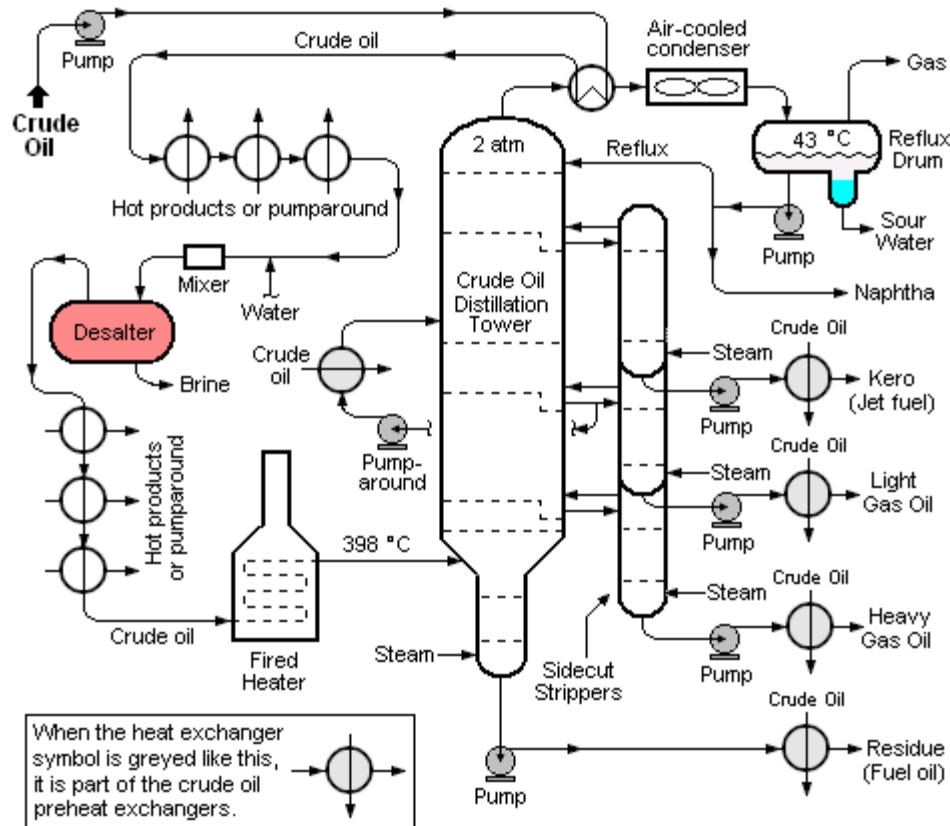


Figure 2-1: Process flow diagram of a typical crude oil refining unit ⁴⁰.

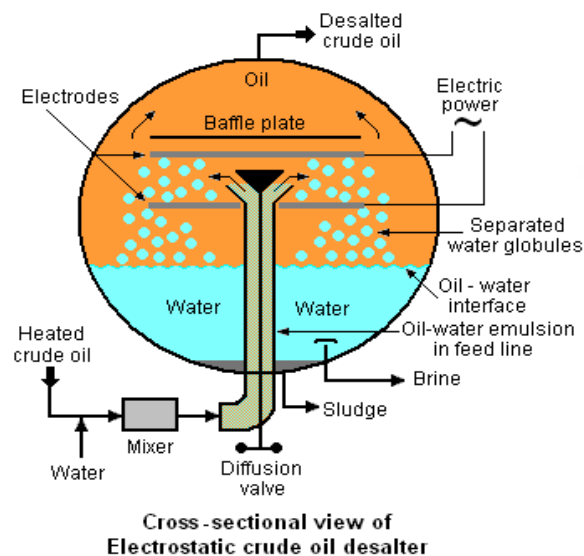


Figure 2-2: Cross-sectional diagram of a crude oil desalter ⁴⁰

2.2.1 Types of desalter units

The two most typical methods of crude-oil desalting are chemical and electrostatic separation which use hot water as the extraction agent. A typical desalting unit operation usually contains the following six major steps: separation by gravity settling, chemical injection, heating, wash water, mixing, and transformer to generate electrical power. The crude oil is heated to 65-176°C (150–350°F) for easier mixing and separation of the water. High temperature reduces viscosity and surface tension ⁵. Depending on the oil reservoir, the crude oil characteristics, and the treated oil specifications, the number of vessels and arrangement will vary in different refineries. In large production facilities, multiple stages are typically used to minimize lost production during maintenance shutdowns. In general, desalters are divided into three types: Natural Desalter, Chemical Desalters, and Electrostatic Desalters. These are further discussed below.

2.2.2 Neutral desalter

In a “Neutral Desalter” time is given to salts, sediments, water, and sludge to settle under gravity and for subsequent draining. Figures 2-3 a. describes a type of desalter which is a typical horizontal type gravity separator. A simplified version of this neutral desalter separator and its external boundary are depicted in Figure 2-3 b. The crude oil stream enters the separator and the associated gas and water are separated from the oil phase. The gas and water leave the separator container through pressure control valves and water dump valves, respectively. The separated oil is then routed to the next stage separator through the oil dump valve

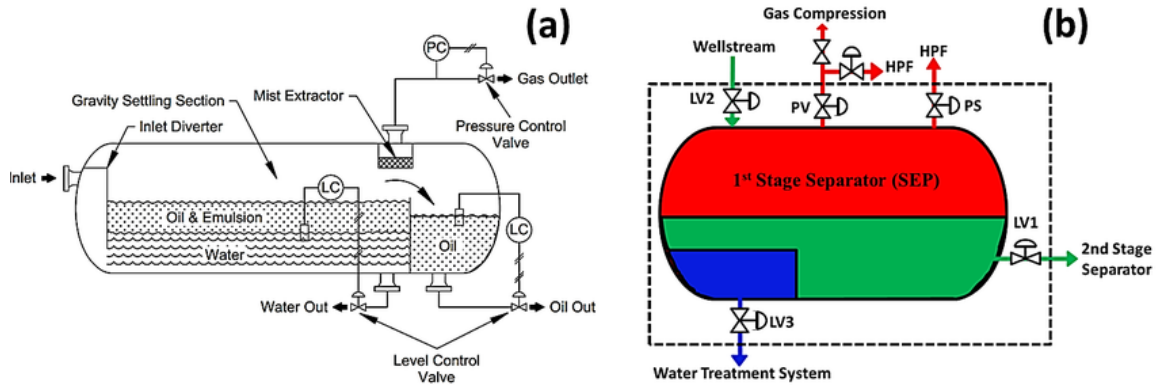


Figure 2-3: (a) Description of a Neutral Desalter Unit; (b) Simplified diagram of the Neutral Desalter operation ⁴¹

2.2.3 Chemical desalter

A second type of desalting operation utilizes chemical removal of salts, sediments, water, and sludge and oil/water separation. In these “Chemical desalters” first, crude oil is heated by the heat exchanger and then fresh water along with the small amount of chemicals are injected to form an emulsion. After the oil is washed and separated, demulsifying chemicals are added for breakage of emulsion. These types of units are efficient for crudes containing low salts or for batch process.

2.2.4 Electrostatic desalter

Figure 2.4 describes a schematic cross section of an Electrostatic Desalter unit. The typical electrostatic desalter is a horizontal, cylindrical vessel as depicted in Figure 3.4. The desalting process operates by use of a chemical agent along with the electric field.

For better separation of water-oil emulsion, the chemical demulsifier injection is added to promote the emulsion breaking. Then an electric field across the settling vessel is applied to charged salty water droplets to attract and combine each other. A potential high voltage

electrostatic charge ranges from about 10 KV to about 25 KV ⁷. The resulting larger water droplets, along with suspended solids, then settle to the bottom of the desalter tank.

The typical electrostatic desalter is a horizontal, cylindrical vessel as depicted in Figure 3.4.

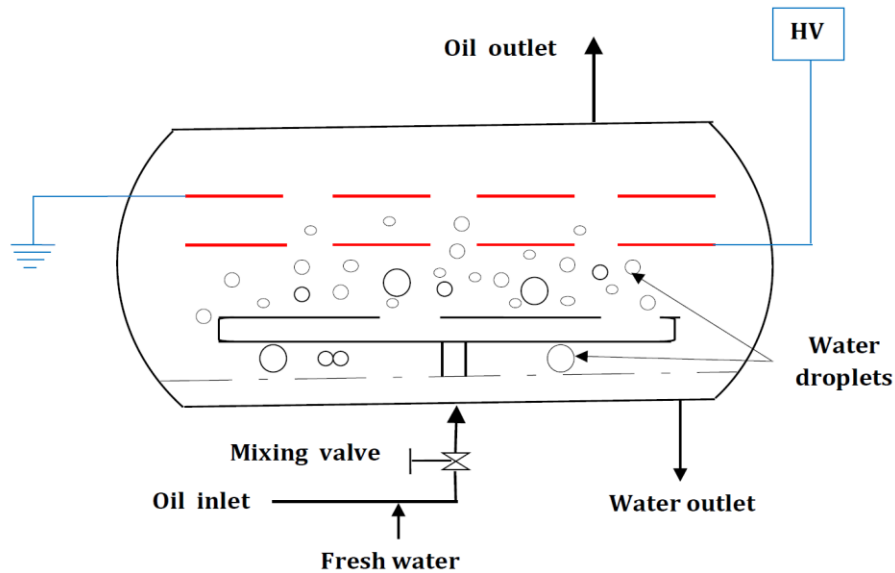


Figure 2-4: Cross section diagram of an electrostatic desalter⁴²

Desalting can be performed in a single stage or in two stages, depending on the requirements of the process. Figure 2-5 shows a process flow diagram for one and two steps desalting process. Dehydration efficiency of the desalter increases when the number of stages increases ²⁸. The typical dehydration efficiency of a one-stage desalter is 95% ⁴³. Dehydration efficiency can increase by up to 99 % when the number of stages increases. In this case, the wash water injected from the first stage flows into the second stage. The effluent water discharged from the second stage is recycled and flow back to the first stage. The multiple sages help further desalting ⁴³.

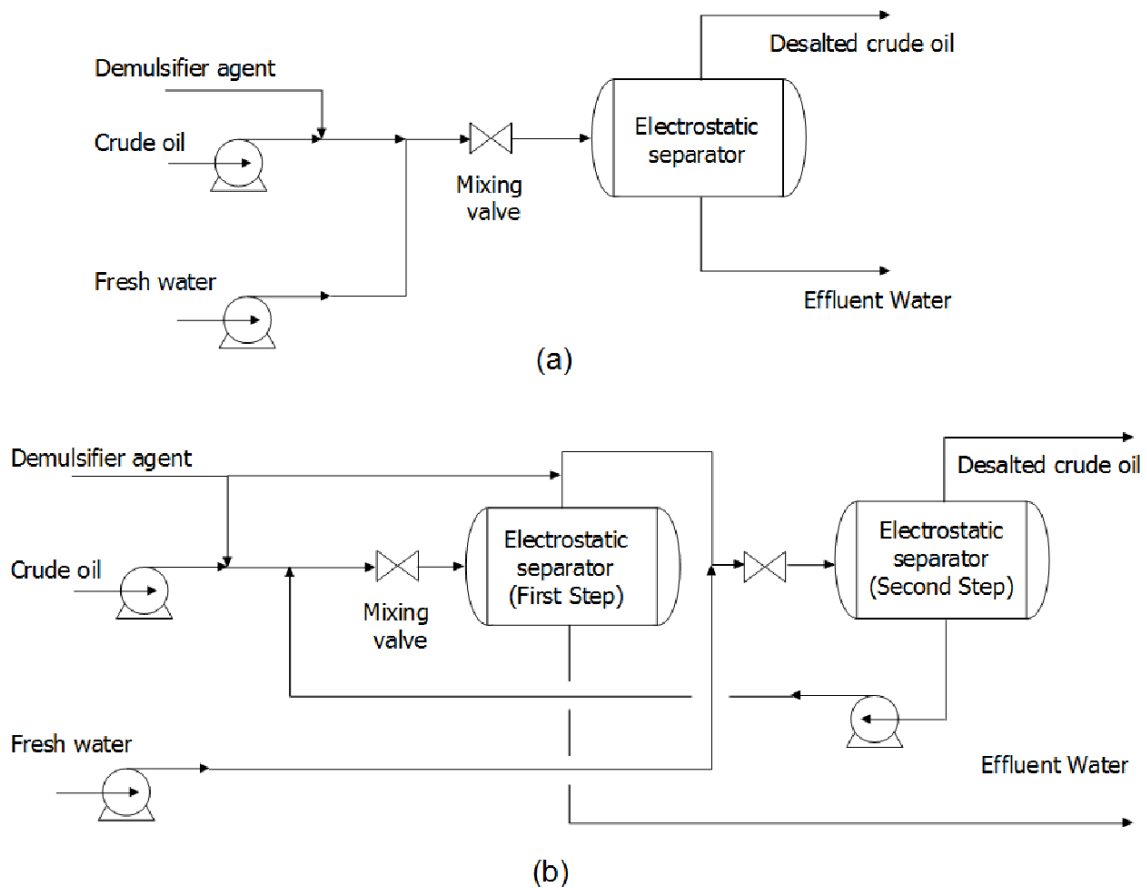


Figure 2-5: Desalting process flow diagrams (a) one-step and (b) two-step.⁴

Demulsifiers change the polarity and so the oil droplets attract each other to merge. The understanding of the different variables that affect the desalting process, especially the effect of the amount of chemical demulsifier used, is imperative in order to optimize operating costs.

2.3 Desalter Effluent Characteristics

Desalters are used for the removal of salts, suspended solids, and water-soluble trace metals/slits, iron oxides that contain in the crude. However, several other contaminants are also removed (H_2S , ammonia, phenol, mercaptans, etc.)^{1,38,44,45}.

The salt content of crude oils depends on geological features of hydrocarbon reservoirs which can be varied up to 200,000 ppm⁴⁶. Consequently, the salinity of produced brine from desalting of the crude oil varies widely. Salt concentration in crude oil depends upon the source of crude. They are inorganic in nature and are soluble in water (inorganic) and insoluble in crude (organics). In one report, four Arabian crude oils contained salt concentrations of 34.2, 28.5, 14.3 and 5.71 mgL⁻¹⁴⁷. The amount of salt in the crude oil for temperatures is up to 373 K and sodium chloride concentrations up to 250,000 mgL⁻¹⁴⁸. In another study, the amount of NaCl in crude oil was reported to be 451.4 mgL⁻¹¹⁶. These salts are mainly chlorides and sulfates of calcium and magnesium like NaCl, MgCl₂, CaCl₂ and MgCl₂. Chlorides hydrolyzed to hydrochloric acid cause severe corrosion⁴. Operating temperature in desalting is 80-150 °C^{12,14,45}. The temperature of effluent is cooling down between 21 and 50 °C^{5,13,49} when it is discharged to a wastewater treatment plant. Optimum pH in desalting is reported 5.4-7.2^{13,24,50}.

2.3.1 Typical desalter effluent characteristics and components

General characteristics of desalter effluent have been reported in several studies. Typical values range as follows: Chemical oxygen demand (COD) 400 to 1000 mgL⁻¹, free hydrocarbons up to 1000 mgL⁻¹, suspended solids up to 500 mgL⁻¹, phenol 10 to 100 mgL⁻¹, benzene 5 to 15 mgL⁻¹, sulfides up to 100 mgL⁻¹, ammonia up to 100³⁸. The total free hydrocarbon including dodecane in typical desalter effluent has been reported up to 1000 mgL⁻¹^{38,51}. However, the oil content in desalter effluent depends on crude oil characteristics and separation efficiency of a desalter. In desalting processes, contaminants such as ammonia, base or acid for pH adjustment can be added. The typical concentrations of cations, anions, COD, Biological Oxygen Demand (BOD), and total dissolved solids (TDS), total hardness (CaCO₃) and toxic hydrocarbons such as benzene and phenol are shown in Table 2-1.

Table 2-1: Characteristics of water discharged after the desalination-dehydration operation

Parameter/Reference	45	1,9	19	24	5	52	13	
Salt							143,054.1	236,509.9
total dissolved solids (TDS)	50-100	3,476	8900	3030			138,012.0	227,2
Oil/emulsified oil	high							
Dissolved hydrocarbons	50-300							
Phenols	5-30			4.7		0.22-6.9-37-63		
Benzene,	30-100					11-12		
BOD	high			1077		700-270		
COD	500-2000	345-12,000		1707		600-1200-2100		
Ammonia	50-100			271		13-47		
Nitrogen compounds	15-20		19.2	1.1		95		
Sulfides (on H₂S basis)	10			60.4	65633		18	19
Na⁺			1926			460-190-400-570	33,157	38,361
K +			10			18-73	270	1832
Ca²⁺			801		8350	86-84-68	12,000	36,000

	Mg⁺²			450		1000	13-19	4865	6075
	Fe⁺²			0.25		12.5	0.95	3.5	350
	Cl⁻¹			4045	1235	118.625	33- 840- 330	86,963	143,775
	HCO₃			285		0.2			
	SO₄⁻¹			1500	164	216		200	650
	CaCO₃		510.3	289	549			279.68	549
			-						
			9,500						

2.4 Current Technologies Of Desalter Effluent Treatment Introduction

Desalter effluents are hazardous to the environment and their discharge into the environment adversely affects ecosystems. Various treatment approaches for desalter effluent are discussed below. However, each method possesses several drawbacks and these are also discussed ⁵³.

Treatment techniques

Currently desalter effluent is mixed with other waste streams and sent to conventional wastewater treatment. Traditional treatment includes a combination of physical and chemical processes such as American Petroleum Institute (API) separators, flocculation, precipitation, filtration, absorption and biological treatment such as activated sludge and biofilm processes. Such treatments are usually effective in reducing organic pollutants to meet standard effluent requirements for disposal into storage for reuse, public sewage or natural waterways. However, they often fail to reduce the concentration of heavy metals and toxic hydrocarbons below permissible limits ⁵⁴. Further, existing technologies usually do not provide the selectivity necessary to create high quality streams suitable for recycling or

reuse, and consequently, the by-product sludge or concentrated wastewater can itself become a disposal problem.

2.4.1 Pre-treatment approaches

Gravity oil separators combined with chemical addition is applied to remove suspended materials and oils some approaches are further discussed below.

2.4.1.1 API Separator (Oil -Water Separator)

API separators are applied in refinery wastewater treatment usually as the first step for primary oil and solids separation. API separators are based on the principle of density difference between oil/water which allows oil to rise to the surface of the device. The API separator represents one of the most important wastewater treatment steps for refineries and petrochemical plants.⁵⁵ The average residence time for APT separators is 30 min and this method is only capable of separating and removal of free oil and not emulsified oil⁵⁶⁻⁵⁸

2.4.1.2 Conventional Flotation Techniques

The removal of solids, ions, macromolecules, fibers, and other materials from water have been the main applications of flotation. In water and waste-water treatment, flotation is the most effective process for the separation of oil and low-density suspended solids. The technical and economic potential of this process are based on selectivity to thicken scums and sludges (6-12% w/w), low operating costs with the use of upcoming flotation devices, efficiency to remove contaminants, flow rates, low detention time and lower foot-print^{57,58}.

2.4.1.3 Electro-flotation (EF)

In this process, the micro-bubbles are generated by the electrolysis of diluted aqueous, conducting solutions leading to the production of gas bubbles at both electrodes. Electro-flotation is effective in treating oily waste-water or oil-water emulsions, waste-water from

coke-production, colloidal particles, heavy metal containing effluents, and applications to many other waters and waste-waters problems^{58,59}. The amount of free and emulsified oil in petroleum refinery wastewater is between 220 mgL⁻¹ and 75 mgL⁻¹. The efficiency of air flotation with no chemical is 75-90% removal of free oil and 10-40% of emulsified oil. When chemicals are applied the oil water removal efficiency increases only in emulsified oil to a range between 50-90%⁵⁶. In the Electro flotation Method (EFM) treatment, oil removal efficiency at an aircraft maintenance facility using 6-9 V, 12-25 Am⁻³ was reported to be 99% from 60 mgL⁻¹ to 0.3 mgL⁻¹⁶⁰. EFM can be applied for removal of heavy metal in the wastewater washing contaminated soil by drilling oil well up 97% using power of 14 kWh m⁻³ with resident time of 20 min⁶¹. EFM was employed for microfiltration pre-treatment that increased permeate flux by reducing mass cake. A review of literature by Kyzas and Matis in 2016⁶² indicated that EFM can apply for removal of heavy metals (97%), minerals, surfactants, and aids in increasing quality of water^{62,63}.

A study was reported EFM removed oil from wastewater at NaCl concentration of 7900 mg l⁻¹ with efficiency of 98% in 720 minutes by consuming energy of 1.47 kWh m⁻³⁶⁴. EFM can remove oil from water 92% at the presence of 3.5 % NaCl by examining operating parameters, electrical current, oil concentration, flotation time and flocculent agent concentrations and Electrical energy consumption between 0.5 and 10.6 kWhm³⁶⁵. Similar research carried out with oil removal of 99.5% consuming less energy than previous literature (0.4 to 1.6 kWhm³)⁶⁶. If this technology can be a good choice for biodegradation of desalter effluent by microorganisms that supply air for their metabolism, size of bubble diameter, in this method can be adjusted regarding increasing of the oil to achieve better separation of oil from water⁶⁷

2.4.1.4 Dispersed (induced) air flotation (IAF)

In this method, the bubbles are mechanically formed by a combination of a high-speed mechanical agitator and an air injection system making use of the centrifugal force developed in the system. The gas, dispersed at the top, in the liquid becomes fully intermixed and, after passing through a disperser outside the impeller, forms a multitude

of bubbles sizes from 700-1500 μm diameter. This method is utilized in the petrochemical industry, and mineral processing for oil-water separation^{57,58}. The combination of IFA and a coagulation process increased COD removal up to 99%. The removal efficiencies increase with the alum concentrations (coagulant). The maximum removal efficiency of 99% in terms of COD was obtained at the optimum pH value and alum concentration range between pH 8–10 and 800 and 1400 mgL^{-1} ⁶⁸. Bubble size, bubble rising velocity, bubble formation frequency and the velocity gradient in flotation process has significant effect on efficiency and operation cost. Integrated IFA with photo-Fenton could remove 100% of organic removal in 20 min⁶⁹.

2.4.1.5 Dissolved air (pressure) flotation (DAF)

DAF was recognized as a method of separating particles in many applications including sludge thickening and separation of biological flocs, treatment of ultrafine minerals, removal of organic solids, dissolved oils and VOCs (dissolved toxic organic chemicals), removal of algae; micro-organisms, etc. The DAF process is by far the most widely used flotation method for the treatment of industrial effluents. It is believed that applications will rapidly expand in waste-water treatment in the metallurgical and mining fields⁵⁸. Another industrial application of DAF is gravity settlement of solid generated by a biological treatment process. This method has high rate process in comparison to traditional gravity settlement systems and highly flexible regard to the systems operating parameters. This method can be applied for treatment of desalter effluent.

2.4.1.6 Nozzle flotation (NF)

This process uses a gas aspiration nozzle to draw air into recycled water, which in turn is discharged into a flotation vessel, to develop a two-phase mixture of air and water with bubbles. This approach in comparison to induced air flotation (IAF) systems, has higher efficiency and lower costs and energy use. Nozzle flotation has been extensively applied for the separation of oil-water emulsions and treatment of oily metal wastewater.⁵⁸. An

optimized Nozzle flotation can remove 81% oil from petroleum wastewater with oil content between 50 and 600 mgL⁻¹ to range between 20 and 30 mgL⁻¹ of oil⁷⁰. The nozzle units compare to induced air flotation (IAF) systems, are lower initial costs and energy use as a single pump provides both mixing and air supply, lower maintenance and longer equipment life because the unit has no high-speed moving parts.

2.4.1.7 Column flotation

This unit operation has been utilized in both mineral processing and wastewater treatment. New developments in column technology include external sparging of gas with and without the addition of surfactant, and columns with internal baffles and coalescers (separation tool) for oil recovery. Column flotation has been applied in the field of oil removal in production waters, and in the recovery of heavy metals precipitates⁵⁸. Flotation columns differ dramatically from mechanical flotation machines in several ways; there is no mechanical agitation/shear, gas bubbles are generated by sparging. Separation of fine mineral particles such as oil proplets was improved by replacing oscillatory air supply with air supply for the first time in 2018⁷¹. Rubio reported in 1996,⁷² modified column, selectively separates drained particles from froth zone and secondary wash water system, recovered gold, copper, Zinc fluorite ore 15%, 33%, 94% respectively⁷². A process utilizing activated carbon adsorption and column flotation by adjusting coal dosage, feed rate, circulation pressure, and gas flow rate has been reported which could achieve 97.7% separation at 2000m³day⁻¹⁷³. Column flotation is an efficient method to separate useful minerals from ores of complex mineral composition used in the mineral industry⁷⁴.

2.4.1.8 Centrifugal flotation (CF)

In this system, the separator and contactor can be either a hydro cyclone or a simple cylinder in which a centrifugal field is developed. The centrifugal flotation unit removes oil, grease, BOD, etc.⁵⁸. The separating efficiency of reduction salt varies from 8 mgL⁻¹

to 3 mg L^{-1} when the Reynolds number is close to 5400²¹. This method produces less wastewater since the dehydration efficiency ranges increased from 86% to 99%.

Modified centrifuge flotation with a disc reduced oil and fat from wastewater up to 20% of COD per cycle in resident time of 1 s⁷⁵. However, energy consumption in this treatment is higher than centrifugal flotation techniques⁷⁵. A synthetic dairy effluent treated by two air flotations methods; flotation column, and centrifugal flotation in hydro-cyclone. Suspended milky wastewater was removed 90% and 50 % respectively. If the flowrate of centrifuge flotation reduces to lower flowrate, the resident time increases to achieve higher removal efficiency⁷⁶. Integration of two flotation techniques induced air flotation and centrifugal filtration can remove oil from water with COD of 85%⁷⁷.

2.4.1.9 Jet flotation

Jet flotation is a unit operation which separates Petroleum oil from water. This approach has a great potential for solid/liquid separations and for liquid/liquid separations as well as in mineral processing. Its main advantage is its high throughput, high efficiency and moderate equipment cost. Moreover, with no moving parts, the jet cell has low power consumption and low maintenance costs. Its use has been extended to waste-water treatment, recovery of solvent extraction liquors⁵⁸. Santander in 2010 modified Jet flotation and oil removal increased from 80% to 85% with optimized design of jet flotation⁷⁰.

2.4.1.10 Cavitation air flotation (CAF)

Cavitation air flotation utilizes an aerator, which draws ambient air down a shaft and injects “micro-bubbles” directly into the wastewater. CAF can remove suspended solids, fats, oils, greases, BOD and COD. A study was carried out for comparison of CAF dewatering efficiency and dewatered sludge (thicken water machine). CAF dewatered sludge 2% higher than thicken water machine (22.4-23.8%)⁷⁸. This method can apply for further

separation of oil from water in desalter effluent, However, there is no fundamental work that has been reported with this flotation technique⁵⁸.

2.4.1.11 Equalization

The equalization is used to steady the flowrate variations. It provides enough mixing and aeration in equalization tank that enhanced biological treatment, and improve process reliability by damping of mass loading⁷⁹. Most water treatment processes are sensitive to changes in flow rate, pollutant concentration, pH, and temperature. Equalization reduce the fluctuations of these parameters, which is effective in optimizing the quality of water treatment. This method was recommended to apply for oil refinery wastewater due to low level of oil removal in dissolved air flotation (DAF) while there is a high concentration of free oil⁵⁶. Table 2-2 displays the list of Petroleum refining effluent treatment technology Performance data that meet quality criteria of Environmental Protection Agency (EPA).⁸⁰ It shows some studies had successful results in removal of contaminations. In 2013, Petrobras applied techniques including EQ, DAF, FI and MBR to remove COD up to 83% in full scale, Tetra tech 77.8% using O/W, AIR, MBR in pilot scale. CH2M HILL in 2014 and 2016 reduced COD from 142.2 to 167 mgL⁻¹(52.9%) using EQ, ANSG, ASG, MBR and from 119.7 to 77.9 mgL⁻¹ (34.9%) by OW, DAF, EQ, MBR in full scale.

Ammonia was removed 94.5% to 98.8% in several techniques OW, DAF, FI, EQ, MBR by Petrobras, and Tetra tech (2013), CH2M HILL (2016) with final concentration between 0.2 and 1 mgL⁻¹. One study monitored the results in 2014 the concentration of nitrate increased in EQ, ANSG, ASG, ANSG, MBR systems from 1.1 to 1.7 mgL⁻¹(CH2M HILL) due to high concentration of ammonia in desalter effluent, the biological oxidation converts ammonia or ammonium to nitrate.

Table 2-2: Petroleum refining effluent treatment technology Performance data identified from data source meeting data quality criteria in pilot and full scale. ⁸⁰

Treatment System	Parameter Name	Influent Conc. (mgL ⁻¹)	Effluent Conc. (mgL ⁻¹)	Update Removal%	Main Author	Year
AIR	COD	522	92	82.4	Siemens Energy Inc.	2013
		2522	560	77.8	Tetra Tech	2013
	COD		296	93	Brown and Caldwell	2011
	Ammonia (as NH ₃)	15	2	86.7	Siemens Energy Inc.	2013
	Ammonia (as NH ₃)	47	1	97.9	Tetra Tech	2013
EQ	COD	119.7	77.9	34.9	CH2M HILL	2016
	COD	2522	560	77.8	Tetra Tech	2013
	COD	142.2	67	52.9	CH2M HILL	2014
	Ammonia (as N)	7.3	0.4	94.5	CH2M HILL	2016
	Ammonia	80	1	98.8	Petrobras	2013
	Ammonia (as NH ₃)	18.1	0.2	98.9	CH2M HILL	2014
	Nitrate (as NO ₃)	1.1	1.7		CH2M HILL	2014
	Ammonia (as NH ₃)	47	1	97.9	Tetra Tech	2013
GAC (Adsorption)	Ammonia	15	2	86.7	Siemens Energy Inc.	2013
ION	Nitrate	25	2.8	88.8	GE Water & Process Technologies	2009
RO	Nitrate	25	2.8	88.8	GE Water & Process Technologies	2009
	Phosphate, total (as PO ₄)	4.5	0.4	91.1	GE Water & Process Technologies	2009
ADSM	Ammonia	0.8	0.7	12.5	MAR Systems Inc.	2012
	Nitrate	4	2	50	MAR Systems Inc.	2012
ANSG	Ammonia (as NH ₃)	18.1	0.2	98.9	CH2M HILL	2014

	Ammonia (as NH ₃)	18.1	0.2	98.9	CH2M HILL	2014
	Nitrate (as NO ₃)	1.1	1.7		CH2M HILL	2014
	Nitrate (as NO ₃)	1.1	1.7		CH2M HILL	2014
	COD	142.2	67	52.9	CH2M HILL	2014
ASG	COD		296	93	Brown and Caldwell	2011
	COD	142.2	67	52.9	CH2M HILL	2014
	COD	458	317	30.8	Georgia Institute of Technology	2012
	COD	704	370	47.4	Georgia Institute of Technology	2012
	COD	874.8	69.2	92.1	Veolia Water Solutions & Technologies Canada	2010
	COD	651.75	177.33	72.8	Sage ATC	2016
	COD	773.33	223.08	71.2	Sage ATC	2016
	COD	865.17	285	67.1	Sage ATC	2016
	Ammonia	14.6	0	100	Veolia Water Solutions & Technologies Canada	2010
	Ammonia (as NH ₃)	18.1	0.2	98.9	CH2M HILL	2014
	Nitrate (as NO ₃)	1.1	1.7		CH2M HILL	2014
BNR	COD	316	42	86.7	ENVIRON International Corporation	2010
	COD	316	42	86.7	ENVIRON International Corporation	2009
	COD	227.6	120.53	47	CH2M HILL	2009
	Ammonia, total	15.8	1.3	91.8	ENVIRON International Corporation	2010
	Ammonia (as N)	15.8	1.3	91.8	ENVIRON International Corporation	2009
	Ammonia (as NH ₃)	29.98	1.49	95	CH2M HILL	2009
	Nitrate	0.01	0.32		ENVIRON International Corporation	2010

	Nitrate (as N)	0.01	0.32		ENVIRON International Corporation	2009
	Nitrate (as NO ₃)	0.14	7		CH2M HILL	2009
DAF	COD			83	Petrobras	2013
	COD	119.7	77.9	34.9	CH2M HILL	2016
	Ammonia (as N)	7.3	0.4	94.5	CH2M HILL	2016
	Ammonia	80	1	98.8	Petrobras	2013
FI	COD			83	Petrobras	2013
	Ammonia (as NH ₃)			97	Petrobras	2013
GAC	COD	522	92	82.4	Siemens Energy Inc.	2013
ION	Phosphate, total (as PO ₄)	4.5	0.4	91.1	GE Water & Process Technologies	2009
MBBR	COD	84	29	65.5	Suncor Energy, Inc.	2014
	COD	165	83	49.7	Suncor Energy, Inc.	2014
	Ammonium-nitrogen (NH ₄ -N)	8.7	0.7	92	Suncor Energy, Inc.	2014
MBR	Ammonia (as NH ₃)	29.98	1.49	95	CH2M HILL	2009
	Ammonia (as NH ₃)	47	1	97.9	Tetra Tech	2013
	COD	227.6	120.53	47	CH2M HILL	2009
	COD			83	Petrobras	2013
	COD	522	92	82.4	Siemens Energy Inc.	2013
	COD	2522	560	77.8	Tetra Tech	2013
	COD	142.2	67	52.9	CH2M HILL	2014
	COD	119.7	77.9	34.9	CH2M HILL	2016
	Ammonia	80	1	98.8	Petrobras	2013
	Ammonia	15	2	86.7	Siemens Energy Inc.	2013
	Ammonia (as NH ₃)	18.1	0.2	98.9	CH2M HILL	2014
	Ammonia (as N)	7.3	0.4	94.5	CH2M HILL	2016
	Nitrate (as NO ₃)	0.14	7		CH2M HILL	2009

	Nitrate (as NO ₃)	1.1	1.7		CH2M HILL	2014
MF	COD	874.8	69.2	92.1	Veolia Water Solutions & Technologies Canada	2010
	Ammonia	14.6	0	100	Veolia Water Solutions & Technologies Canada	2010
	Nitrate	25	2.8	88.8	GE Water & Process Technologies	2009
	Phosphate, total (as PO ₄)	4.5	0.4	91.1	GE Water & Process Technologies	2009
OW	COD			83	Petrobras	2013
	COD	522	92	82.4	Siemens Energy Inc.	2013
	COD	119.7	77.9	34.9	CH2M HILL	2016
	Ammonia (as NH ₃)			97	Petrobras	2013
	Ammonia (as NH ₃)	15	2	86.7	Siemens Energy Inc.	2013
	Ammonia (as N)	7.3	0.4	94.5	CH2M HILL	2016

2.4.2 New directions in desalter effluent treatment

The approaches discussed below have been reported at laboratory and pilot plant scale applied for the treatment of water from the crude oil desalting process and similar wastewater in other industries. Electrochemical methods; electro-photo-oxidation and electro-disinfection also are considered to be promising technologies²⁴. Microfiltration (MF), VSEP Membrane Filtration offers advanced, precise, and promising separation technologies for crude oil refining and processing.

2.4.2.1 Ion Exchange

New ion-exchange resins and zeolite materials are reported for the selective removal of specific heavy metal cations from wastewater. The use of clinoptilolite, another natural zeolite, for the removal of the soluble ammonium was reported⁸¹. However, the ion

exchange processes are limited by the difficult elution step and this operation needs to be improved to develop an easier, cheaper industrial process. In this instance, alternative technology is required. The use of a solid matrix for adsorption and ion-exchange of contaminants provides such an alternative. The volume of adsorbent material required increases proportionately with the solute load so that at higher solute concentrations, equipment size makes such processes economically unfeasible. Applications are typically limited to levels of contaminants in the ppm range. Synthetic ion-exchange resins have long been used in commercial scale applications for the softening or demineralization of water⁸².

This technique with combination of other separation methods was applied in oil refinery located in Texas, USA to achieve reducing its potable water consumption and wastewater disposal costs. A pilot study consisted of three-unit operations: ultrafiltration (UF), cation exchange softening (IX) and reverse osmosis (RO). These results indicated that the amount of discharged wastewater reduced by more than 50%⁸³. The major disadvantage of ion exchange is the need to regenerate the resin after use for recycling⁸⁴. This requires using a concentrated solution, often sodium chloride, to displace the heavy metals from the resin replacing them by either sodium or chloride ions as appropriate. This regeneration process produces a spent regeneration solution containing relatively high concentrations of heavy metals in brine that results in a costly disposal problem. Recent research has been investigating ways of reducing this regeneration problem. RenixUIX™ is modified ion exchange approach maximizes the power of separation, with 60% of conventional platforms operating expenses. This separation technique is combination of adsorption vessel with steady-state, uninterrupted resin regeneration.⁸⁵

2.4.2.2 Adsorption

Solid-liquid adsorption is a useful approach to remove heavy metals from desalter effluent. Many substances can be used as adsorbents for various metal ions. These include activated carbon, alumina, and silica gel. Activated carbon is quite frequently applied⁸⁶. Most heavy metals, (arsenic, mercury) can be removed by adsorption on carbon. To avoid reduced

capacity after regeneration, the carbon should be acid-washed prior to reuse. Commercial activated carbon is obtained from waste plant materials such as coconut shell, wood, coal, etc., often obtained locally thereby minimizing transportation costs. Studies have also shown that plant materials can be used to adsorb metals from aqueous solution and several laboratory studies have been carried out on industrial effluents. In addition, very inexpensive and readily available substances such as mineral slimes and fly ashes have also been suggested as adsorbents for aqueous metal ions.⁵⁸ Adsorption is a non-destructive process with the advantage of being simple, effective and adaptable to any treatment formats, and applicable for wide range of commercial products with an excellent ability to separate a wide range of contaminants⁸⁷. It can be applied for removal of heavy metals and salt from desalter effluent. This method had been investigated in the petroleum industry, but it has not been applied for desalter effluent too. Selenium (Se) concentrations was reduced by alumina adsorption media, to below these detection limits⁸⁸.

One major drawback of adsorption technologies, especially if it is dealing with removing toxic compounds and micro pollutants, is that the pollution is transferred from the aqueous to the solid phase and further disposal is still needed. Biological materials are effective at binding or adsorbing metals and toxic compounds in various solutions. These biological materials cover a wide range of species from shrubs and grasses to mosses, fungi, algae, and bacteria.^{58,84}.

2.4.2.3 Biological approaches

Desalter effluent contains phenol. Biological treatment can be effective for phenol or another hydrocarbon treatment. A previous study showed that the efficiency of biological methods employed in the sequencing batch reactor system at the plant was effective in the removal of total phenols from the effluents, with an average removal efficiency of about 98%. Additional removal capacity in reducing the level of total phenols is sorption by activated carbon with an average removal efficiency of 30%.⁸⁹.

The total Naphthenic acids (NAs) concentration in the desalter brine, decreased by 33 and 51% in PAC-free and PAC-containing mixed liquor microcosms, respectively⁹⁰. This method required to develop by manipulation operating parameter to achieve optimum biosorption. A drawback to biosorption is inconstant sorbent due to the selectivity and competitive of sorption from all the cations, ionic size, stability of bonds between metal ions and biosorbent⁹¹. Biological treatment removed 99.5 % of influent mercury in petroleum waste water while other approaches like sand filters and granular activated carbon adsorption removed mercury 80% ⁹². The MBR approach results demonstrated that the target parameters and compounds (BOD₅, COD, TSS, oil and grease, ammonia, thiocyanates and phenols) and benzo(a) pyrene and naphthalene were removed at range of 80 to 99 % within direct discharge limitations⁹³.

Some bacteria are useful in reduction pollution such as leptothrix ochracea, clonothrix putealis, siderococcus sp. and toxothrix thricogenes. These microorganisms, are added to a slow sand filter to eliminate iron and manganese from water by oxidizing the metals to precipitate able compounds⁵⁸. Biological materials such as fungi, algae, and bacteria are effective at adsorbing metals, including arsenic, present in various solutions. However, chemical reaction and microbial metabolism were responsible for the formation of the mineral deposits. However, microorganisms in this treatment possess high biodegradability capacity, efficiently eliminating biodegradable organic matter, NH₃, NH₄⁺, iron, reduces color well, high removal of biochemical oxygen demand and suspended solids. ⁹⁴

Some anaerobic bacteria reduce sulfate to sulfide as a part of their metabolic cycle, and such species are termed sulfate-reducing bacteria (SRB).⁹⁵ This process can remove heavy metals and toxic inorganic species to very low concentration levels with several advantages. It produces hundreds to thousands of times less sludge than conventional precipitation but the achievable sludge reduction levels and the full-scale capital and operating costs, are both site and waste-water dependent. ⁵⁸ Table 2-2 shows further research of different biological treatment to remove ammonia, nitrate, BOD, COD toxic metals and aromatic compounds in petroleum refinery wastewater plants and their residual concentration is within environmental standard limit of EPA for petroleum refinery effluents. These biological approaches are aeration (AIR), aerobic suspended growth

(ASG), Anaerobic Suspended Growth (ANSG), Biological Nutrient Removal (BNR), microfiltration (MF), Membrane bioreactor (MBR), Ion exchange (ION), Reverse Osmosis (RO), Equalization (EQ), Activated Sludge Digestion Model (ASDM), Dissolved air flotation (DAF), Oil water separation (O/W), Moving bed biofilm reactor (MBBR), Filtration (FI). However, these methods with current microorganisms in petroleum refinery plants were deteriorated by adding desalter effluent to the system. If biological treatments are still in the interest of petroleum refinery plants due to their low price and high performance, robust microorganisms are appropriate for removal of contamination.

2.4.2.4 Solvent extraction (liquid-liquid)

Solvent extraction is separation technique of removing organic solution from aqueous phase. This is a successful technology for metal recovery from large-scale operations where the concentrations of contaminants are high⁵⁸. Ethylene glycol can dissolve inorganic salts strongly. Glycol was taken as a solvent for extraction to separate the salts in crude oil in order to achieve highly efficient removal of salt from crude oil. The results showed that the optimum total desalination rate is 94%. When ethylene glycol is applied for separation, the extraction desalination does not require additional power and demulsifier, which saves the cost significantly. Ethylene glycol can be recycled, as it can be recovered from the alkoxide solution via adsorption and separation after extraction⁹⁶. However, the capital expense for the equipment can be costly, the required organic extractants is high volume and performance is often limited by hydrodynamic constraints such as flooding and entrainment. There is also the potential for cross contamination of the aqueous stream with the organic solution and allow the organic phase to recycling to treat more wastewater. For wastewater with low concentrations of metal ions, such technology is limited by the need for high aqueous to organic phase ratios and ion exchange will generally be preferred. High phase ratios lead to difficulties with the design of equipment, and organic losses through entrainment in the aqueous phase⁵⁸. It is not convenient at low toxic solute concentrations from effluent⁸⁷. Therefore, this approach is not appropriate to apply for desalter effluent.

2.4.2.5 Membrane technology

Reverse Osmosis (RO) and Ultrafiltration (UF) can apply for Removal of salt and water from the oil ^{26,27,58,97} and requires high energy^{87,98}. Membrane distillation (MD) was recommended for treating desalting effluents ⁵. There is a potential risk of contamination of distillate due to presence of volatile and toxic hydrocarbons ⁸⁷. VSEP is a new technology for Desalter Effluent in comparison with evaporators, clarifiers, or filter press units result in dramatic construction cost savings⁹⁹. The performance of a vibratory shear enhanced process (VSEP) combined with an appropriate membrane unit, MF, UF, and RO, for the treatment of the wastewaters ^{94,100}.

Nanofiltration (NF) is a promising technology for separation⁵⁸. The best effect on nanofiltration performance for desalter effluent was obtained by a nanoparticle concentration of 0.5% (wt)^{1,101}. However, it has low flow rate. Electrodialysis (ED) is another type of membrane that can remove some metal ions such as recovery of nickel ⁵⁸ and total organic carbon removal ⁹⁴. Emulsion liquid membrane (ELM) technology has been commercialized for removal of heavy metal cations and the removal of anions^{58,101}. The main drawbacks of ELM are poor long-term stability, rupture and swelling the membrane ^{102,103}.

2.4.2.6 Other separation technologies

Emerging membrane process was applied for desalter effluent using RO, UF and MD. This method was introduced as low energy usage, high flux, low fouling and low capital cost simple operation^{5,9}.

Activated sludge combined with membranes represents a promising process to reduce organic content at lower cost.⁵⁸ Electrochemical technologies successfully treated wastewater from the crude oil desalting process via electrochemical oxidation and degrade toxic organic and oil compounds into CO₂ and water^{22-24,58,94}. However this treatment contains and requires post-treatment to remove high concentrations of iron and aluminum

ions to avoid deposition on the electrodes⁹⁴. Bauxol method can be applied for removal of metal ions.

Bauxol (red mud) cannot be re-used but must be landfilled as industrial waste^{58,104,105}. This technology has not been applied for petroleum wastewater treatment.

Evaporation process can be performed through different techniques like falling film evaporation (FFE), multi-effect distillation (MED) or the multi-stage flash (MSF) and thermo-vapor compression (T- VC). These methods are applied for desalting. The major disadvantages of the techniques are expensive costs for high energy consumption¹⁰⁶ for high volumes of waste-water⁹⁴, high contamination load in the concentrates, scaling of the boiler and heat exchanger surfaces and potential contamination of the distillate preventing reuse due to presence of some VOC or hydrocarbons in the waste-water^{20,58,107}.

Photocatalytic degradation has been introduced to be a highly effective treatment technology. This technique in comparison to other advanced oxidation processes (AOPs), such as homogeneous photo-Fenton, UV/H₂O₂, UV/O₃, UV/H₂O₂/O₃¹⁰⁸ has complete mineralization and high COD removal¹⁰⁹⁻¹¹¹. Catalyst has inhibition for high COD concentration⁵⁸. Treatment specified wastewater by TiO₂ is more expensive than photo-fenton and UV¹⁰⁷. TiO₂ needs high cost for running and produce dioxins and other pollutants⁹⁴.

2.4.3 Economy and energy requirement

There are only a few studies in desalter effluent globally, the number and capacity of industrial desalination plants are 7757 with 28, 8 m³d⁻¹ respectively¹¹² and the industrial Brine effluent is 27.4 m³d⁻¹¹¹². Table 2-3 shows the energy requirements for the different desalination processes. However, different method with pros and cons including operation cost, energy consumption, and capital expense, were discussed in this review earlier. Thermal and membrane desalination procedure operations consume heat and electricity for evaporation and process flows by high pressure flow respectively Table (2-3). RO

consumes less energy in comparison with MSF, MED, and VC⁹⁸. Due to high energy consumption, biological treatment of wastewater has become an attractive desalination alternative because it demands lower energy than RO.

The energy consumption, in desalination processes, depends on variety of factors, such as feed water concentration of salts, temperature of operation in membrane processes, performance ratio, heat losses by convection and radiation from the top and bottom of the cell, etc, for thermal processes. Thermal processes that rely on a change on water phase (MED, MSF), involve higher energy consumption than processes that do not require a change of phase Table (2-3). However thermal processes can utilize exhaust steam from turbines for electrical generation, solar system or hot gases from diesel engines or geothermal energy and so are economically attractive and comparable with RO energy cost.

Table 2-3: Equivalent electrical energy consumption for major desalination processes ⁵³

Process	Steam energy (kWh/m ³)	Electrical energy (kWh/m ³)	Equivalent electrical energy (kWh/m ³)
MSF (Multi-Stage Flash Distillation)	7.5–11	2.5–3.5	10–14.5
MED (The multiple effect distillation)	4–7	2	6–9
VC	–	7–15	7–15
SWRO (Seawater reverse osmosis)	–	4–6 (with energy recovery) 7–13 (without energy recovery)	4–6 (with energy recovery) 7–13 (without energy recovery)
BWRO (Brackish water reverse osmosis)	–	0.5–2.5	0.5–2.5
ED	–	0.7–2.5	0.7–2.5

2.4.3.1 Operating and maintenance costs

Operating and Maintenance Costs (O&M) costs consist of fixed costs and variable costs. Fixed cost or investment cost is insurance and amortization (0.5% and 5-10% of the total capital cost respectively). Variable of cost includes energy requirements (11- 44%), labor (4-9%) and process consumables including chemicals (3-10%) and maintenance (12-16%)^{113,114}. Table 2-4 describes the total costs of the major desalination technologies for applying sea water and brackish water. Capital cost of different separation technologies was obtained from IDA Worldwide Desalting Plants Inventory Report¹¹⁵. The maintenance includes pre-treatment, periodic cleaning of the system, replacement of mechanical equipment and control instruments. The membrane processes require membrane replacement, which constitutes a major cost factor. Chemical requirements for pre-treatment and post-treatment depend on the feed water quality. Distillation processes require fewer chemicals for the feed water pre-treatment than membrane processes. Labor requirements are more or less the same for both distillation and membrane process. Generally, O&M costs are less for thermal processes¹¹⁶.

Table 2-4: Total specific costs of the major desalination processes

Process	Investment (\$m ⁻³ day ⁻¹)	Energy (\$m ⁻³)	Consumable (\$ m ⁻³)	Labor (\$ m ⁻³)	Maintenance (\$ m ⁻³)	Total O&M costs (\$ m ⁻³)
MSF	1120-2240	0.67- 2	0.03-0.10	0.03-0.22	0.02-0.07	0.76-2.41
MED	1000-2000	0.42-1.25	0.02-0.17	0.03-0.22	0.02-0.07	0.50-1.71
VC	1000-2800	0.63-2.7	0.02-0.17	0.03-0.22	0.02-0.09	0.71-3.17
SW-RO	890-1790	0.34-1.43	0.10-0.28	0.03-0.22	0.02-0.06	0.52-1.99
ED	297-367	0.07-0.45	0.06-0.15	0.03-0.22	0.007-0.01	0.16-0.83

2.4.3.2 Fresh water supply cost

Average water supply costs in various countries are shown in Table 2-5. Some of the European countries have to pay much higher water prices than other developed countries due to different contexts including policy, economic and environmental. Water prices are heavily subsidized in some countries such as China and India¹¹⁷. This promotes changes

in user behavior mainly irresponsible use of the clean water. An ideal water pricing policy should also provide to encourage efficient resource utilization leading to reduce pollution and protect resource. According to a recent water tariff survey by Global water intelligence in 2014, global water costs have risen by 4.3% an average cost of \$2.14 m⁻³ for water and wastewater services combined ¹¹⁸. The price of water and wastewater services is growing fast in the US, which saw average combined tariffs rise by 7% in 2014 for reviving aging infrastructure and combatting the water scarcity due to drought especially in California ¹¹⁹. A study estimated costs of the transported freshwater from coastal desalination plants ¹²⁰. The water supply cost for the city of Beijing in China from the nearest ocean source located at a distance of 135 km was estimated as \$1.13m⁻³ (Table 2-5). Similarly, for transportation distances of 1050 km from Delhi, India transported desalinated water costs will be \$ 1.90. Since the desalinated water costs have reached to the levels of conventional water supplies in recent years, the difference is acceptable, but the transportation costs will be unavoidable. The dedicated costs for the transportation distance must be considered as a part of total cost and the water must be supplied to the communities at any cost.

Table 2-5: Comparison of water costs for conventional and transported desalination water supply options

	Water supply cost(\$/m³) ¹¹⁸		Transport of desalinated water cost ¹²⁰
Canada	0.31 \$	China	1.1-1.4 \$; 135 km
USA	0.4-0.8 \$	USA	1.34 \$; 280 km
Spain	0.47 \$	Spain	1.36; 163 km
Sweden	0.69 \$	India	1.90 \$; 1050 km
UK	1.3 \$	Yemen	2.38 \$; 135 km
Germany	2.16 \$	Brazil	1.33 \$; 240 km

2.4.3.3 Desalinated water cost by using current technologies

The desalination systems have been categorized to three: domestic, small-scale, and large-scale systems. A domestic desalination system can be considered for the freshwater needs with capacity of less than $1\text{ m}^3\text{ day}^{-1}$. A small-scale desalination system can be considered for small populations in rural areas, small villages up to 10,000 people for the freshwater needs only with the range of a capacity between $1\text{--}1000\text{ m}^3\text{ day}^{-1}$. A large-scale desalination system can be considered for cities and towns where the electricity costs are reasonable, and the volume is between 1000 and $100,000\text{ m}^3\text{ day}^{-1}$. Table 2-6 presents representative production costs for different desalination capacities $> 100\text{ m}^3$.

From Table 2-6, it can be noted that membrane processes are used for small to medium size desalination capacities and thermal processes for large size desalination capacities. The desalination cost is lower for higher desalination capacities whether they are powered by conventional energy or renewable energy. However, considering high capital costs required for renewable energy sources for large-scale applications, thermal processes may be considered where the cost for thermal energy is attractive as in the case of Middle Eastern countries.

For example, an MSF process of capacity $528,000\text{ m}^3\text{ day}^{-1}$ produces desalinated water at a cost of $\$0.42\text{ m}^{-3}$. The desalination cost can be reduced by 15% if the MSF unit is combined with an RO unit for the same production capacity¹²¹. In dual-purpose plants (cogeneration), the desalinated water cost can be minimal or as low as $\$0.08\text{ m}^{-3}$ ¹²² in Bahrain (Table 2-6). A hybrid NF–RO–MSF–crystallization unit can produce desalinated water at a cost as low as $\$0.37\text{ m}^{-3}$ ¹²³. Similarly, pre-treated wastewater can be recovered using membrane processes for reuse at costs much lower than conventional seawater desalination. The recovered water can be recommended for other potable uses except drinking, cooking, and personal hygiene needs.

Table 2-6: Desalination costs for different desalination processes based on capacities.

	Desalination process	Capacity (m ³ /day)	Energy source	Energy cost (\$/kWh)	Desalinated water cost (\$/m ³)	Reference
Small-scale applications	Reverse osmosis	250, 300, 350, 500, 600	Diesel generators	0.07, 0.06, 0.07	1.25-3.21	¹²⁴ , ¹²⁵ , ¹²⁶
	VC	1000, 1200	Conventional		1.51, 3.22	¹²⁷ , ¹²⁸
	VC	3000	Conventional		0.7	¹²¹
	MED	20,000	Conventional		0.88	¹²⁹
	MSF	20,000	Natural gas		1.6-2.02	¹²⁹ , ¹²²
Large-scale applications	Dual-purpose MSF	20,000	Natural gas/steam	0.0001	0.08	¹²²
	Reverse osmosis	2000 - 50000	Diesel generator	0.06, 0.05	0.86-2.23	¹²⁵ , ¹²²
	Reverse osmosis	95,000, 100000	Conventional		0.83, 0.43	¹³⁰
	Reverse osmosis	100–320 × 10 ³	Conventional		0.45–0.66	¹²¹
	MED	91–320 × 10 ³	Conventional		0.52–1.01	¹²¹
	MSF	23–528 × 10 ³	Conventional		0.52–1.75	¹²¹

2.5 Review of microorganism for desalter effluent treatment

Two microorganisms were candidates to be investigated for biological treatment of petroleum desalter effluent; i.e. yeast *Debaryomyces hansenii* strain (LAF-3 10 U) and green microalga *Parachlorella kessleri*, strain CCALA 255. The biotechnology of these microorganisms is described below:

2.5.1 Biotechnology of halotolerant yeast *Debaryomyces hansenii*

2.5.1.1 Microbiology

Debaryomyces hansenii is a unicellular, strongly halotolerant (0-24%(w/v) NaCl, heavy-metal-resistant yeast widely distributed in nature¹³¹⁻¹³⁵. This organism is osmotolerant and does not adversely affect macromolecular structure and function which has led to the introduction of the concept of compatible solute.^{133,136} All *Debaryomyces* species are haploid yeasts (*a cell that contains a single set of chromosomes*) that reproduce vegetatively by multilateral budding.¹³⁷ It has a halo-xerotolerance trait (tolerant of dry conditions) and shows a broad spectrum of carbon source assimilation and fermentation¹³⁸.

2.5.1.2 Source

Debaryomyces hansenii is one of the most common yeast species in nature and isolated from food such as dairy products, including soft, brine, and all types of cheese^{137,139-141}. *D.hansenii* is a marine yeast, and it can be found in salty food and brine including and in various types of cheese¹⁴² wine, beer, and meat^{134,137}. *Debaryomyces hansenii*, is a cosmopolitan species in aquatic ecosystems and the most common fungus in marine environments because of its broad salinity tolerance and ability to utilize a wide range of carbon sources.¹⁴³

2.5.1.3 Characteristics

This yeast has high respiratory and low fermentative activity. Growth, fermentation and respiration of this yeast are limited when KCl and NaCl is more than 1 M¹⁴⁴. However, another study has been reported that *D.hansenii* can grow in saline media containing up to

4M NaCl¹³⁷. *D.hansenii* can grow in a wide range of pH between 3 and 10¹³⁷ and temperature (20°C-35°C)¹⁴⁵ but growth up to zero °C has been reported.¹³⁷

2.5.1.4 Applications of *D.hansenii*

D. hansenii has been reported to metabolize n-alkanes and benzenoid compounds such as phenol, dihydroxybenzenes (catechol, resorcinol) and dihydroxy- benzoic acids¹⁴⁶. Earlier, Cerniglia and Crow¹⁴⁷; in 1981 reported oxidation of more saturated polyaromatic hydrocarbons, naphthalene, benzo(a)pyrene and biphenyl, by this organism. Interestingly, the ability of ascomycetous yeasts to assimilate phenol and n-alkylamines has been reported to be correlated with n-alkane assimilation.^{148,143} *D.hansenii* has an ability to accumulate lipids in salt stress. In high salt condition, the intracellular salt level of yeast is not sufficient to make an osmolarity balance with media. To resolve this crisis condition, yeast accumulate glycerol and polyhydroxyalcohol that are the basic unit of lipids in triglyceride^{131,149}. *D.hansenii* was recognized as a source of high capacity to accumulate lipids. There are more than 600 yeast species and lipid accumulation characteristic is found in less than 30 of them^{150,151}.

2.5.2 Biotechnology of *Parachlorella kessleri*

2.5.2.1 Microbiology

The green microalgae genus *Chlorella* is one of the most important commercial microalgae¹⁵². A taxonomy of the genus *Chlorella* was published by Fott & Novakov A (1969)¹⁵³⁻¹⁵⁵. This microalgae in some characteristics resembles *Chlorella vulgaris*. *Chlorella kesslerii* was formerly *Chlorella vulgaris*.¹⁵⁶ It was reported that it is one of species in taxonomy of *Chlorella* including *vulgaris*, *C. lobophora*, and *C. sorokiniana*. Later on, the *Chlorella* genus was reduced to *C. vulgaris*, *C. lobophora*, and *C. sorokiniana*. The new phylogenetic studies *C. kesslerii* belonged to the new genus *Parachlorella*

(Chlorophyta, Trebouxiophyceae)¹⁵². *Chlorella kessleri* is freshwater, non-motile, unicellular green algae (eukaryote)^{155,157,158} (2-10 μm).¹⁵⁹ These species are easily cultured in the laboratory as they reach exponential growth 3-4 days after inoculation. Some strain of Para *Chlorella Kessleri* such as ATCC 11468, CPCC 266, and 262 misidentified at the genus or species level in *Chlorella vulgaris*^{152,158}

2.5.2.2 Characteristics

Most of the strains in the genus *Chlorella* are acid tolerant and salt tolerant. They have limited growth at pH 2.0 - 2.5 and NaCl 4 - 5 % (wv). And temperature between 34–36°C.^{153,160} Extracted cell walls of *C. kessleri* strongly resemble that one's of *C. vulgaris*¹⁵⁴. The author cultivates this microalga at room temperature. *P.kesslerii*, grows faster in comparison to other microalgae. The trend of cell growth vs time in other studies demonstrates *P.kesslerii* can grow faster in first 4 to 6 days¹⁶¹. *P.kesslerii* grow in the range pH between 7-8, the range of absorbing pb increased.¹⁶²

2.5.2.3 Application of *Parachlorella kessleri*

The main market for *Chlorella* is human nutrition, the dried biomass being processed as powder, capsules, or tablets.¹⁵² *C. kessleri* are capable to transform toxic metals such as selenium to organic compounds and of producing selenomethionine^{156,163}. Media contain SE between 1.6 to 46.9 ($\mu\text{g l}^{-1}$) has been up taken and reduced from 0.1 to 10.62 ($\mu\text{g g}^{-1}$)¹⁶⁴. The significant growth of *C.kessleri* over a wide range of free Zn (16pM to 1.6 M) indicated a high tolerance of *C. kessleri* to zinc¹⁶⁵. Microalgae, *Chlorella kessleri* absorbs Pb (lead)^{157,158,166–170}. Literature shows this microalga can uptake other metal ions such as Cd and Cu^{171–173}, Ni¹⁷⁴, Zn¹⁷⁵ and Ca¹⁷⁰. Some *Chlorella* strains including *Parachlorella kessleri*, strain CCALA 255 green algae (Chlorophyta) grown under optimal condition under limitation and deficiency of nitrogen, sulfur or phosphorous, the biomass accumulates and produces lipid up to 10-60% DW^{176–178}.

2.6 Conclusion

In this review, all physical, chemical and biological separation and treatment methods in the petroleum industry were investigated. There are two potential solutions to solve the challenge and treat desalter effluent. The first solution is to desalinate the desalter effluent and to be discharged into the wastewater treatment plant. Second alternative approach is to treat desalter effluent in a separate process.

The price of freshwater transportation is less than the cost of desalinated effluent process (Freshwater in Canada $0.31 \text{ } \$\text{m}^{-3}$, desalination ($0.52\text{-}2.41 \text{ } \m^{-3}). This approach for desalting desalter effluent will be costly. It can be emphasized that desalination and water reuse technologies limits tremendous potential for efficient utilization of impaired and saline water sources. However, high energy and cost-related issues should be addressed with innovative, energy-efficient and cost-effective technologies that are socially acceptable and environment-friendly.

Numerous technologies designed to limit polluting components from saline effluents which contain a high concentration of salt and heavy metals. Each technique only applies to certain pollutants in the waste stream, which is required to emerge several techniques as a complementary or combined application for removal of suspended solids, oil, ions and other components in a particular effluent. Before designing the method and techniques, it is important to define the characteristic effluents of the desalter effluent and to study the most appropriate technologies for the industry. Efforts should be continued to minimize energy demand and maximize resource utilization. Some effective and novel technology is recommended to be installed in new facilities. Petroleum refinery plants with old facility requires to optimize desalter effluent with minimum change due to the expense of installation. Naturally, the technical and economic considerations of the challenge must be noticed such as a load of effluent, production rates, treatment plant capacities. It is essentially significant to ensure that the treated effluent will not have any negative effects on the environment, and the quality of the treated desalter effluent. Biological treatment

has excellent potential with major challenges to be overcome. There is still a need for better engineering design and innovation.

We found two robust and halotolerant microorganisms have been chosen to treat desalter effluent efficiently with opportunity to have alternative biofuel. We provided further information about the result in the next reports.

Chapter 3

3 Investigation of Growth Kinetics of *Debaryomyces hansenii* (LAF-3 10 u) in Petroleum Refinery Desalter Effluent

3.1 Introduction

The process water from petroleum refineries commonly contains a large quantity of desalter effluent¹. Due to the presence of BTEX (benzene, toluene, ethyl benzene, and xylenes), phenol, dissolved inorganic compounds and minerals, the desalter effluent is required to be treated before being discharged into the environment¹⁷⁹. Many regulatory bodies such as Canada and the USA have imposed requirements that refinery effluent must be treated to meet acceptable standards^{80,180}. In addition, recent concerns with fresh water shortages in the developing world and the demand for relatively high volumes of raw water in the refinery have increased the pressure to recycle and/or reuse water¹⁸¹. In the past few years, several water treatment techniques have been investigated to treat refinery effluent streams e.g., biodegradation, adsorption, ion exchange, electrochemical separation, flotation and oxidation¹⁸². Desalter effluent could potentially be used as a source of recycled water after the oil content is removed below 120 ppm according to Refinery Liquid Effluent Regulations, CRC 828¹⁸⁰ and may provide a cost-effective approach for water reuse in refineries.

Debaryomyces hansenii is an osmo-tolerant and halo-tolerant yeast that can be found in many habitats with low water activity, such as sea water, cheese, meat, wine, beer, fruit and soil and as well in high-sugar products¹³⁷. *D.hansenii* has a high ability to degrade

phenol¹⁸³ as a sole carbon and energy source¹⁸⁴. In addition, a number of phenol derivatives are metabolized by this yeast¹⁸⁵. The effect of several environmental factors such as medium composition, pH and temperature on the growth of *Debaryomyces* cells has been previously explored^{186,187}. This yeast grew well in mineral wastewater containing carbon sources and supplemented by NaCl or KCl¹⁴⁴. *D. hansenii* strains are able to produce the volatile compounds e.g., mainly ester compounds, ethyl and methyl esters, sulfur, alcohols, aldehydes and ketones¹⁸⁸⁻¹⁸⁹. It was shown that the yeast can grow in oil mill wastewaters with (NH₄)₂SO₄¹⁹⁰. Thus, the growth of this yeast on desalter effluent offers strong potential for petroleum wastewater treatment.

Many substances found in desalter effluent potentially inhibit the growth of microorganisms. The specific growth rate of microorganisms increases with an increase in substrate concentration to a threshold level. Above this, the growth rate decreases with increase in initial substrate concentrations. Several unstructured mathematical models have been discussed in literature which describe substrate inhibited growth kinetics¹⁹¹. The Andrews model¹⁹², based on specific growth rate, is one of the most commonly used models due to its mathematical simplicity and wide acceptance for describing the substrate inhibition kinetics of microorganisms. The Andrews inhibitory growth kinetic equation¹⁹³ Equation (3-1) is as follows:

$$\mu = \frac{\mu_{max}S}{K_s + S + \frac{S^2}{K_I}} \quad (3-1)$$

where K_s , K_I , μ , μ_{max} , and S are the saturation constant (mgL⁻¹) (substrate-affinity constant), substrate inhibition constant (mgL⁻¹), specific growth rate (h⁻¹), maximum specific growth rate (h⁻¹), and substrate concentration (mg L⁻¹), respectively.

Aiba ¹⁹⁴ proposed an alternative semi-empirical model to express microbial growth inhibition rate as given by Equation (3-2) (where the symbols have the same meaning as in Equation 3-1 above):

$$\mu = \frac{\mu_{max} \frac{S}{K_I}}{K_S + S} \quad (3-2)$$

Another unstructured mathematical model proposed by Edward ¹⁹⁵ to predict substrate inhibition at higher substrate concentration as given by the equation 3-3 (the symbols have the same meaning as in Equation 3-1 above):

$$\mu = \mu_{max} [e^{\frac{-S}{K_I}} - e^{\frac{-S}{K_S}}] \quad (3-3)$$

In this study, *D. hansenii* yeast was investigated for the first time to understand its growth on desalter effluent and for phenol removal which is one of the major components of desalter effluent. The experimental results were simulated using the above described models to identify a suitable kinetic model.

3.2 Materials and methods

3.2.1 Materials

Debaryomyces. hansenii SWING YEAST LAF-3 was provided by Parmalat Inc (London, Canada). The desalter effluent water was supplied from an Imperial refinery operation. All

chemicals used in this study were analytical grade and purchased from Sigma Aldrich (Oakville, Canada).

3.2.1.1 Preparation for growth medium

In this present study, two types of growth media were prepared for yeast cultivation. The first medium (real desalter effluent) contained: total ammonia 13 mg L^{-1} ; total chemical oxygen demand (COD) 1200 mg.L^{-1} ; orthophosphate (P) 0.22 mg L^{-1} ; phenols-4 AAP 2.1 mg L^{-1} ; total phosphorus 0.48 mg L^{-1} ; total potassium (K) 0.013 mg L^{-1} ; and total sodium 600 mg L^{-1} . The second synthetic growth medium (synthetic desalter effluent) was prepared as follows: phenol COD $120\text{-}4000 \text{ mg L}^{-1}$, $(\text{NH}_4)\text{Cl}$ 60 mg.L^{-1} ; K_2HPO_4 30 mg.L^{-1} and NaCl 1 g L^{-1} . Both of the growth media were additionally supplemented with $(\text{NH}_4)\text{Cl}$ 60 mg L^{-1} and K_2HPO_4 30 mg L^{-1} . The pH of the two growth media was adjusted to 5.5-6.0. Both of the growth media were autoclaved at 121°C for 20 min prior to yeast cultivation.

3.2.1.2 Shake flask experiments

In this study, the shake flask experiments were carried out as follows. The yeast cells were first transferred into fresh yeast extract peptone dextrose (YEPD) agar slants and then incubated at 28°C for 24 h. After that, the cell cultures were inoculated into 250 mL Erlenmeyer flasks containing 50 mL of YEPD medium. The flasks were incubated at 25°C for 24 h with a shaking speed of 180 rpm. The optical density of cell cultures (550 nm) was measured every two hours. After the optical density reached around 1, *D.hansenii* cells, which were at the late exponential growth phase, were inoculated into flasks (at 5% v/v) containing prepared synthetic or real desalter effluent as described earlier. The culture was cultivated in a rotary shaker (VWR, Mississauga, Ontario, Canada) at 25°C and 180 rpm. The yeast growth was carried out for 72 h and samples were withdrawn from the test cultures at intervals of 4 h. The residual concentrations (COD) of phenol and culture

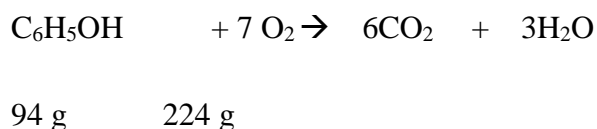
turbidity (OD_{550}) were measured to examine cell growth in the presence of different concentrations of phenol and salt.

3.2.2 Analytical methods

The cell concentration was measured using the optical density (OD) of cell culture. The OD was measured using a spectrophotometer (50 Bio, UV-visible, Evolution 60S, Thermo) spectrophotometer at 550 nm.

3.2.2.1 COD measurement

The chemical oxygen demand (COD) was used as a measure of substrate concentration. For experimental determination, the microbial culture from the shake flasks were filtered through a 0.2 μm filter paper (Whatman, Michigan, USA) to remove the cells. The remaining filtrate was then used for COD analysis using Hach 8000 (Hach Inc, Loveland, USA). The initial COD of phenol in this study was the theoretical COD based on the equation:



Thus 1 g of phenol has a theoretical COD of 224/94 or approximately 2.38 g.

3.2.2.2 Mathematical modelling of growth kinetics

The specific growth rate (μ) value was calculated for the exponential phase in each growth curve using Equation 3-4 below.

$$\mu = \frac{\ln \frac{X}{X_0}}{t} \quad (3-4)$$

where X_0 and X indicate the initial biomass and the biomass at time t , respectively.

3.2.2.3 Relationship between optical density and dry weight

Dry weight and optical density of *D.hansenii* biomass in different dilution of samples were measured. The equation (3-5) shows a linear equation between OD₅₅₀ and Dry weight with R-squared of 99%.

$$\mathbf{D.W = 6.88 OD_{550} + 3.47} \quad (3-5)$$

D.W demonstrated dry weight of yeast *D.hansenii* (mgL⁻¹) and OD is optical density of cell in desalter effluent at wave length of 550 nm.

3.2.2.4 Modeling the kinetics of simulated desalter effluent

The growth of *D.hansenii* in simulated desalter effluent was examined using three different unstructured mathematical models described earlier. Data fitting was carried out using nonlinear regression method using MATLAB (R2017b).

3.3 Results and discussion

Growth kinetics of *D.hansenii* on simulated desalter effluent

Desalter effluent is a major source of contaminated wastewater effluent in the refinery and

can contains hydrocarbon emulsions, heavy metals, salts such as chlorides and carbonates, suspended solids, hydrogen sulfide (H₂S), ammonia, and phenolic compounds. Due to the presence of a large number and variety of organic contaminants, chemical oxygen demand (COD) measurement is an appropriate approach to describe the level of organic contaminants. Previously, few studies have conducted to evaluate the effect of COD on the growth of *D. hansenii*.

Therefore, in this study, the growth kinetics of *D.hansenii* were investigated in the simulated desalter effluent containing COD in the range of 120 and 4000 mg L⁻¹. Figure 3-1 describes the growth kinetics in the simulated desalter media. Phenol was used as the substrate to simulate the COD in the simulated desalter effluent and in order to elucidate the growth kinetics of the yeast in a well-defined medium with known substrate. As seen in Figure 3-1, the cell concentration increased with increasing initial COD from 120 to 900 mg L⁻¹. The cell growth is dependent on the amount of organic carbon substrate and very little growth was observed at 120 to 300 mg L⁻¹ initial COD. At higher CODs, the cell concentration increases rapidly then growth slows as COD increased beyond 1200 mg L⁻¹ indicating substrate inhibition by phenol. Several microorganisms including yeast can utilize aromatics as carbon energy sources. Previously it was reported that the yeast *Trichosporon cutaneum* utilizes an ortho oxidation pathway of the benzene moiety¹⁹³. Several inducible enzymes are involved which are suppressed by excess concentrations of the substrate leading to reduction in the cell growth. Similarly, Hill and Robinson¹⁹⁶ reported on bacterial inhibition by phenol and applied a substrate inhibition model to simulate the growth kinetics. Yan et al.¹⁹⁷ investigated the yeast *Candida tropicalis* (obtained from activated sludge) for phenol degradation. Substrate inhibition was noted with an increase of phenol concentration over a threshold concentration. While several studies have appeared on phenol biodegradation by yeasts and bacteria, very limited or no studies have been published on microbial growth kinetics of *Debaryomyces hansenii* using phenol as the carbon source. An understanding of growth kinetics can provide a fundamental knowledge for better design of petroleum or other aromatic effluent treatment systems.

An average specific growth rate was obtained for the exponential phase of each growth

curve in Figure 3-1 and this was plotted against initial phenol COD as in Figure 3-2. As seen in Figure 3-2, the specific growth rate increases to a maximum then decreases as the initial COD increases which is consistent with the data in Figure 3-2. These values of μ versus S were applied for the model simulations and are discussed below.

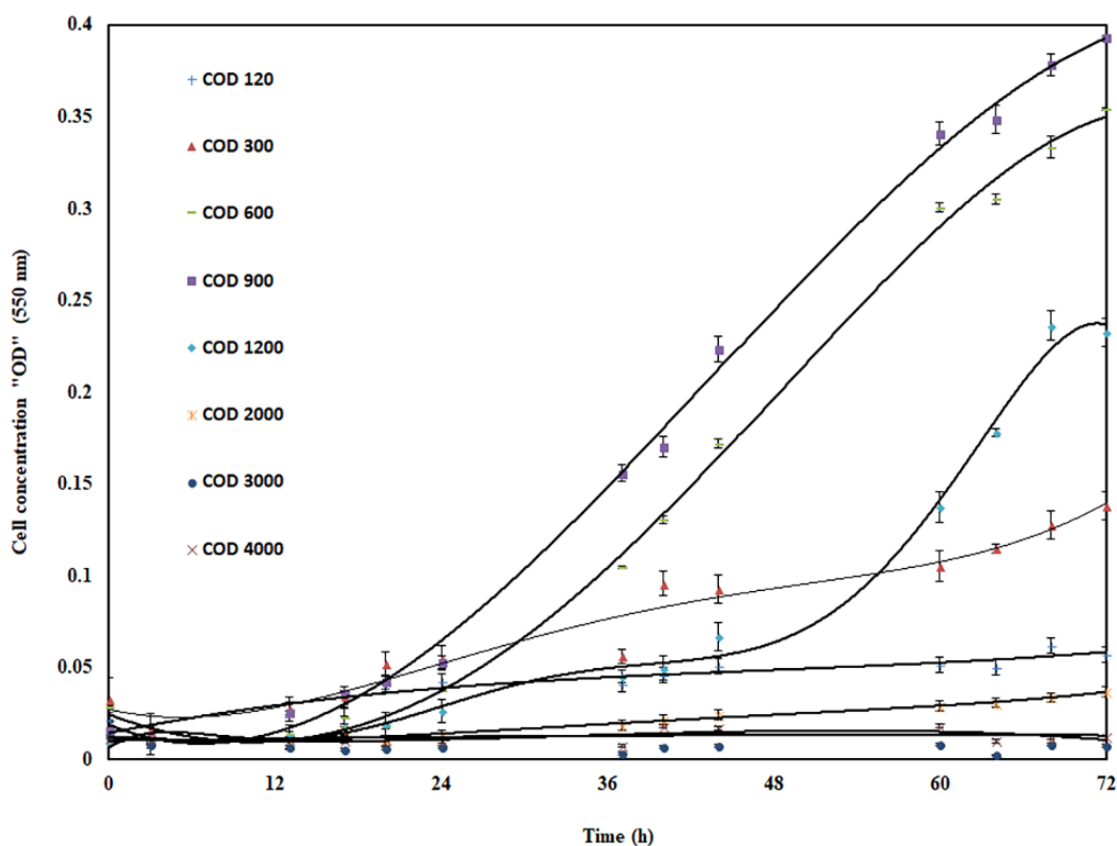


Figure 3-1: Growth kinetics of *D.hansenii* in high-salt media in simulated desalter effluent at various COD values (120-4000 mg L⁻¹).

3.3.1 Investigation of kinetic models

Three different unstructured models, the Andrews model Equation (3-1), Aiba Equation (3-2) or Edward model Equation (3-3) were applied to simulate the batch growth kinetics.

Non-linear least squares regression was applied by varying the three model constants μ_{\max} , K_s and K_I . Figure 3-3 shows the plot of model simulations using the best available fit with experimental data of specific growth rates. As seen in Figure 3-3, the Aiba and Edward model which have similar exponential terms produced almost identical results while the Andrews equation predicted higher specific growth rates for initial COD values of 2500 mg/L or higher. Table 3-1 shows the best fit parameters μ_{\max} , K_s , and K_I . Since different combinations of model parameters can be applied to model experimental data in the response space, it was important to calibrate the obtained results with reported literature in order to select the most appropriate mathematical growth kinetic model.

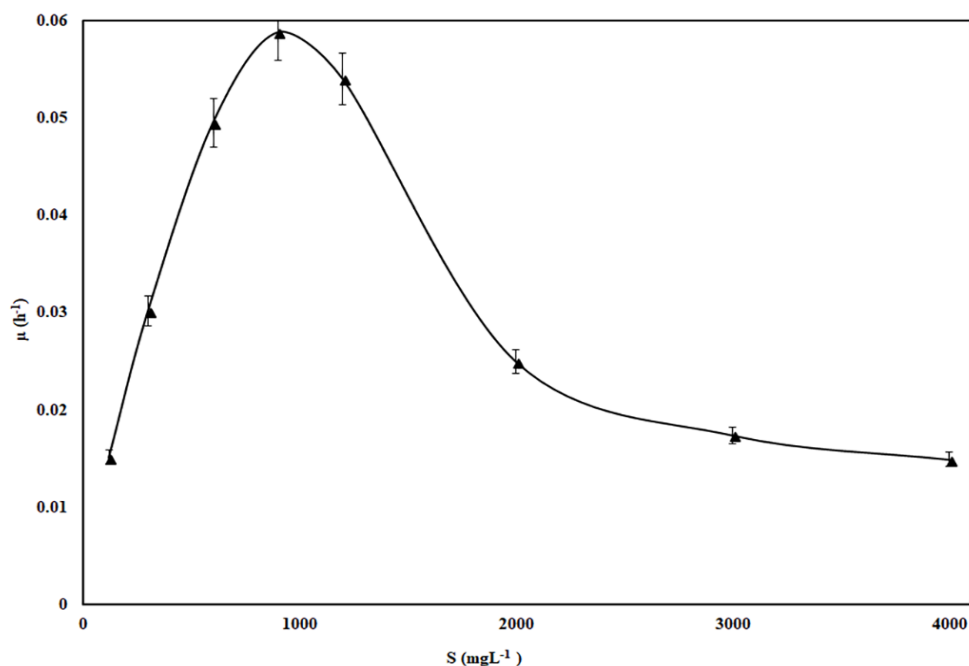


Figure 3-2: Average specific growth rate as a function of COD for a range of COD values in simulated desalter effluent containing 1g L⁻¹ sodium chloride solution.

Previously Prista et al.¹⁹³ examined the specific growth rate of *Debaryomyces hansenii* in the presence of different salts and varying concentrations. They found the specific growth rates to be in the range of 0.02 to 0.24 h⁻¹ at salt concentrations up to 2.5 M. Thus in our

case (at a salt concentration of 0.02 M), the Edward model most realistic simulates the experimental data and is an appropriate kinetic model to represent the growth of the *D. hansenii*.

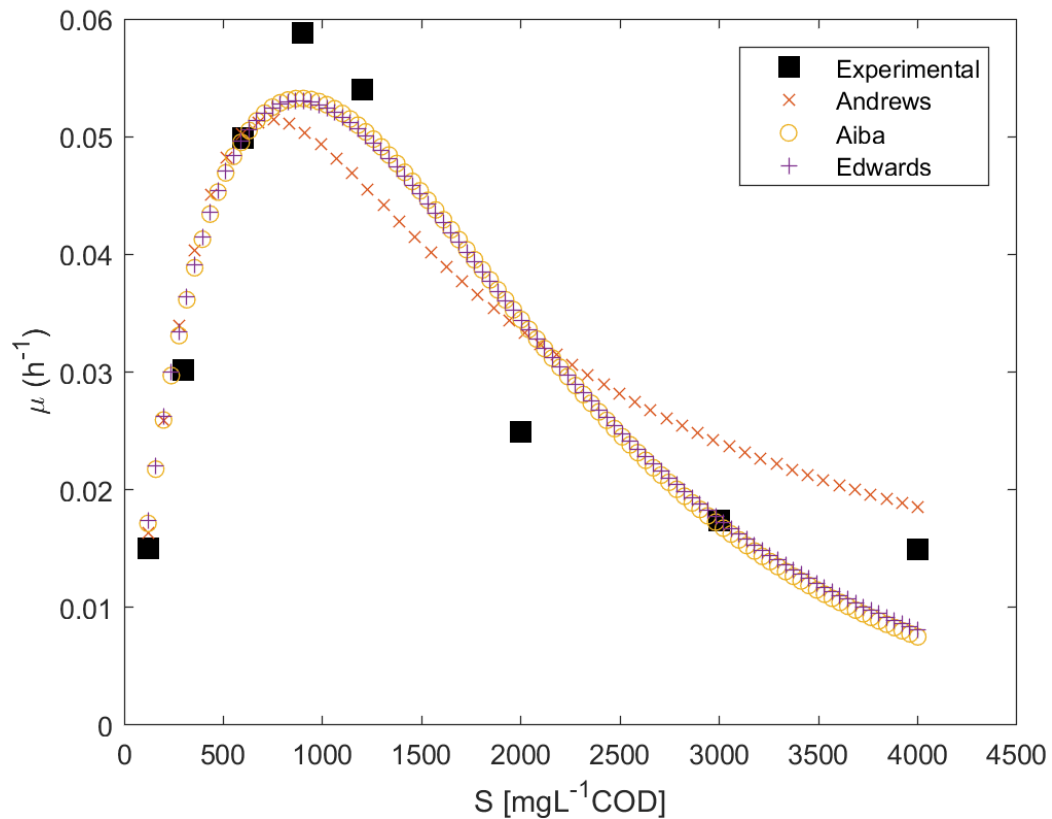


Figure 3-3 : Experimental and model simulations for specific growth rate of *D.hansenii* growth in 1 g L^{-1} salt as a function of initial COD using Andrews, Aiba and Edward models (Equations 3-1). (The line represents different kinetic models using least squares non-linear regression and exponential curve fitting (MATLABTM)).

Table 3-1: Best-fit biokinetic constants using non-linear regression with three different unstructured models applied to *Debaryomyces hansenii* cultivation on synthetic desalter effluent degradation compared to reported literature values.

Kinetic Model	$\mu_{\max}(\text{h}^{-1})$	$K_s (\text{mg L}^{-1})$	$K_I (\text{mg L}^{-1})$
Andrews	11.31	81136.6	6.647
Edward	0.210	633.95	1263.61
Aiba	0.998	6187.8	1108.3

3.3.2 COD removal rates in simulated desalter media

Figure 3-4 describes the COD removed as a function of initial COD of the simulated desalter effluent. At low initial CODs, the COD removal was approximately 50%. As the initial COD increased to above 300 mg L⁻¹ the COD removal rate was greater than 80%. Above an initial COD of 1200 mg L⁻¹, the COD removal rate decreased due to the phenol substrate inhibition of growth. This figure provides useful data for the range of CODs in a desalter effluent in order to achieve high COD removal. These results were reexamined by cultivation of the yeast in real desalter effluent media.

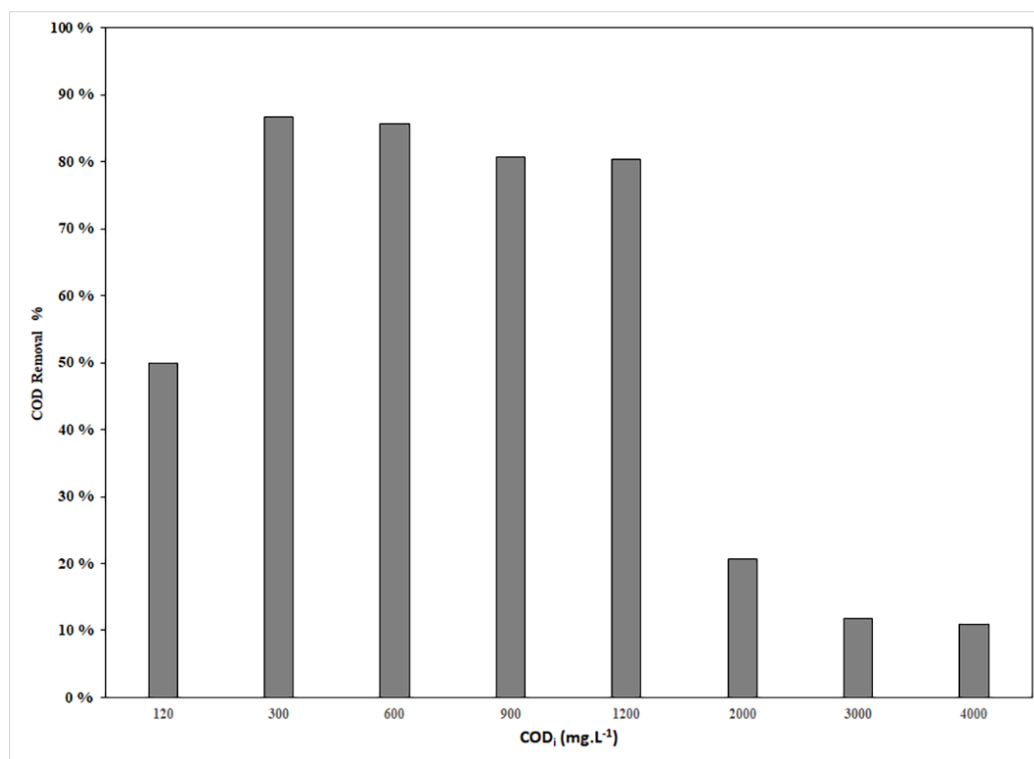


Figure 3-4: Various Phenol COD removal by using *D.hansenii* cultivation in simulated desalter effluent in 1 g L^{-1} NaCl.

3.3.3 Investigation of growth kinetics in real desalter effluent media

Figure 3-5 describes the growth of *D.hansenii* in actual desalter effluent. The cells grew well in the undiluted effluent with a COD of around 1200 mg.L^{-1} . The cell concentration obtained was lower at lower CODs. This trend agrees with the simulated desalter experimental results as the specific growth rate decreases with decreasing initial COD. As mentioned previously, there are many organic compounds present in a real desalter effluent. While COD is a measure of the total organic loading, not all the COD may contribute to biodegradability. There may be also more toxic effects due to other compounds present in the complex environment of the actual desalter effluent. Thus realistically a biochemical oxygen demand (BOD) may provide a better description of cell cultivation in real media. This should be examined further in other studies.

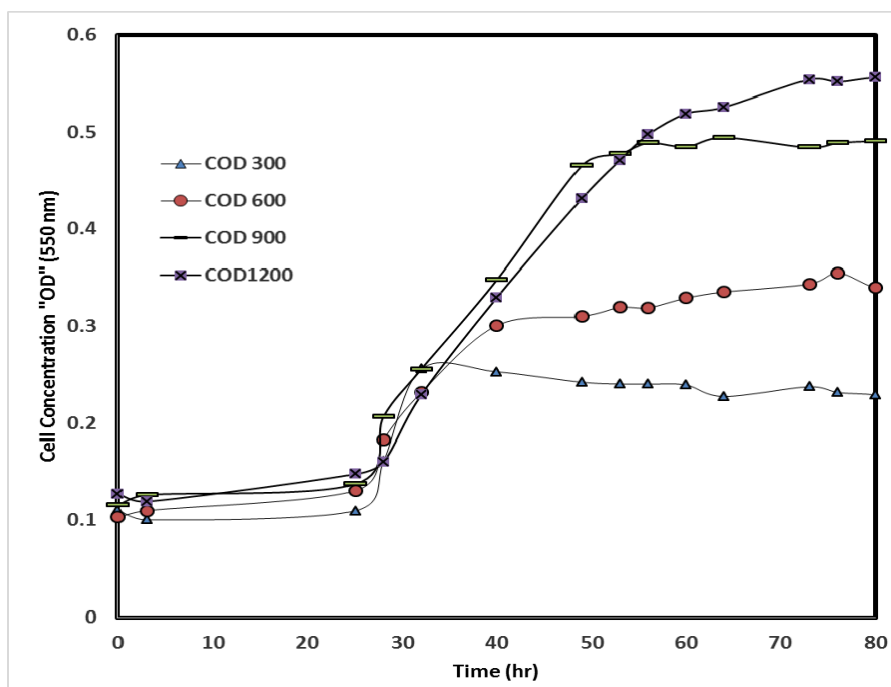


Figure 3-5: Growth of *D.hansenii* in actual desalter effluent with dilution of initial COD to 300,600,900 and 1200 mgL⁻¹.

Figure 3-6 describes the COD removal rates in the actual desalter effluent. The COD removal rate is in the range from 69 to 88%. Overall, the phenol degradation efficiencies were relatively high at the pH range studied (5.5 to 7.5). The COD removal in real desalter effluent wastewater was about 1.3-8X higher than that obtained in simulated desalter effluent containing phenol as the only carbon substrate. The salt concentration in the actual desalter effluent was 600 mg L⁻¹ and lower than in the simulated effluent. This may also contribute to higher efficiencies of COD removal.

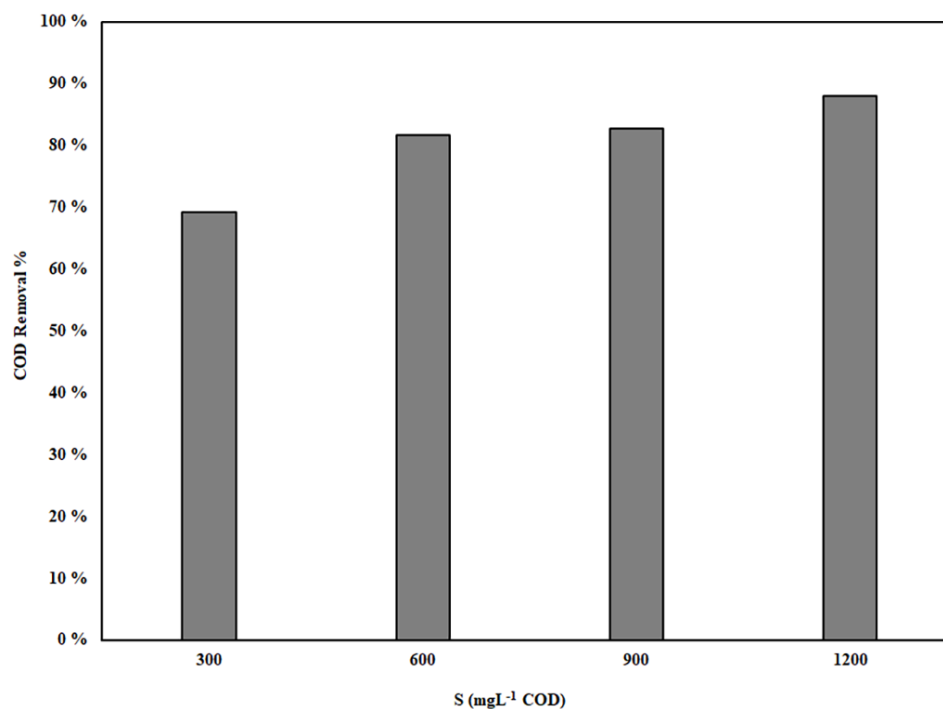


Figure 3-6: Desalter effluent COD removal by using *D.hansenii* at different initial CODs in actual desalter effluent media.

3.4 Conclusions

In this study, for the first time, an osmo-tolerant and halophilic yeast *D. hansenii* (*LAF-3 10 u*) was investigated for the treatment of petroleum refinery desalter effluent. A single organic substrate, phenol was utilized in order to identify suitable kinetic models to represent the growth kinetics in batch culture as the limiting substrate at 25°C and in a pH range of 5.5- 7.5. The yeast also grew well in real desalter effluent and can provide a high COD reduction. Kinetic constants applicable to the Edward equation were obtained to describe substrate inhibition model for yeast growth as a function of COD. The *D. hansenii* can effectively degrade organic carbon in synthetic and real desalter effluents. Further studies on reactor development are needed to design suitable bioprocessing configurations for the efficient treatment of petroleum refinery desalter effluents.

Chapter 4

4 Investigation of Degradation of N-Dodecane By *Debaryomyces Hansenii* In Simulated Desalter Effluent

4.1 Introduction

The first step of the petroleum refining process uses a desalter to dissolve impurities, including hydrocarbons, metals, soil, amines, ammonia and different salts. In the desalter operation, water and demulsifiers are added to the crude oil and then heated to extract salts and other impurities into the water^{198,199}. The operating temperature in the desalter is between 80 and 130°C^{12,14}. Cooling water then reduces discharged desalter effluent temperature down to between 21 and 50°C^{5,13,49}.

The presence of salt in the desalter effluent makes the effluent treatment challenging hence alternatives need to be explored. There has been limited research on the biological treatment of desalter effluent”.

N-dodecane, a straight-chain alkane with 12 carbon atoms, is one of the many hydrocarbons found in crude desalter effluent²⁴. The research literature describes many techniques using the biological treatment of petroleum wastewater for degradation of aliphatic compounds by an alkane-degrading organism such a bacteria, yeasts, fungi during 3-4 weeks or months at the low range temperature²⁹⁻³⁷. However, the efficiency of crude oil degradation by microorganism depends on molecular weight and length of the

hydrocarbon chain in crude oil³¹. About 61 bacterial (aerobic and anaerobic) and 28 yeast strains utilize petroleum hydrocarbons including n-alkanes for growth^{31,200}.

Several bacteria could degrade 930 mgL⁻¹ of dodecane in 1% salt up to 60% during 90 days²⁰¹. Some yeasts such as *Candida tropicalis*, *Candida albicans*, *Yarrowia lipolytica*, and *Debaryomyces hansenii* can degrade hydrocarbons²⁰². Yeast, *Yarrowia lipolytica*, degrades dodecane with concentration of 100gL⁻¹ at Temperature of 15 °C up to 73% after 5 days but this yeast grow up 20 °C^{31,203} and over 9% NaCl²⁰⁴, while *D.hansenii* grow up to 25% NaCl¹³⁷ and 35 °C. Certain yeast can accumulate large amounts of lipids, a characteristic found in less than 30 of about 600 yeast species¹³⁷.

D. hansenii is an alkane-metabolizing yeast¹⁴³ with metabolic machinery for a wide range of organic substrates^{202,205} at different specificities among its forty-three strains²⁰⁶. *D. hansenii* can grow in media up to 4 M KCl, and 4 M or 10 to 25% NaCl^{144,207}. Primary application of this yeast is in food and dairy operations, including the production of cheese, meat, beer and fruit^{137,208}. *D. hansenii* has been reported to grow and metabolize across a broad range of pH values, from 3 to 10^{4,26}, temperatures from 10 to 35°C^{144,207}, and salinities from 10 to 25% NaCl (w/v, salt)) (Kockova- Kratochvilova et al., 2009). These properties render it highly suitable for desalter effluent bioremediation, as the effluent is characterized by alkane hydrocarbons and high salt concentrations. The biomass of this yeast is also amenable to commercialization for biofuel production due to its high lipid content.

This study first examined the growth of *D. hansenii* in simulated desalter effluent (SDE) with concentrations of *n*-dodecane (*n*-alkane hydrocarbon) ranging from 3.85 gL⁻¹ to 30 gL⁻¹. Next, response surface methodology (RSM) was applied to investigate the effects of different environments on yeast performance. Our findings demonstrate that a significant efficiency boost in dodecane concentration removal can be achieved under a set of easily optimized environment conditions.

4.2 Materials and methods

4.2.1 Materials

The simulated desalted effluent (SDE) was prepared from a mineral media solution²¹⁰ with equivalent properties of real desalter effluent, with dodecane the only yeast-degradable carbon source. Tween 20 (non-ionic surfactant) was added to dissolve the nonpolar hydrocarbon dodecane into the aqueous medium of SDE to help yeast access this carbon source.

4.2.1.1 Chemicals and preparation of synthetic desalter growth medium

All chemicals used in this study were purchased from Sigma Aldrich (Oakville, Canada) at analytical grade. The SDE in 1 L distilled water was prepared as described in Table 4-1. The pH of the growth media was adjusted to between 6 and 6.5. All growth media were autoclaved at 121°C for 20 min prior to yeast cultivation. Experimental specifications are provided in Table 4-2. Dodecane was added to the synthetic effluent as a petroleum hydrocarbon representative at concentrations ranging from 3.75 to 30 g.L⁻¹ (high range), and 150 mgL⁻¹ to 750 mgL⁻¹ (low range) to the simulated media. The theoretical oxygen demand (ThOD) for the oxidation of 1 g of dodecane is 3.43 g (adapted from Pitter and Chudoba, 1990). Experiment 2 used a ThOD of dodecane ranging from 522 to 2610 mgL⁻¹; this is within the range of the COD in Imperial Oil desalter effluent.

Total free hydrocarbon content, including dodecane, in typical desalter effluent has been reported as high as 1,000 mgL⁻¹ ^{38,211}.

Table 4-1: Synthetic desalter effluent (SDE) components without hydrocarbon

Mineral component	media	Concentration in 1 litre distilled water	SDE (MM) mgL ⁻¹	
KH₂PO₄		1 g	Total potassium (K ⁺)	73.6
K₂HPO₄		1 g		
(NH₄)₂SO₄		1 g	Total ammonia (NH ₃)	27.3
MgSO₄		0.2 g	Magnesium (Mg ²⁺)	40
FeCl₃		0.05 g	Ferrous (Fe ²⁺)	17.3
CaCl₂		0.02 g	Total calcium (Ca ²⁺)	72
NaCl		1 g	Total sodium (Na ⁺)	393.3
FeCl₃, CaCl₂, NaCl		0.05 g, 0.02 g, 1 g	Dissolved chloride (Cl ⁻)	651
Tween 20		1 mL	-	-

4.2.1.2 Yeast preparation and growth experiments

Debaryomyces hansenii SWING YEAST LAF-3 (Parmalat Inc., London, Canada) was used for all experiments. Pre-cultivation of fresh and sterilized yeast extract peptone dextrose (YEPD) agar slants was conducted, and the cultures were then incubated at 25°C and 180 rpm on a rotary shaker (VWR, Mississauga, ON, Canada) for 24 h. Growth in liquid media was facilitated by 50 mL of sterilized malt extract medium. Optical density (absorbance percentage) at a wavelength of 600 nm was measured every four hours on an Evolution™ 60S UV-visible spectrophotometer (Thermo Fisher Scientific) during the 24 hours of incubation. Once the cultures reached the late exponential phase, the *D. hansenii*

cells were added to SDE in 250 mL flasks with a suspended yeast cell concentration of 1% v/v (1 mL *D. hansenii* inoculum in 100 mL of desalter effluent) and incubated at 25°C in a rotary shaker set to 180 rpm for five days.

Table 4-2. Experiment dodecane concentrations

Experiment	Dodecane per liter mineral media			
high range	3.75 gL ⁻¹	11.25 gL ⁻¹	18.75 gL ⁻¹	30 gL ⁻¹
low range	150 mgL ⁻¹	450 mgL ⁻¹	750 mgL ⁻¹	
	experimental design (central composite design)			

4.2.2 Analytical methods

Organic carbon (dodecane) concentration was measured by assessing COD. SDE, mineral media (MM) and surfactant (Tween 20), were maintained at the same concentrations for all runs of all experiments, with dodecane concentration as the only variable.

4.2.2.1 Cell concentration

Yeast (*D. hansenii*) is a unicellular microorganism, and growth (cell concentration) was measured using the optical density (OD) of the cell culture by measuring absorbances at 600 nm.

4.2.2.2 Chemical oxygen demand (COD) analysis

Chemical oxygen demand (COD) is a good way to measure organic loadings in wastewaters such as desalter effluent as the organic composition can be highly variable. In this study, COD was also applied as a measure of dodecane concentration. For experimental determinations of COD, the microbial culture samples from the shaker flasks were centrifuged with an IEC Micromax (Hyland Scientific Company, WA, USA) at 1,000 rpm for 45 min. The supernatant was then filtered using sterile 0.2-micron cellulose acetate membrane syringe filters (VWR) to remove any remaining cells. COD analysis of the filtrated SDE was conducted with a Hach 8000 (Hach Inc., Loveland, USA).

The presence of salinity in the media affects COD measurements; therefore, the correlation between initial *n*-dodecane concentration and COD was determined by measuring correlations at different NaCl concentrations. For low dodecane, concentrations of 150, 450 and 750 mgL⁻¹ with salt concentrations of 0 and 5 gL⁻¹ at a pH of 6.4 were used, and COD% was measured and compared with the results of COD removal described earlier in this section. For high dodecane, a 200 mL volume of mineral media in shaker flasks was supplemented with *n*-dodecane (0.5% to 4% v/v) at concentrations of 3.75, 11.25, 18.75, and 30 gL⁻¹ for five days in a rotary shaker. Dodecane removal was calculated using Equations 4-4 and 4-5. Each experiment was repeated three times.

Table 4-3 shows equivalent CODs for dodecane concentrations of 150, 450 and 750 mgL⁻¹ at salt concentrations of zero and 5 gL⁻¹ when the pH was 6.4.

4.2.2.3 *n*-dodecane removal measurement

Dodecane removal was evaluated using Equation 4-5 and the following formula

$$\Delta\text{COD}\% = \frac{(\text{COD}_{\text{Total}(i)} - \text{COD}_{\text{Total}(f)})}{\text{COD}_{\text{(Total)}i}} \times 100 \quad (4-1)$$

here COD_i is the initial dodecane concentration before adding yeast and COD_f is the final dodecane concentration at the end of the experiment.

Table 4-3. COD of dodecane in synthetic desalter effluent at NaCl concentrations of zero and 5gL^{-1} , pH = 6.4

NaCl (gL^{-1})	COD _{MM} + COD _τ mgL^{-1}	D = 150 mgL^{-1}		D = 450 mgL^{-1}		D = 750 mgL^{-1}	
		COD _{Total} mgL^{-1}	%ΔD	COD _{Total} mgL^{-1}	%ΔD	mgL^{-1}	%ΔD
0	534 ± 1	621 ± 1	14. ± 0.1	644 ± 2	17.08 ± 0.1	679 ± 1	21.3 ± 0.1
5	728 ± 2	977 ± 1.2	25.5 ± 0.2	1173 ± 3	37.94 ± 0.11	1221 ± 3	40.4 ± 0.12

4.2.2.4 *D. hansenii* biodegradation of n-dodecane in simulated desalter effluent

A four-factor central composite design (CCD) was developed to evaluate *n*-dodecane removal responses and determine the optimal combination of temperature, pH, NaCl, and initial *n*-dodecane concentration. The effects of temperature (A), initial pH (B), salt (C), and initial concentration of *n*-dodecane (D) were assayed over a range of 20 to 35°C (A), 3 to 9 (B), 1 and 5 g L^{-1} (C), and 150 and 750 mg L^{-1} (D).

All cell cultivations were carried out in 250 mL shaker flasks using SDE and Tween 20. The un-coded values for each parameter were low star point, low center point, center

point, high center point, and high star point as star points help to fit the curvature model. Temperature (A) in °C, initial pH (B), initial NaCl or salt concentration (C) in gL^{-1} , and *n*-dodecane concentration (D) in mgL^{-1} are shown in Table 4- 4. Each flask contained 100 mL SDE in the combinations described in Table 4-5. The flasks were mixed in a Multitron (INFORS HT, Anjou, QC, Canada) shaking incubator at 180 rpm for five days. After five days, dodecane concentrations remaining in the supernatants were determined using Equation 4-6. The experimental design was developed using Stat-Ease Design Expert v.11.1.0.1, which suggested 27 conditions. All conditions were assayed in triplicate, including 3 center points. The resulting 81 conditions ($3 \times [16 \text{ factorial} + 8 \text{ augmented} + 3 \text{ center points}]$) were fully randomized.

Linear regression analysis was applied to fit experimental data with a second order model, as shown in Equation 4-10. The significances of each parameter, interaction and quadratic effect were determined based on an α of 0.05 using an F test. The fitted model was evaluated by normal probability plots, R^2 , and adjusted R^2 , and lack of fit coefficient to evaluate adequacy. An analysis of variance (ANOVA) was used to assess the accuracy of the model. A *p*-value of less than 0.05 was considered statistically significant. Regression analyses and optimization were performed by Stat-Ease Design Expert v.11.1.0.1 software to maximize the removal of dodecane from the desalter effluent. Error bars indicate standard deviations of triplicate measurements.

Table 4-4: Experimental design with four factors and three levels

Level	Low star	Low center	Center	High center	High star
	-	-1	0	1	+
Dodecane (D) mgL^{-1}	25	150	450	750	874.5
NaCl (C) gL^{-1}	0.17	1	3	5	5.8
pH (B)	1.2	3	6	9	10.2
T °C (A)	16	20	27.5	35	38.1

4.3 Results and Discussion

4.3.1 COD analysis

The strong linear relationship between total organic carbon (TOC) and COD indicates that a COD assay can reliably replace the TOC test normally used in the evaluation of specific wastewater and treatments²¹². Amounts of consumed dodecane were evaluated by measuring reductions in COD after five days using Equation 4-2

$$COD_{Total} = COD_{MM} + COD_D + COD_T \quad (4-2)$$

where COD_X denotes the COD of component X, MM represents mineral media, T represents Tween 20 and D represents dodecane.

Equation 4-3 illustrates that COD_{Total} has linear regression with the TOD of Tween 20 (T) and dodecane (D)

$$COD_{Total} = \alpha TOD_{\tau+D} + \delta \quad (4-3)$$

where α is the slope and δ is the intercept of the straight line.

Equation 4-4 similarly illustrates that COD_{Total} has linear regression with the TOD of Tween 20 (T) and dodecane

$$COD_{Total} = \alpha D + \beta \quad (4-4)$$

where α is the slope and β is the intercept of the straight line.

Tween 20 is not degradable by yeast, so amounts thereof at the first (i) and final (f) days remained constant (equation 4-5):

$$[\text{COD Total}_{(i)} - \text{COD Total}_{(f)}] = \alpha\beta [D_{(i)} - D_{(f)}] = \Delta D \quad (4-5)$$

Since chloride levels can affect the COD²¹³, COD correlations were developed for the different salt and *n*-dodecane concentrations and are described below.

Equation 4-6 demonstrates the correlation line between COD and high dodecane concentration.

$$(\text{high range of dodecane}) \text{ NaCl } 1 \text{ gL}^{-1}; D = 14.647 \times \text{COD} - 15885, R^2 = 0.97 \quad (4-6)$$

4.3.2 Kinetics of *D. hansenii* *n*-dodecane biodegradation in simulated desalter effluent

Aerobic degradation of *n*-dodecane by *Debaryomyces hansenii* starts with the oxidation of *n*-dodecane to a primary alcohol that is subsequently oxidized into fatty acid. Fatty acids then undergo further processing to release the energy they store²¹⁴; yeasts can accumulate and store these lipids, as well. One limitation to the utilization of *n*-dodecane as a substrate is its extremely poor solubility in water. In our study, Tween 20 (polyoxyethylene sorbitan fatty acid ester), a nonionic surfactant, was added to increase the miscibility of *n*-dodecane²¹⁵. A control sample of SDE with Tween 20 in the absence of *n*-dodecane was tested to ensure the yeast degraded *n*-dodecane only and not the surfactant. Biodegradation of *n*-dodecane in SDE by adding surfactant was compared with control using the equations described in the Methods section.

Figure 4-1 shows the growth kinetics of *D. hansenii* in SDE at initial, low range dodecane concentrations from 0.3 to 1.5 gL⁻¹. Three growth phases, lag, exponential, and log were observed in the SDE (Fig. 4-1). Yeast concentration, as evaluated at OD₆₀₀, increased from

0.18 to 0.7 in the Tween 20 containing SDE over a period of 48 h. Negligible growth was observed in the control flask containing no dodecane, indicating Tween 20 was not appreciably metabolized by the yeast (Fig. 4-1).

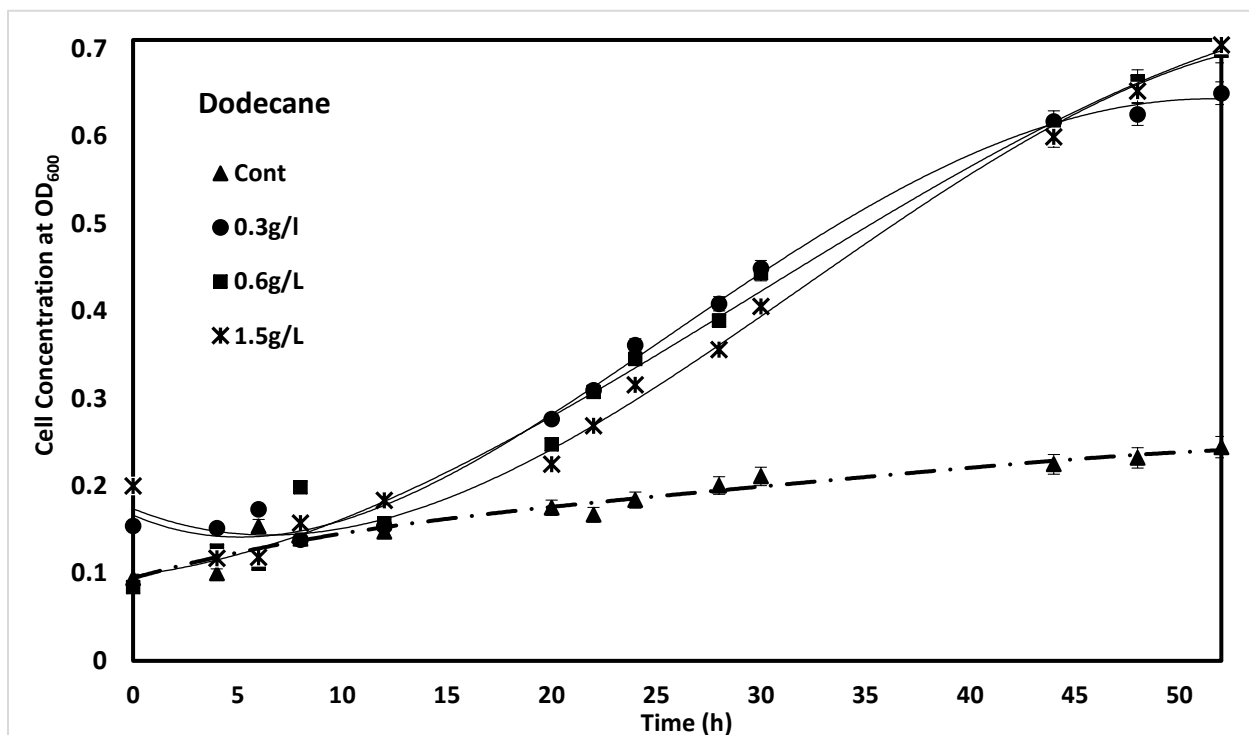


Figure 4-1. Degradation of *n*-dodecane with Tween 20 over 50 hours with control Error bars indicate standard deviations of triplicate measurements.

Figure 4-2 describes the growth of *D. hansenii* in SDE at high initial *n*-dodecane concentrations of 3.75 gL⁻¹, 11.25 gL⁻¹, 18.75 gL⁻¹ and 30 gL⁻¹. The OD₆₀₀ of the cells increased from 0.3 to 2.0 in the SDE media. No lag phase was observed during the growth period under these conditions; however, cell concentration trend lines were closely aligned. These results demonstrate that the yeast *D. hansenii* can grow in concentrations of *n*-dodecane up to 30 gL⁻¹. Of note, cell growth increases at initial substrate concentrations of

up to 3.75 gL^{-1} but not significantly after that (Figs. 4-1, 4-2). This could be because dodecane has low solubility in water, limiting the amount of the substrate dissolved in the effluent at any given time²¹⁶.

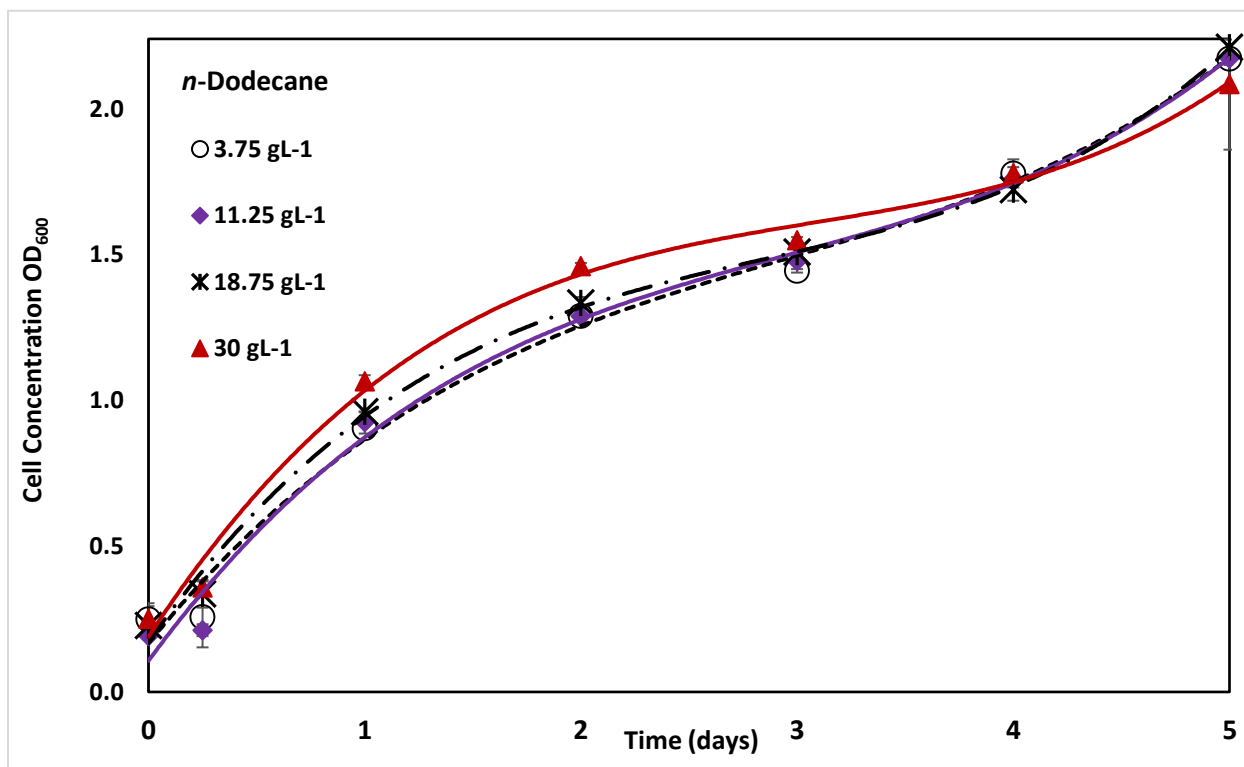


Figure 4-2: Growth of *D. hansenii* in different dodecane concentrations of 3.75, 11.25, 18.75 and 30 gL^{-1} in the presence of Tween 20 Error bars indicate standard deviations of triplicate measurements

At low concentrations (up to 1.5 gL^{-1}) the driving force for mass transfer of dodecane may be low enough for growth to be limited by supply (Fig. 4-1). As dodecane concentration increased (Fig. 4-2), the driving force for mass transfer increased concomitantly and was associated with increased cell growth. The increase in cell growth plateaued at a substrate concentration of 3.75 , with increases up to 30 not associated with

significant increases in cell growth rate, suggesting limiting factors such as other nutrients, oxygen supply constraints or substrate inhibition.

Once the surfactant exceeds critical micelle concentration (CMC), the amount of solubilized dodecane increases with increases in surfactant concentration²¹⁷. In this experiment, concentrations of surfactant in the four samples were approximately equal; however, the concentration of Tween 20 in SDE was higher than the reported CMC of 60 mgL⁻¹²¹⁸, suggesting that the solubilization power (SP) of a surfactant is equivalent to the free energy of solubilization (ΔG_s) for the four different concentrations of dodecane in water, as indicated here

$$SP = \frac{S_{total} - S_{wat}}{C_{surf} - CMC} \quad (4-7)$$

where S_{total} is the molar solubility of the hydrophobic hydrocarbon (dodecane) in the aqueous system (SDE); S_{wat} is the molar solubility of the hydrocarbon in water; and C_{surf} is the molar concentration of the surfactant.

Figure 4-3 shows *n*-dodecane removal from SDE at *n*-dodecane concentrations of 3.75, 11.25, 18.75 and 30 gL⁻¹; which were reduced after five days by *D. hansenii* to 2.06, 6.53, 7.5, and 9 gL⁻¹, respectively. *N*-dodecane removal is displayed as a function of initial dodecane concentration. As the initial dodecane concentration increased, the level of dodecane removal decreased, indicating that mass transfer from the two-phase system controlled the overall removal rate. Mass transfer can be increased by higher agitation speeds or Tween 20 concentration.

The effects of *n*-dodecane concentration on specific growth rates and dodecane removal from SDE were investigated, with the specific growth rate (μ) determined from the initial slope of cell growth at OD₆₀₀ versus time curves for each *n*-dodecane concentration in equation 4-8 as indicated here

$$\mu = \frac{\ln \frac{X_2}{X_1}}{t_2 - t_1} \quad (4-8)$$

where X is cell concentration, and t is time.

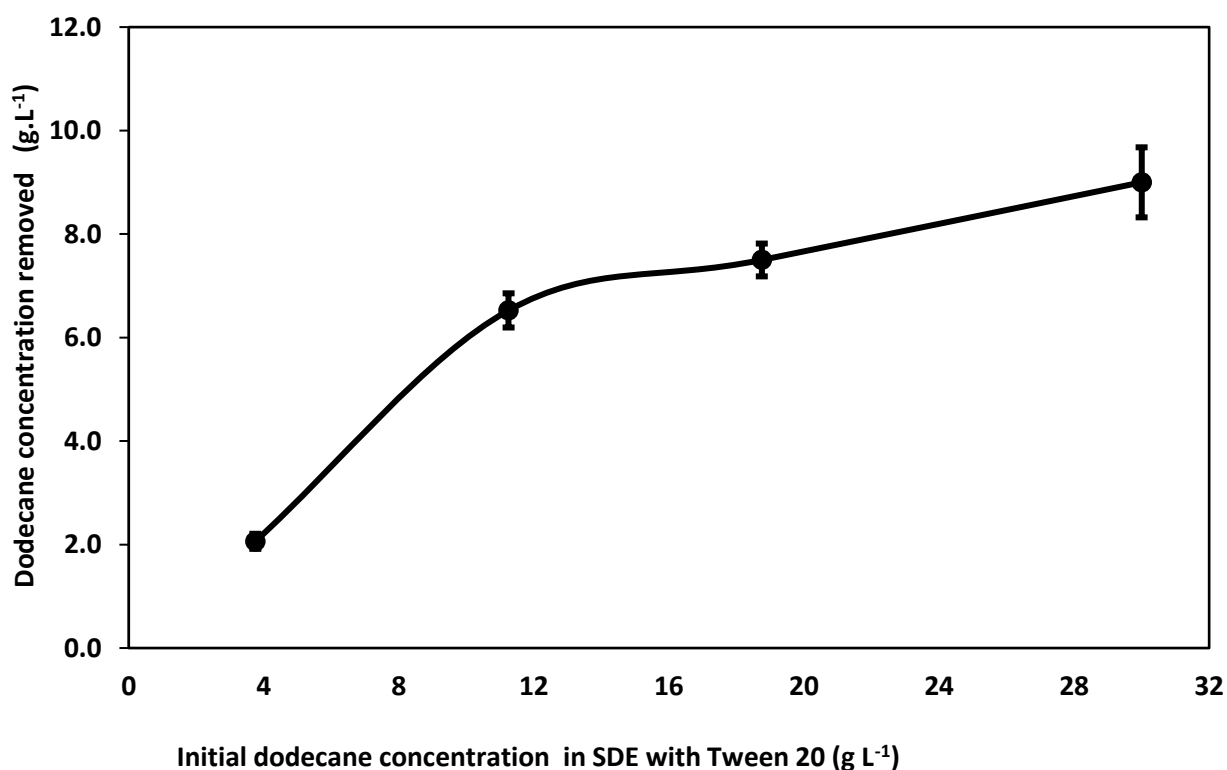


Figure 4-3. Dodecane removal as a function of initial dodecane concentration after five days. Error bars indicate standard deviations of triplicate measurements.

Specific growth rates were calculated as indicated in Equation 4-8. *N*-dodecane concentrations of 0.3, 0.6, 1.5, 3.75, 11.25, 18.75 and 30 gL⁻¹ yielded specific growth rates of 0.010, 0.012, 0.044, 0.055, 0.055, 0.044 and 0.045 h⁻¹, respectively. In previous work, the Andrews, Aiba and Edward models were compared using phenol as the substrate for *D. hansenii*⁵². In this study, the Aiba semi-empirical model²¹⁹ as shown in Equation 9 was applied to assess specific growth rate as a function of initial substrate concentration

$$\mu = \frac{\mu_{max} \frac{S}{K_I}}{K_S + S} \quad (4-9)$$

where μ is the specific growth rate (h^{-1}), μ_{max} is the maximum specific growth rate (h^{-1}), K_S is the half saturation constant (gL^{-1}), K_I is substrate inhibition constant (gL^{-1}), and S is the initial dodecane concentration or substrate (gL^{-1}). Figure 4-4 shows model simulation versus experimental results, indicating a slight inhibition of specific growth rates at higher initial dodecane concentrations. Values for μ_{max} , K_S and K_I were calculated by the least square method in MATLAB, and were 0.085 (h^{-1}), 1.74 (gL^{-1}) and 45.53(gL^{-1}), respectively; these were compared with the Aiba model in Equation 4-9.

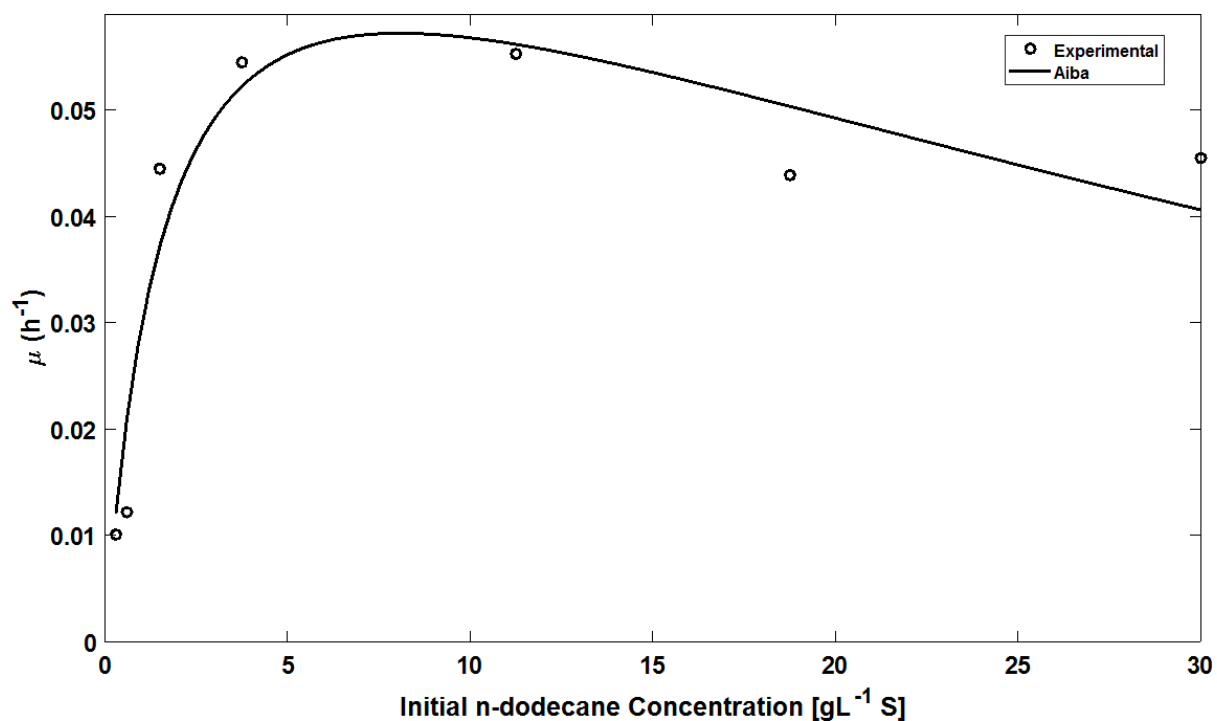


Figure 4-4: Experimental data and Aiba model simulations for the specific growth rate of *D. hansenii* growth as a function of initial *n*-dodecane concentration of 0.3 to 30 gL⁻¹.

(Equation 4-9) The curve represents the Aiba kinetic model fitting with experimental data using the least squares method in MATLABM

Several studies have been carried out for the microbial metabolism of dodecane and other hydrocarbons. In one approach, sawdust and peat absorbents were applied to degrade petroleum spills with an initial dodecane concentration of 38 gL⁻¹ for 68 days²²⁰. The average removal of COD using mixed cultures in a trickling filter was 75% over a minimum period of 11 weeks²²¹. Our results showed a much faster removal of high *n*-dodecane concentrations (up to 31% in 5 days) in saltwater using the yeast, *D. hansenii*. Another study used bacteria for dodecane degradation, and mycobacterium *austroafricanum* GTI-23 has also been shown to grow on aliphatic hydrocarbons, such as dodecane, in a mineral salt medium of 3.3% (v/v)²²².

However, only a limited number of microorganisms are known to grow on crude oil at concentrations from 6 gL⁻¹ up to 250 gL⁻¹. These microorganisms include *Actinomyces* sp., PRCW E1, *Acinetobacter* sp. E11, *Burkholderia cepacia* RQ1, *Corynebacterium* sp. BPS2-6, *Pseudomonas* sp. BPS2-5, and *Rhodococcus* spp. Moj-3449 and BPS1-8^{223,224}. *Geobacillus stearothermophilus* A-22, *Pseudomonas stutzeri* NA3, *Acinetobacter baumannii* MN329, *P. aeruginosa* NCIM 551427, *bacterium* SH-1 *Geobacillus* sp.²²⁵, and *Dietzia* sp. DQ12-45-1b²²⁶ can degrade more than 10% of *n*-alkanes over a period of five to 14 days. The biosurfactant rhamnolipid is also used to increase the biodegradability of raw wastewater in the petrochemical industry and has been shown to remove up to 72% of hydrocarbon content after 45 days²²⁷.

The results of our investigation demonstrate that the yeast *D. hansenii* degraded dodecane at a maximum rate between 9 to 30 gL⁻¹ in the ranges investigated. Results did indicate potential substrate inhibition as dodecane concentration increases. Our previous results on phenol showed phenol inhibition at a COD of 1,200 mgL⁻¹ when phenol was the only

carbon source⁵². The results obtained in our study led us to examine in more detail the different parameters affecting cell growth using dodecane as a nonpolar substrate. This study demonstrates the growth rates of *D. hansenii* from low to high concentrations in SDE with a salt concentration of 1 gL⁻¹. These results are comparable with other research focused on the removal of oil, dodecane, *n*-alkane and aliphatic hydrocarbons.

4.3.3 Optimization of *n*-dodecane removal and response surface model validation

Response surface methodology was used to study the interaction effects of the four factors. Measured responses for dodecane removal percentage, parameters and levels are shown in the last column of Table 4-5. The quadratic model for *n*-dodecane removal in terms of actual factors are shown based on the selected significant variables

$$\begin{aligned} \mathbf{COD\ \% \ removal} = & +20.55 - 5.76 A + 4.99B - 0.5324 C - 8.67 D - 4.58AD + \\ & 4.25 BC - 2.58 BD + 2.56 CD + 11.53D^2 \end{aligned} \quad (4-10)$$

Where *COD % removal* is the response data in linear correlation with *n*-dodecane removal percentage (%ΔD).

The resulting model parameters are shown in Table 4-6. The *F* value of the model was 16.89, much higher than the critical value, indicating that model parameters are highly significant. The significance of each parameter coefficient was determined by *p*-value, with smaller *p*-values indicating increasing significance of the coefficient. In this study, the lack of fit obtained for this model was 16.7%, and temperature, initial pH, and dodecane concentration all significantly affected dodecane removal. The quadratic effects of *n*-dodecane concentration and pH and the interaction between temperature and dodecane also significantly affected COD (dodecane removal). The goodness of fit of the model was

confirmed by the coefficient of determination $R^2 = 0.90$ and adjusted determination coefficient of $R^2 = 0.85$. A ratio of 15.22 for adequate precision indicates an adequate signal to noise ratio for navigating the design space. Data were analyzed statistically and found to fit with the model.

Table 4-5: Chemical oxygen demand percentage (average of triplicates \pm standard deviation) under conditions determined for CCD

Run	Factor 1 (A) Temperature (OC)	Factor 2 (B) pH	Factor 3 (C) Salt gL^{-1}	Factor 4 (D) Dodecane mgL^{-1}	Response COD Removal %
1	16.9	6	3	450	13.8 \pm 1.3
2	20	3	1	150	27.2 \pm 0.7
3	20	3	1	750	51.3 \pm 0.4
4	20	3	5	150	12.3 \pm 0.7
5	20	3	5	750	51.3 \pm 0.54
6	20	9	1	750	47.5 \pm 0.25
7	20	9	5	150	44.9 \pm 0.77
8	20	9	1	150	32.3 \pm 0.31
9	20	9	5	750	61.6 \pm 0.79
10	27.5	1.7	3	450	16.6 \pm 0.9
11	27.5	6	0.17	450	20.5 \pm 0.75
12	27.5	6	3	25	21.4 \pm 0.52
13	27.5	6	3	450	20.7 \pm 0.2
14	27.5	6	3	450	19 \pm 0.54
15	27.5	6	3	450	21.5 \pm 1
16	27.5	6	3	874.5	60.9 \pm 0.73

17	27.5	6	5.8	450	18 ± 0.8
18	27.5	10.2	3	450	22.6 ± 0.4
19	35	3	1	150	27 ± 0.7
20	35	3	1	750	22.4 ± 0.15
21	35	3	5	150	8.3 ± 0.43
22	35	3	5	750	28.7 ± 0.42
23	35	9	5	150	35.5 ± 0.33
24	35	9	1	750	31.7 ± 0.8
25	35	9	1	150	28.4 ± 0.51
26	35	9	5	750	38.5 ± 0.66
29	38.1	6	3	450	12.3 ± 0.73

4.3.4 Combined effects of pH, temperature, sodium chloride, and n-dodecane concentration on dodecane removal

Figure 4-5 describes the three-dimensional surface plots of the combined effects of temperature and dodecane on COD removal at a constant salt concentration of 3 gL⁻¹ and pH of 6. *N*-dodecane removal was also found to be a function of temperature and dodecane individually. Figure 4-5 illustrates the relationship of yield increases at pH 6 in temperatures ranging from 20 to 35°C. When the dodecane concentration was 750 mgL⁻¹ at pH 6 and 20°C, dodecane removal was quite high; a dodecane concentration of 150 mgL⁻¹ at pH 3, 20°C was significantly lower. Table 4-6 shows the *p*-value of the interaction between dodecane and temperature to be lower than 0.05 (*p* = 0.0039). Table 4-6 also shows the *p*-value of the interaction between pH and salt as less than 0.05 (*p* = 0.0062).

Table 4-6: Analysis of variance of fitted model

Source	Sum of squares	df	Mean square	F-value	p-value
Model	4489.00	9	498.78	16.89	< 0.0001
(A) T	662.90	1	662.90	22.45	0.0002
(B) pH	499.23	1	499.23	16.91	0.0008
(D) dodecane	1502.71	1	1502.71	50.89	< 0.0001
AD	335.81	1	335.81	11.37	0.0039
BC	293.27	1	293.27	9.93	0.0062
Lack of Fit	471.05	15	31.40	21.73	0.1670
R²	0.90	-	-	-	-
Adjusted R²	0.85	-	-	-	-

Design-Expert® Software
Factor Coding: Actual

COD Removal %

● Design points above predicted value

○ Design points below predicted value

8.2  61.6

X1 = A: T
X2 = D: Dodecane

Actual Factors

B: pH = 6

C: Salt = 3

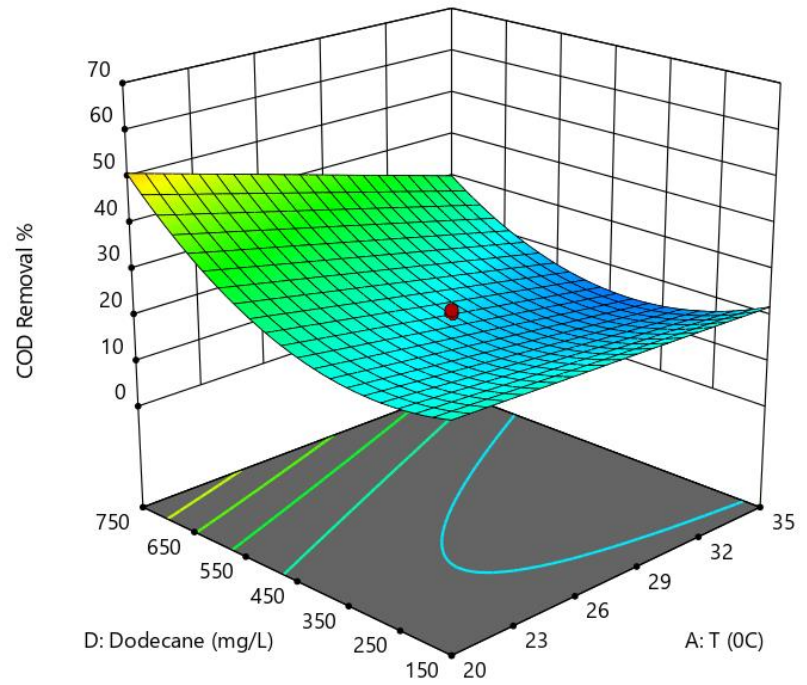


Figure 4-5: Surface plots of combined effect of process variables temperature and dodecane concentration on dodecane removal

4.3.5 Single factor effects on dodecane removal

4.3.5.1 Effect of salt on n-dodecane removal

Table 4-5 shows that optimal dodecane removal occurs at a NaCl concentration of 5 gL⁻¹; in our experiments, this level was associated with removal of 61.6% of the dodecane. *D. hansenii*, a yeast predominantly isolated from cheese brines, is characterized as having a high salt tolerance. When salt concentration increases over 1M, enzyme activity ramps up and increases fermentation, and metabolic pathways are inhibited via inhibition of respiration. Metabolism shifts from aerobic to anaerobic, producing alcohol and glycerol. This mechanism is evidenced by increased utilization of the carbon source by the enzyme at high salt concentrations²²⁸. In the present study, *D. hansenii* metabolism was less sensitive to Na⁺; growth continued undisturbed for concentrations up to 1 M or over 4% w/v^{229,230}. Breuer also confirmed that *D. hansenii* grows faster in high NaCl concentrations up to 1M than in lower ones^{137,231}. Other studies report that the growth of *D. hansenii* slows as salt concentrations increase^{230,232} in media with a salt content of at least 0.2 M. In this investigation, levels of salt between 1 and 5 gL⁻¹ did not affect yeast cell reproduction rate ($p > 0.05$). Table 4-7 shows the growth rate of 16 factorial tests at different salt levels, dodecane concentrations, pH values, and temperatures and demonstrates that growth rates in the different salt concentrations were close to one another other and deviated as a function of temperature or dodecane concentration. Salt concentration did not inhibit growth rate or cell concentration of *D. hansenii*.

4.3.5.2 Effect of pH on n-dodecane removal

Table 4-5 lists the experimental results of dodecane removal from SDE at initial pH values from 3 through 9. The starting values of this parameter were kept constant to investigate the effects of pH on dodecane removal, and were measured each day for continuous control during sampling for optical density. The results of Table 4-5 demonstrate that maximum dodecane removal at a pH of 9 was slightly higher than at a pH of 3 or 6. Praphailong and

Fleet (1997) studied the effect of pH on yeast growth over pH values ranging from 1 to 10 in the presence of a salt-free inorganic buffer (similar to basal medium) and found that *D. hansenii* grew between a pH of 4 and 8. No growth at a pH of 3 or below, or above 9 and 10, was observed. In the present study, the pH of the medium also affected growth in the presence of salt. *D. hansenii* was more salt tolerant at a pH between 5 and 7 (15% NaCl) and a pH of 3 (10% NaCl)²³³. Of note, *D. hansenii* grew more at a pH of 8 than 6 when the NaCl concentration was increased to 2M. In high salt concentrations (1M NaCl), *D. hansenii* demonstrated a longer lag phase at pH 8 than pH 6; cells grew more slowly in the former than in the latter²³⁴. In our study, a pH of 9 also resulted in a longer lag phase than pH values of 3 or 6 (data not shown). We also did not observe high cell growth at a pH of 6 when the temperature was 27.5°C, although in our study, NaCl concentrations were lower than those evaluated in previous literature. Kinetic growth at a pH of 9 approximated the specific growth rate is similar with pH 3 and was changed based on dodecane concentration (Table 4-7). COD changes when pH is adjusted at the beginning of the experiment and the oxidation of the sample changes in accordance with initial COD. Results of an ANOVA in Table 4-6 show a highly significant relationship between initial pH and initial COD oxidation.

The experimental data from cell concentrations as evaluated at OD₆₀₀ and different pH levels confirmed that pH has little effect on the kinetic growth of *D. hansenii*²³⁵. Table 4-7 shows that the specific growth rates for the different pH values at constant temperatures and dodecane or salt concentrations are approximately equal. Other studies have reported the optimal reduction of dodecane with different microorganisms, including yeast and bacteria, was at pH values between 6 and 8, and temperatures lower than 30°C. Recently, the degradation capacity of the thermophilic bacterial strain *Geobacillus A-2* was investigated in basal salt media and crude oil. Degradation of aliphatic hydrocarbons as the sole carbon source, including *n*-dodecane, at 60°C and a pH of 7.2 was over 50%²⁰⁰.

4.3.5.3 Effect of temperature on n-dodecane removal

Table 4-5 shows the influence of temperature on *D. hansenii* kinetic growth in dodecane. Our results indicated that the optimal temperature for dodecane removal was 20°C and not the expected 35°C. Yeast *D. hansenii* can grow in temperatures up to 35°C¹³⁷; the latter temperature is considered optimal for fermentation.²³⁶ The rate of growth in yeast depends on the level of autolysis that occurs at a given temperature, and temperature also affects the solubility of the surfactant. When the temperature increases, the hydrogen bonding between the water and surfactant molecules ruptures, increasing the hydrophobicity of the surfactant. Surfactant micellization then occurs at lower concentrations²³⁷, with the water solubility of surfactant molecules at less than one in lower temperatures. This result could explain why the growth rate at higher temperatures was lower than that at 20°C; the surfactant mass transfer resistances in the SDE were increased at 35°C. Results of the ANOVA analysis in Table 4-6 demonstrate the dependence of dodecane removal on dodecane concentration, which is dependent on mass transfer level.

4.3.5.4 Effect of dodecane concentration in n-dodecane removal

D. hansenii utilized hydrocarbons at salt concentrations of 1, 3 and 5 gL⁻¹. Growth rates were evaluated at OD₆₀₀ once daily for five days. Results demonstrated that the yeast could utilize *n*-dodecane and grow across a range of salt concentrations, temperatures, pH values, and hydrocarbon concentrations. Table 4-6 shows that as *n*-dodecane concentration increased, the specific growth rate rose, as did the consequential removal of *n*-dodecane. A previous study on *Acinetobacter* strain ADH-1 investigated its activity across a range of temperatures, initial pH values, NaCl concentrations and different hydrocarbon chemical structures, and reported optimal degradation of *n*-dodecane between 25 and 30°C²³⁸. A study carried out in 2018 using the fungi strains *Penicillium* sp. RMA1 and RMA2 showed these yeasts degraded up to 80% of the *n*-alkane in crude after 14 days of kinetic growth in a NaCl concentration of 0.5 g.L⁻¹²³⁹. Other studies have shown that certain bacteria can degrade shorter chain hydrocarbons (C6 to C21) in NaCl concentrations of up to 20% NaCl (w/v) provided the initial salt concentration was 0.5 gL⁻¹^{200,225,226,240,241}. Results in Table

4-7 show that at a constant temperature, growth rate increases in accordance with *n*-dodecane concentration and ultimately decreases as dodecane concentration drops ($p < 0.05$ (0.01)).

Table 4-7: Specific growth rate of yeast *D. hansenii* in different experimental conditions of the four main factors (SD of factors ± 0.005)

$\mu(\text{day}^{-1})$		T = 20 °C		T = 27.5°C	T = 35°C	
		Salt = 1 g L^{-1}	Salt = 5 g L^{-1}	Salt = 3 g L^{-1}	Salt = 1 g L^{-1}	Salt = 5 g L^{-1}
D = 150 mg L^{-1}	pH = 3	0.34	0.40	-	0.17	0.19
	pH = 9	0.33	0.39		0.22	0.18
D = 450 mg L^{-1}	pH = 6	-		0.26	-	
D = 750 mg L^{-1}	pH = 3	1	1.12	-	0.46	0.45
	pH = 9	1.09	1.00		0.47	0.37

4.3.6 Response optimization and model validation

Optimal conditions for maximum dodecane yield were obtained when at least two of the following factors were: a dodecane concentration of 150 mg L^{-1} , a temperature of 20°C, and a pH of 9. Yields also rose across at range of NaCl concentrations between 1 and 5 g L^{-1} when pH increased and temperature and dodecane concentration were low.

The center point applied and replicated at runs 22, 26 and 27, with the parameters of 27.5°C, pH 6, dodecane 450 mgL⁻¹ and salt 3 gL⁻¹, resulted in a better fit curvature. The optimal parameters for yeast growth yeast in desalter effluent are 20°C, pH 9, and dodecane 750 mgL⁻¹, experiments at the center point yielded moderate results and partial substrate degradation.

To validate the applicability of this RSM model, *n*-dodecane removal from three types of simulated desalter effluents with different pH, temperature, salt and *n*-dodecane concentrations (Table 4-8) were measured and compared with predicted *n*-dodecane removal using this empirical model; predicted and experimental yields are listed in Table 4-8. The predicted results were well-aligned to the actual values obtained from the experiment. A *t*-test with a 95% confidence interval found no significant differences between the predicted and actual values. These findings indicate that the proposed RSM model could be useful in predicting optimal hydrocarbon yield.

Table 4-8: Predicted and measured dodecane removal yields according to maximum model parameters

Initial pH	Temperature (° C)	Salt (gL ⁻¹)	Dodecane (mgL ⁻¹)	COD Yield (%)	
				Predicted	Experimental
8.8	20.1	4.9	750	60.35	59.5 ± 0.9
8.9	25.8	5	750	52.7	53 ± 0.7
9	20	3.5	750	55.35	56±.75

4.4 Conclusion

This report discusses a novel approach to the removal of hydrocarbons from desalter effluent, a substance generally difficult to treat biologically due to its high salt concentration. The method described here was both rapid and efficient in high salt

concentrations. This study evaluated a simulated desalter effluent containing dodecane as the hydrocarbon source for degradation of high concentrations of *n*-dodecane by the yeast *D. hansenii*. The yeast rapidly reduced high concentrations of *n*-dodecane in shorter time periods compared to previous findings for biodegradation of this effluent, suggesting *D. hansenii* could be useful for bioremediation and enhanced microbial oil recovery in high salinity environments. A dodecane removal of 2.06 gL⁻¹ was obtained after five days in a starting concentration of 3.75 gL⁻¹ of *n*-dodecane. As such, we then evaluated *D. hansenii* biodegradation capacity over a range of dodecane and salt concentrations close to typical aliphatic concentrations in real desalter effluent. COD removal results demonstrated that dodecane could be removed from these different concentrations in just five days. Results also showed that salt concentration did not affect yeast growth rate and that dodecane removal was instead dependent on *n*-dodecane concentration, initial pH, and temperature as mediated by the interaction between temperature and dodecane. The presence of a surfactant enhances the degradation of aliphatic and polycyclic aromatic hydrocarbons by increasing their bioavailability; however, mass transfer resistance increases when temperatures increase. The results of this study found that the surfactant Tween 20 at a concentration of 1% enhanced the degradative capacity of *D. hansenii* in both high and low concentrations of aliphatic dodecane hydrocarbons. This yeast could potentially also be applied to other types of saline wastewater containing aliphatic components such as *n*-dodecane alongside high salinity and significant heavy metal presence. Its low cost of bioremediation, biocompatibility, and effective acceleration of degradation render *D. hansenii* an attractive option for all types of desalter effluent in the petroleum industry.

Chapter 5

5 Investigation of *Parachlorella Kessleri* strain CPCC 266 on refinery desalter effluent for lipid production

5.1 Introduction

Desalting is the first unit operation to handle and process crude oil in a refinery. This operation is designed to mix crude oil and water in order to transfer inorganic salts and other contaminants contained in the crude to the water phase and to finally remove them as a brine stream (desalter effluent) ^{4,7}. The desalter effluent stream has a high COD and pH. ¹⁰ Discharged desalter effluent will cause aquatic ecosystem upsets due to the presence of salt, heavy metals, ammonia, and toxic hydrocarbons ¹, and depending on the crude oil source, it may also contain hydrogen sulfide (H₂S). An upset in the desalter can cause upsets in the biological wastewater treatment plant and put that system at risk of not meeting discharge requirements²⁴².

Current technologies for desalter effluent management are focused on conventional approaches such as gravity settlers. With new regulations on emissions, demand for high product quality, and increasing energy costs, traditional separation methods cannot achieve the purity or efficiency levels required for effluent discharge into receiving bodies of water ¹⁶⁻¹⁹. Crude oil refiners facing global competition are looking for new technologies to minimize waste and develop processes that can improve operations performance, reduce

operating costs, and stem pollution problems before they occur^{5,10,99}. Innovative technologies and environmental sustainable methods are needed for this changing environment^{1,5,9,20-27}. Several approaches have been proposed including membrane filtration, such as microfiltration (MF) and Vibratory Shear Enhanced Processing (VSEP), for crude oil refining and processing^{94,99}. Capital and operating costs have been reduced, with less consumption of energy and chemicals. However, one major drawback of the membrane and other separation technologies is that they accumulate and transfer toxic compounds and contaminants from the wastewater to the adsorbent or concentrate phase but they are not eliminated⁸⁷. Biological treatment is required to degrade toxic compounds. Such processes have high removal of biochemical oxygen demand (BOD) and Chemical Oxygen demand (COD) properties²⁹⁻³⁷.

Microalgal cultivation in industrial wastewaters with various nutrients, such as nitrogen, phosphorus, and an organic carbon source, offers a cheap, alternative source of growth media. Productive microalgae strains that are resistant to pathogens in wastewater and degrade toxic compounds instead of collecting or absorbing them should be selected. For example, *Chlorella* and *Scenedesmus* species were reported as having good algal growth rates, nutrient removal efficiency biomass, and lipid productivities²⁴³. Culturing of microalgal strains in mixotrophic mode gives a higher biomass than phototrophic growth and may be useful for the commercial production of microalgal products. Both fixed carbon compounds as well as light are used as sources of energy in mixotrophic growth²⁴⁴. In the petroleum industry, increased interest has been focused on microalgae not only due to their pollutant consumption and high photosynthetic efficiency, but particularly due to the possibility of controlling their metabolism to produce relatively high contents of energy-rich lipids as an alternative to conventional fossil fuels. Many algae can optimize their lipid biosynthetic pathways towards the synthesis and accumulation of neutral lipids under unfavorable environmental or stress conditions (20–50% cell dry weight)²⁴⁵.

Parachlorella kessleri is a eukaryotic microalga in the phylum of Chlorophyta. Previous studies indicate that these photosynthetic micro-organisms have high metabolic flexibility and are capable of both mixotrophy and heterotrophy. A previous study indicated that the microorganism can grow in wastewater that contains BTEX and removes 40% of

benzene²⁴⁶ in low salt concentrations like Bold's Basal Medium (BBM), or in high ranges of salt concentration.²⁴⁷ *Parachlorella kessleri*, is characterized by its high biomass and lipid productivity, and is the focus of many studies.¹⁷⁷ The treatment of wastewater using beneficial microalgae such as *Parachlorella kessleri* to produce high value, biomass containing lipids, antioxidants, and amino acids allows the wastewater stream to be treated as a resource.^{248,249}

The aim of the present study is to investigate the growth and lipid production by green alga, *P. kessleri*, at different concentrations of desalter effluent and in two different types of desalter effluent. Two different modes of cultivation, heterotrophic, and mixotrophic were studied and the production of lipids in the microalgae was also evaluated.

5.2 Materials and methods

5.2.1 Materials

5.2.1.1 Microalgae Strains and Growth Medium for Cultivation

Parachlorella kessleri strain CPCC 266 cultures were obtained from the Canadian Phycological Culture Centre at the University of Waterloo, Waterloo, Ontario, Canada. The *Parachlorella kessleri* cultures were maintained on Bold's Basal Medium (BBM) plates. The components of BBM media were as follows: KH_2PO_4 ; 9.5 gL^{-1} (10ml), $\text{CaCl}_2 \cdot 2\text{H}_2\text{O}$; 25 gL^{-1} (1ml), $\text{MgSO}_4 \cdot 7\text{H}_2\text{O}$; 75 gL^{-1} (1ml), NaNO_3 ; 250 gL^{-1} (1ml), K_2HPO_4 ;

75gL⁻¹ (1ml), NaCl; 25g⁻¹(1ml), Na₂EDTA•2H₂O; 10g⁻¹(1ml), KOH; 6.2 gL⁻¹, FeSO₄•7H₂O; 4.98 g⁻¹(1ml), H₂SO₄ (concentrated) 1ml l⁻¹, H₃BO₃; 11.5g⁻¹ (0.7ml), Trace Metal Solution (1ml) contains H₃BO₃;2.86 gL⁻¹, MnCl₂•4H₂O; 1.81 gL⁻¹, ZnSO₄•7H₂O; 0.22 gL⁻¹, Na₂MoO₄•2H₂O; 0.39 gL⁻¹, CuSO₄•5H₂O; 0.08 gL⁻¹, CuSO₄•5H₂O; 0.08 gL⁻¹, Co(NO₃)₂•6H₂O; 0.05 gL⁻¹. The media was sterilized by autoclaving at 15 psig for 20 min and cooled to ambient temperature before use.

P. kessleri was grown on a BBM medium with pH 6.5 ± 0.4. *P. kessleri* grown to the logarithmic phase was inoculated into a 500 ml Erlenmeyer flask containing 250 mL BBM medium. The mixture was then placed at 24±1 °C, and under 12 h light, 12 h dark conditions using a white light source (150 µmol photons m⁻²s⁻¹) and mixed by spargers to introduce air into media.

5.2.1.2 Desalter effluent media

Desalter effluent was sourced from two desalting systems, Coker Brine and AV Brine, from the Imperial Oil refinery located in Sarnia, ON, Canada. The effluents originate from treatment of Alberta crude oil. The composition and characteristics of these desalter effluents were analyzed at the Maxxam Analytics Laboratories in London, Ontario, and the results are displayed in Table 5-1. The desalter effluent was centrifuged for 40 min at a speed of 3000 rpm, filtered using 45 µm filters to remove suspended solids and microorganisms. Growth of *C.Kessleri* were investigated in (i) two types of wastewater media, (ii) without supplementation and with (50% v/v) Bold basal media (BBM), and (iii) in two cultivation conditions, heterotrophic and mixotrophic. The experiments were designed with three main factors (variables) and two levels: Nutrient BBM (A) [50 ml/ 0 ml], Light intensity (B) [heterotrophic/mixotrophic], and desalter effluent (A) [Coker Brine/ AV Brine]. Synthetic desalter effluent was made using chemicals purchased from Sigma Aldrich (Toronto, Canada).⁵² The components of the simulated desalter effluent were 1 gL⁻¹ NaCl in 1 L mineral media.

Table 5-1: Analyses of desalter effluent from two sources Coker Brine (CB), AV Brine (AVB) by Maxxam Analytics Laboratories

Hydrocarbons	AV BRINE (AV)(mgL ⁻¹)	COKER BRINE (CK) (mgL ⁻¹)	Dissolved Metals	AV BRINE (AV) mgL ⁻¹	COKER BRINE (CK) mgL ⁻¹
Benzene	12	11	Aluminum (Al)	0.032	Not Detected
Toluene	11	7.6	Arsenic (As)	0.051	0.025
Total Xylenes	5.1	2.9	Barium (Ba)	0.48	0.67
F2 (C10-C16 Hydrocarbons)	5.8	3.7	Boron (B)	1.3	1.1
F3 (C16-C34 Hydrocarbons)	1.7	3.9	Calcium (Ca)	86	84
F4 (C34-C50 Hydrocarbons)	ND	0.81	Lithium (Li)	0.21	0.11
Total BOD	700	270	Magnesium (Mg)	13	19
Chemical Oxygen Demand (COD)	1100	600	Manganese (Mn)	0.15	0.16
Phenols-4AAP	6.9	37	Phosphorus (P)	0.73	1.5
Dissolved Chloride (Cl)	840	330	Potassium (K)	18	7.3
Total Ammonia-N	47	13	Silicon (Si)	3	5.7
Total Phosphorus	0.48	0.22	Sodium (Na)	400	190
Total Kjeldahl Nitrogen (TKN)	45	95	Strontium (Sr)	2.8	1.3

5.2.1.3 Microalgal Batch Cultivation

After growing microalgae to the mid-logarithmic phase. Before the start of the experiments, 1 ml of the Microalgae inoculum cultures (50 ml media) (with 242×10^4 cells/ml) were transferred to 8 samples with defined specifications as in Table 5-3, (in 250 ml flasks). Table 5-2 explains the abbreviation of the experimental protocols (4 factors) for Table 5-3.

Table 5-2: Explanation of abbreviations of different conditions for Experimental protocol in Table 5-3 below.

Description	Abbreviation	Description	Abbreviation
AV Brine:	AV	Heterotrophic	H
Coker Brine:	CK	Mixotrophic	M
Simulated Desalter effluent + Benzene (25 mgL ⁻¹)	Sim D.E + Benzene (25)	BBM	B
AV Brine+ Coker Brine+ Phenol (65 mgL ⁻¹)	AV+ CK+ Phenol (65)	AV Brine+ Coker Brine+ Benzene (35 mgL ⁻¹)	AV+ CK+ Benzene (35)

Table 5-3: Experimental protocols and response for two sources of desalter effluent

Run	Factor 1	Factor 2	Factor 3	Response 1	Response 2	Response 3	Response 4	Response 5
	Á:Supplement %	β:Mode of Cultivation	Ç:Desalter effluent (50 ml)	COD Removal	Phosphorous Removal%	Ammonium Removal	Lipid Production	Biomass Production
	%	H, M	CK, AV	%	%	%	mg Lipid/mg dry weight	mgL ⁻¹
1	0	H	CK	1.4	88.5	43.6	0.39	225
1	0	H	CK	1.1	84.5	69.2	0.34	200
2	B	H	CK	28.6	93.3	50	0.48	366.7
2	B	H	CK	18.8	97.4	60	0.41	150
3	0	M	CK	0	90.7	24.6	0.64	216.7
3	0	M	CK	0	88.7	0	0.70	200
4	B	M	CK	21.2	92.7	7.4	0.11	225
4	B	M	CK	28.8	98.1	16.7	0.10	274.1
5	0	H	AV	61.5	100	36.8	0.43	450
5	0	H	AV	77.7	100	60.2	0.41	483
6	B	H	AV	78.5	91.9	58.5	0.76	514.3
6	B	H	AV	81.7	91.7	37.5	0.78	500
7	0	M	AV	76.2	100	64.3	0.37	458.3
7	0	M	AV	62.6	100	90.9	0.42	566
8	B	M	AV	72.7	97.6	90.6	0.50	446.7
8	B	M	AV	80.8	100	72.3	0.57	500
9	B	M	AV+CK+ Phenol (65ml)	86.4	98.8	47.4	0.24	483
9	B	M	AV+CK+ Phenol (65ml)	79.4	100	89.4	0.4	300

10	B	M	AV+CK+ Benzene (35)	65.5	94.1	41.8	0.71	225
10	B	M	AV+CK+ Benzene (35)	61,8	88.6	66,1	0.85	300
11	B	M	Sim D.E + Benzene (28)	GC and OD analysis				

To investigate the growth of *P. kessleri* in desalter effluent containing phenol and benzene, the experiments were designed as described in Table 5-3. One flask and two serum bottles 250 ml in volume were used for the investigation of *P. kessleri* growth in phenol and benzene. At Run 9, phenol was added to the mixture to study the growth of microalgae in the media containing phenol. Run 10 was conducted similarly to Run 9; however, benzene was added to the culture instead of phenol. The culture was sealed in a serum bottle using a rubber-metal cap to avoid volatilization. The lid was opened once a day for sampling, and this influenced the air inside the bottle. Run 11 was benzene and simulated desalted effluent as a control sample was provided without microalgae.

The effect of the application of the desalter effluent as a culture medium on the growth and biochemical composition of *P. kessleri* biomass was studied. Eight samples in 250 ml flasks were prepared as illustrated in Table 5-3. One flask of phenol with a concentration of 65 mgL⁻¹ was added and the second flask, 35 mgL⁻¹ benzene, was added as displayed in Table 5-3. To each flask, 1 ml of *P. kessleri* with an average 242×10^{-4} cells ml⁻¹ was added. The growth of *P. kessleri* in 11 flasks was monitored. These flasks (batch photobioreactors) at temperature 24 ± 1 °C were placed in the shaker and exposed to the white light source (130 μ mol photons m⁻² s⁻¹, 12/12 h light/dark). The heterotrophic condition was applied by wrapping an aluminum sheet around the flasks to prevent light. The algal solution was shaken in the rotary shaker (VWR, Mississauga, Ontario, Canada) at 170 rpm. The cell density of the culture was measured using the cell counter once every day for 12 days. All experiments were performed in duplicate and the initial culture conditions were the same as above for 12 days.

5.2.2 Analytical Methods

5.2.2.1 Determination of algal growth

Cultures were periodically monitored by cell counting under an optical microscope (40×/0.65). Leica was performed by using a hemocytometer. The specific growth rate and doubling time of microalgae were calculated according to the following equations:

$$\text{Specific growth rate (d}^{-1}\text{)} \quad \mu = \frac{\ln \frac{n_a}{n_b}}{t_a - t_b} \quad (5-1)$$

5.2.2.2 Biomass determination

For dry weight determination, biomass was separated from the medium by centrifugation of 2 ml samples in preweighed microtubes at 10000 RPM for 5 min (Micromax Centrifuge, (Hyland Scientific Company, WA, USA) and washed twice with distilled water. The residue was dried at 105 °C for 12 h and weighed on an analytical balance (METTLER TOLEDO AB204-S, Giessen, Germany). The difference in quality between the two values was recorded as the algal dry weight (DW). The formula is as follows in Equation 5-2:

$$DW = \frac{W_2 - W_1}{V} \quad (5-2)$$

where DW is the microalgal dry weight (g L⁻¹), W₁ (g) is the constant dry weight of the microtube, W₂ (g) is the total weight of the microtube and algal solution after drying in the oven, and V (L) is the volume of the algal cultivation.

5.2.2.3 Determination of wastewater treatment quality from desalter effluent

To determine the desalter effluent, the 2 mL microalgal suspension in liquid samples were centrifuged at 10000 rpm and 4 °C for 40 min, and then, the supernatant was separated to measure the concentrations of the Chemical Oxygen Demand (COD, mgL⁻¹), Ammonia Nitrogen (NH₃-N, mg l⁻¹), and total phosphorus (P_{tot}, mg L⁻¹). These parameters were measured using Hach Kits (HACH, USA) and hatch method, Spectrophotometer (HACH DR 2800) and DRB200 Reactor. Nutrient removal efficiency (RE, %) was calculated according to Equation 5-3

$$\mathcal{R} = \frac{C_i - C_f}{C_i} \times 100 \quad (5-3)$$

where C₀ and C₁₂ are the nutrient concentrations (mg L⁻¹), Ammonia(N) and Phosphorous (P) at the initial concentration on Day 0 and C₁₂ at their initial and final concentrations on Day 1 and Day 12, respectively.²⁴³

5.2.2.4 Determination of total lipid content

The neutral lipid content was obtained after 12 days cultivation. Lipid extraction and the determination of the oil content was conducted following a modified version of the Bligh and Dyer method (Bligh and Dyer 1959) described by Gao in 2019.²⁵⁰ Zonouzi reported that the optimum solvent to maximize oil extraction yield from microalgae was chloroform/methanol with a ratio of 2:1²⁴⁹. For lipid extraction, a pre-weighed, known amount of dried algae was weighed and placed in a 10-mL centrifuge bottle. Then, 3 mL methanol and 1.5 mL chloroform (ratio 2:1)^{251,252} were added to the bottle. The solution was mixed. Cell walls were broken with a mini-bead beater for 8 min, and for 30 minutes by an ultrasonic bath (BRANSON-1210). Next, the mixture samples were centrifuged

(5430R, Eppendorf, Hamburg, Germany) at 3500 rpm for 40 min. Methanol and chloroform 1:2 were added with the same ratio, and the above procedure was repeated using the bead beater and ultrasonic bath (sonicator). The mixtures were then centrifuged at 3000 rpm for 40 min, and the lower liquid layer was taken by pipet and added in the preweight pan to dry in the open air and then weighed. Extraction of biomass was repeated twice as described above. The total lipid content productivity for each sample was calculated using Equation 5-4:

$$\text{Total lipid} = \frac{w_3 - w_2}{w_1} \times 100 \quad (5-4)$$

where Total Lipid (%) is the weight percentage of the total lipid in dried algal, w_1 (g) is the dry weight of the microalgae, w_2 (g) is the weight of empty aluminum pan, and w_3 (g) is the total weight of the algal lipids and aluminum pan after the algal lipids were extracted in Equation 5-4.²⁵⁰

5.2.2.5 Analysis of phenol and benzene removal

According to the experiment listed in Table 5-3, removal of phenol and benzene by *P. kessleri* from desalter effluent was studied by observing the kinetic growth of microalgae, cell counting, and by measurement of COD, N, and P percent removal.

5.2.2.6 Determination of benzene in simulated desalter effluent

To be sure of the reduction of benzene resulting from the growth of *P. kessleri* in desalter effluent, Gas chromatography (GC) analysis was applied.

5.2.2.7 Materials, sample preparation, equipment and chromatography condition

Benzene anhydrous (99.8%) as a certified standard and anhydrous (99.8%) diethylene glycol as an internal standard²⁵³ were used in Benzene determination in simulated desalter effluent. Analytical-grade acetone, Dichloromethane was used for extraction of benzene from the sample. Agilent 7890, a gas chromatograph, was employed with FID (Flame Ionization Detector), which had J&B DB-Wax 122-7032 column; 30 m x 0.25 mm and ID 0.25 μm .

5.2.2.7.1 Chromatographic conditions

The gas chromatography Methods 1501 and 2005 Column were used for the analysis of benzene Chromatographic conditions. The following conditions were used in the investigations. The oven temperature program was 40 °C for 5 min and ramped to 220 °C (20 min) at 10 °C/min. The injection split was 1:100 and the temperature was 250 °C. Then 1 μl of the extract was injected into the GC system in CS_2 , Detector FID, at 300°C, Nitrogen makeup gas at 30 mLmin^{-1} .

5.2.2.7.2 Preparation of standard solutions

From a benzene sample with a purity of 99.8% and density of 874 000 $\mu\text{g mL}^{-1}$, preparation of work standard solutions was made at known concentrations of benzene, DCM, and the internal standard. The internal standard work solution (Diethylen Glycol) was prepared in acetone from its certified standard of reference. Then, each benzene standard and the extracted sample were added with the same amount, in such a way that it kept a constant concentration in all solutions. Standard solutions were stored in amber glass containers and kept under refrigeration.

5.2.2.7.3 Extraction and chromatographic analysis

The extraction and analysis process of benzene from simulated desalter effluent was performed based on Grzegorz Boczkaj's instruction with some modification.²⁵⁴ A 10 ml sample of the effluent was placed in a centrifuge tube. Next, 0.5 g of NaCl, 0.4 mL acetone and 0.5 mL of dichloromethane were added to the sample. The pH was adjusted to 7.0 and the sample was shaken for 1 min, followed by centrifugation at 3500 rpm for 40 min. Then, 200 μ l of benzene (lower layer) was transferred to HPLC glass vial (1ml) to be injected in the GC/FID to determine and analyze benzene.

5.2.2.7.4 Determining BTEX concentration in the extract

For determining benzene concentration, calibration curves were built for each analyte. The process was performed through the chromatographic analysis of a blank of reagents and a series of standards prepared from a benzene standard with an internal standard (diethylene glycol) in dichloromethane solvent. Benzene determination requires the construction of one calibration curve interval; one interval within the high and low range of 2 and 24 μ g ml^{-1} concentration. Response factor and analyte concentration was calculated using the Gallego-Díez procedure.²⁵³

5.2.2.8 Statistical analysis

The analysis of variance one-way (ANOVA) was employed to measure the significance of regression coefficients with a confidence level of 95% to establish statistical significance. Model accuracy was evaluated by the regression coefficients of R^2 and adjusted R^2 (adj- R^2). Linear regression correlation and two factor interaction analysis were conducted with the data using Design-Expert® Software Version 11 - Stat-Ease. To analyze the effect of desalter effluent, light, and nutrient (BBM) on wastewater treatment quality, analysis of variance of the COD removal, phosphorous and ammonium removal, biomass production, and lipid content, were used and p -values below 0.05 were considered significant. All the experiments were at least duplicated unless stated. The mean of the samples was reported

and the STDEV was shown as an error. The data were examined if they met the assumptions of normality and homogeneity of variance before calculation.

5.3 Result and Discussion

5.3.1 Growth of *Parachlorella kessleri* in desalter effluent

The performance of microalgal growth, *P. kessleri* is shown in real desalter effluents, AV Brine, CK Brine, and mix of desalter effluent AV and CK Brine in Figures 5-1, 5-2, and 5-3, respectively. Figure 5-1 displays the growth of *P. kessleri* in AV Brine under heterotrophic / mixotrophic condition, and with/ without 50% BBM (additional supplement). No lag phase was observed in the microalgal growth curves with different media compositions in AV Brine, which indicated that the microalgae *Parachlorella kessleri* adapted well to the conditions of real desalter effluent. When the real desalter effluent was inoculated with *P.kessleri*, the number of green algae gradually increased with time. After 12 days of cultivation, *P. kessleri* in AV brine desalter effluent achieved higher cell concentrations ranging from 112 to 326, 40 to 274, 58 to 304, 90 to 620 *10⁻⁴ cells ml⁻¹ for Runs 5, 6, 7, and 8, respectively, as demonstrated in Table 5-3. Figure 5-2 displays the growth of *P. kessleri* in CB compared to AB. The biomass production of *P. kessleri* in CK desalter effluent was relatively lower during the initial two days compared to AV. *P. kessleri* in CK desalter effluent at runs with the condition of 1, 3 and 4 had moderate biomass concentrations from 56 to 174, 57 to 167, and 52 to 227*10⁴ mg L⁻¹, respectively. Run 2 had a very limited growth of alga compared with initial cells on the first day of cultivation. Since Run 2 was diluted in BBM, the amount of COD was reduced. However, COD_{AV} was much more than COD_{CK}.

Figure 5-1 shows that *P. kessleri* in desalter AV has more cell growth than desalter effluent CK in Figure 5-2 at different nutrient levels (0, B), light (H, M). Figure 5-3 shows the growth of *P. kessleri* in a mixture of two types of desalter effluent and BBM 50% (v/V) under mixotrophic condition (Runs 9 and 10). Mixture of desalter effluents with phenol is

a proper culture for the growth of *P. kessleri* because the number of cells increased from initial cells of 64×10^4 cells ml^{-1} to 330×10^4 cells. ml^{-1} .

Phenol did not inhibit *P. kessleri* growth in the mixture of the two types of desalter effluent while benzene stopped further growth on Day 3. It grew from 58 to 110×10^4 mgL^{-1} and was inhibited at the same level of growth until Day 12. This sample was exposed to air for 1 month, after which the cells began to grow. This result revealed that this species of cells are resistant to benzene. This microalga can grow in desalter effluent when toxic chemicals such as phenol and benzene are present.

In general, all presented results suggested that the growth of microalgae in real desalter effluent was dependent on the desalter effluent type. Desalter AV has twice more COD than the CK type.

Table 5-4 presents the specific growth rate for 10 experimental runs. The specific growth rate differed significantly among desalter effluent types. *P. kessleri* achieved the highest specific growth rate when it was grown in ABBM. The CB and AB at heterotrophic conditions and CBB in mixotrophic conditions displayed a moderate growth rate. Despite adding nutrients in CB, the growth of microalgae, *P. kessleri* under heterotrophic condition demonstrated the lowest specific growth rate, when the one is the specific growth of *P. kessleri* in “mixotrophic + no BBM” with a slight difference.

P. kessleri achieved the highest growth potential in AV Brine with supplement media (AVB) compared with the other 10 tested conditions listed in Table 5-3. The specific growth rate of *P. kessleri* has been investigated in other studies under different conditions: heterotrophic, autotrophic, mixotrophic, with and without carbon source is between 0.31d^{-1} and 0.8d^{-1} .²⁵⁵ In another study, the range of specific growth rate was reported between 0.17 to 0.5d^{-1} in Day 6.²⁵⁶ In our investigation the rate of growth after 6 days is higher than 12 days (Figures 5-1 and 5-2). Hanafy reported in 2013 the specific rate of *P. kessleri* increases by increasing glucose (carbon source) from 10 to 80gL^{-1} , but a further increase in glucose concentration resulted in decrease in specific growth rate.²⁵⁷ Specific growth rate reduced from 0.12d^{-1} to 0.037d^{-1} when the initial inoculum in a wastewater increased from 25mgL^{-1} to 400mgL^{-1} .²⁵⁸ Maximum specific growth rate (μ_{max}) of *P. kessleri* in

different bioreactors was obtained after 20 days. The μ_{\max} varied between 0.19 d^{-1} and 0.39 d^{-1} .²⁵⁹ Based on the above literature, the specific growth ranged between 0.037 d^{-1} to 0.5 d^{-1} after 6 days and more. Thus, in our case the specific growth rates in the two types of desalter effluent in Table 5-4 represent appropriate kinetic growth and for *P. kessleri*.

While the physicochemical analysis of the wastewater indicated the presence of most essential nutrients required for algal growth and organic carbon substrate (COD), the AV Brine effluent had a better balance of nutrients and organic carbon than the CK Brine effluent. These organic carbon compounds can be consumed by *P. kessleri* and promote their growth allowing efficient mixotrophic and heterotrophic metabolism as illustrated in Figures 5-1 and 5-2. Phenol cannot inhibit the growth of *P. kessleri* in desalter effluent (Figure 3). Figure 5-3 shows an initial inhibition until Day 6 and then the cells were duplicated until Day 12. However, there is low growth of microalgae in desalter CK compared with growth in desalter AV, and in phenol (Run 9, when two types of desalter effluent were mixed) due to toxicity of phenol and low COD.

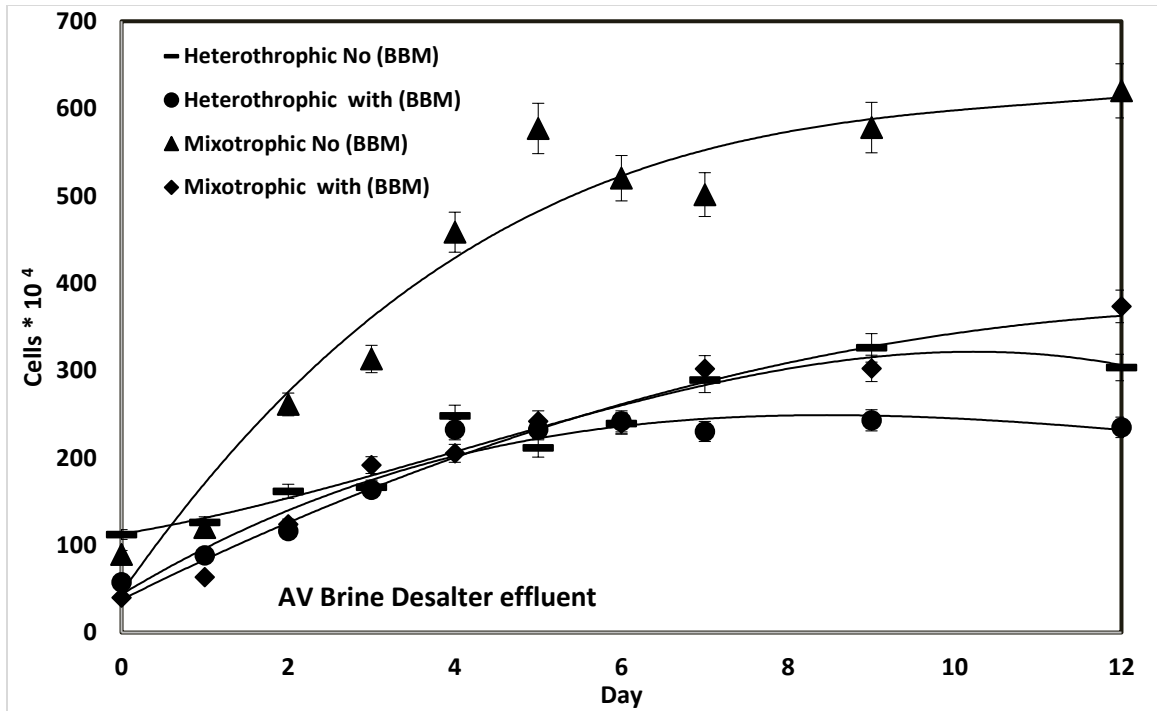


Figure 5-1: Cultivation of *P. Kessleri* cells in AV media under different modes as described in Table 5.3

Because ammonia at high concentrations inhibits the uptake of nitrate (NO_3) by microalgae. In the presence of ammonium, nitrate uptake was depressed in light (mixotrophic) conditions; however, this phenomenon was more pronounced in the heterotrophic condition. Many studies have demonstrated the preference of algae for ammonia nitrogen over nitrate nitrogen and have indicated the inhibitory effect of ammonia on the rate of nitrate uptake.^{261–263}

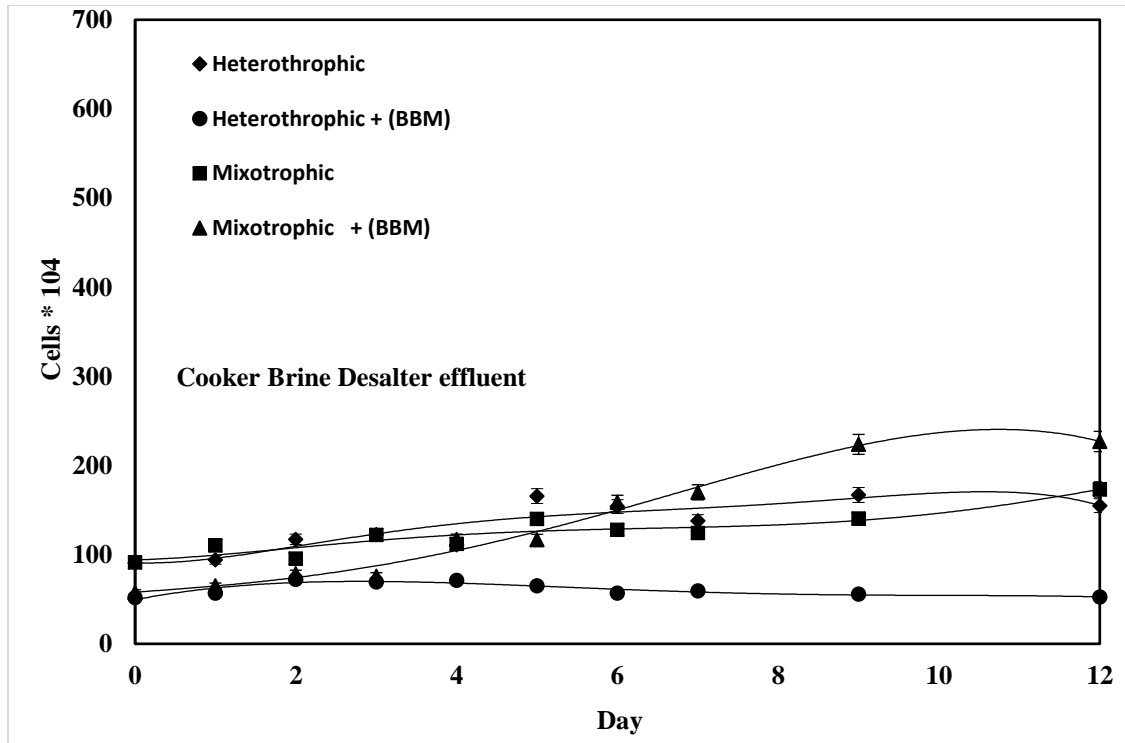


Figure 5-2: Cultivation of *P. Kessleri* cells in CK media under different modes as described in Table 5.3

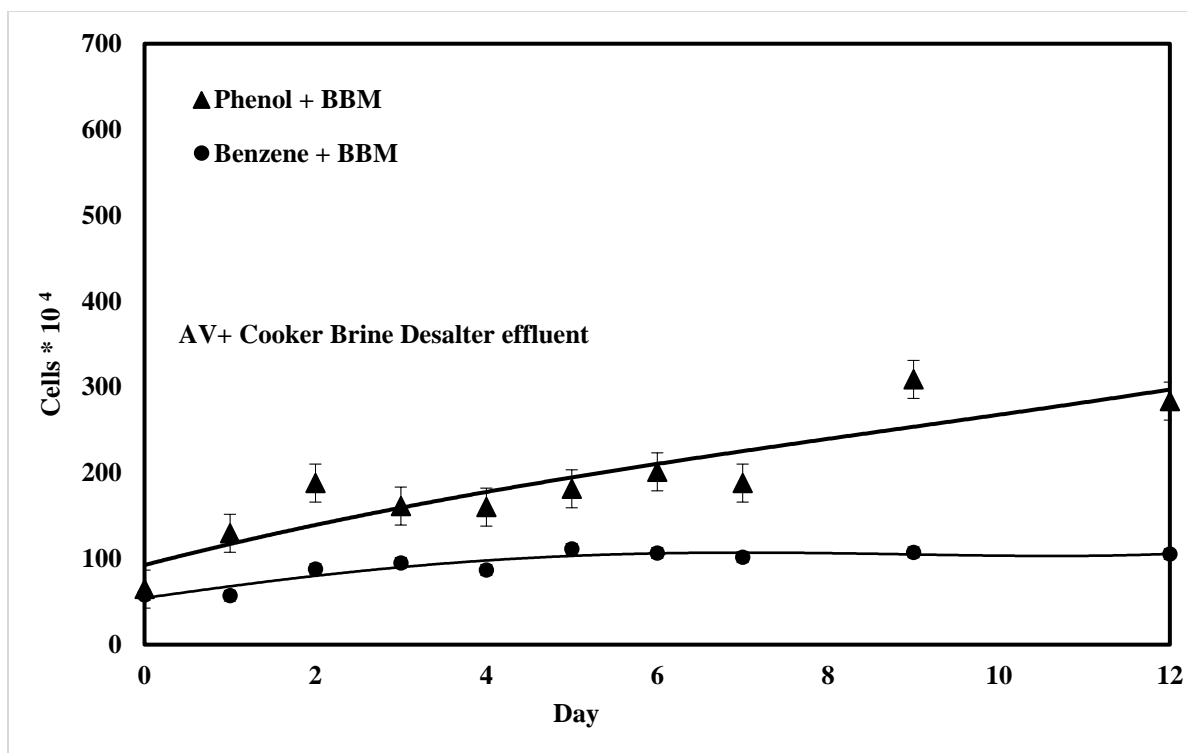


Figure 5-3: Cultivation of *P.Kessleri* cells in CB+AV under different modes as described in Table 5.3

5.3.2 Biomass production

Figure 5-4 displays the dry weight of *P. kessleri* growth in AV and CK Brine desalter effluents in 10 different runs. The maximum biomass concentration (dry weight) of *P. kessleri* was in AV Brine—512 mg l⁻¹. As shown in Figure 5-4, the dry weight differed significantly among desalter effluent types ($p < 005$), nutrient (0, 50% BBM) and light intensity (H, M) conditions.

Table 5-5 contains an analysis of the effect of three main factors in biomass production. The response model of biomass production was linear. The model F -value of 92.63 implies that the model is good fit. There is only a 0.01% chance that an F value this large could occur due to noise.

P-values less than 0.05 indicate that the model terms were significant. In this case, desalter effluent type was a significant model term. The lack of fit *F value* of 0.29 implies the lack of fit was not significant relative to the pure error. There is a 92.70% chance that a lack of fit *F value* this large could occur due to noise. Non-significant lack of fit shows that the model is fit. The Predicted R^2 of 0.83 predicts a regression model response for new observations. Adeq Precision measures the signal to noise ratio. A ratio greater than 4 is desirable. Adeq Precision of 13.6 indicates an adequate signal. This model can be used to navigate the design space. The biomass in CK in mixotrophic condition was significantly lower than that of biomass inoculated in AK ($p < 0.05$).

Table 5-4: Specific growth rate and doubling time of *P. kessleri* growth under different modes as described in table 5.3

Mode of cultivation	Desalter effluent	Media	μ (day ⁻¹)
Mixotrophic	CK		0.060
		B	0.216
	AV		0.149
		B	0.442
Heterotrophic	CK		0.082
		B	0.057
	AV		0.136
		B	0.117
Mixotrophic	AV+CK	Phenol, B	0.130
		Benzene+ B	0.168

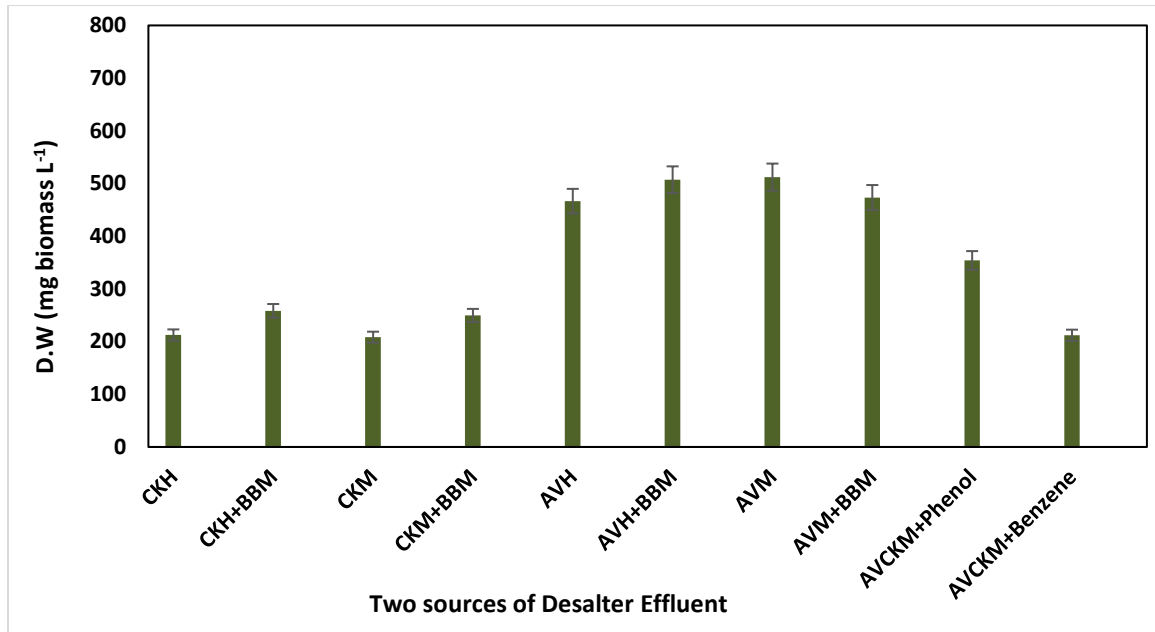


Figure 5-4: Mean of *P. kessleri* dry weight under different modes as described in Table

5.3

5.3.3 COD removal and desalter effluent treatment quality

The pollutant removal abilities of the 10 different conditions in the two types of real desalter effluent are depicted in Figures 5-5. The pollutant concentration in all the tests displayed a sharp decrease after 12 days. The maximum removal efficiency of COD, nitrate, ammonium, and total phosphorus were 82.9%, 22.2%, 77.6%, and 100%, respectively. The COD, nitrate, ammonium, and total phosphorus removal efficiencies from desalter effluent without adding BBM were 62.4%, 2.5%, 77.6%, and 100%, respectively. When desalter effluent CK or AV Brine were used as only media for *P. kessleri*, lack of nutrient inhibited algae growth and resulted in reduced microalgae growth. Figures 5-5 display the results of the two types of desalter effluents and mix of both. The levels of COD were compared with CK or AV Brine, when *P. kessleri* was used to inoculate AV and CK separately. The high removal efficiency of pollutants with microalgae was

mainly dependent on the amount of the carbon source. Mixing desalter effluents and adding hydrocarbon (phenol or benzene) removed the excess nitrate and increased the quality of mixed desalter effluent more so than was the case in CK Brine. The results of pollutant removal rates for COD, ammonia (NH₃) and total phosphorous (P), suggests that desalter effluent types are effective in pollutant removal ($p < 0.005$). In addition, the partial removal of COD was attributed to supplement media (BBM) and interaction between desalter effluent type and BBM interfere. The p values of the model in Table 5-5 for COD confirms this analysis.

Microalgae *P. kessleri* exhibited high pollutant degradation capability in real desalter effluent, while rare microalgae were able to grow and remove pollutants while being exposed to toxic compounds and high salt concentrations. Because of *P. kessleri* growth, COD, total nitrogen ammonia and total phosphorous levels in AV desalter effluent were reduced by up to 100%, 90%, and 100 %, respectively. Biological assimilation in desalter effluent with culture supplemented (BBM) was considered the main mechanism of nitrogen removal in ammonia. Assimilation by *P.kessleri* appeared as the principal mechanism of phosphorous remediation in desalter effluent. Overall, cultivation of microalgae in desalter effluent may be more favorable from an economical and sustainability perspective due to the elimination of the costly and energy-intensive separation technologies and biological treatment steps. These findings demonstrate that when AV Brine desalter effluent is diluted by BBM and when two types of desalter effluent (AV Brine and Coker Brine) are mixed together, this can serve as critical nutrient source for biomass generation and that robust microalgae can play potential roles in desalter effluent phycoremediation.

Table 5-5 reveals that the response of COD removal is significant. The Model F value of 185.81 implies the model is significant (p -values < 0.05). In this case, nutrient (BBM), types of desalter effluent, and interaction between these two were significant model terms. The lack of fit F value of 0.09 implies *the Lack of fit* was not significant and the model fits well. The predicted R² value of 0.96 is in reasonable agreement to predict responses for future observation. Adeq Precision of 28.7 indicates an adequate signal. This model can be used to navigate the design space.

5.3.4 Investigation of ammonia removal

Ammonia is added to the desalter effluent for pH adjustment; therefore, ammonia is the main component in desalter effluent. In addition, amines are used in the production process as H₂S scavenger is associated with crude, which partition into the water phase in the desalter, also lead to the wastewater treatment plant. This leads to very large COD and nitrification (TKN) loads in desalter effluent biotreatment.

Inorganic nitrogen compounds are typically toxic for aquatic animals, compared with phosphate. In particular, unionized ammonia (NH₃-N) and nitrite exceed the toxicity of nitrate.^{266,267} According to water quality guidelines from the ministry of environment in Canada in 2009, the nitrogen and ammonia concentration should not be more than 10 and 25 mgL⁻¹ for the protection of aquatic Life.²⁶⁷ High nutrient concentration in AVB led to higher growth of microalgae compared with the same desalter effluent with no nutrient.

While CKBH demonstrated a better growth in heterotrophic conditions (see Figure 5-5). The NH₃-N concentration in desalter effluent inoculated with microalgae decreased significantly to 3 to 5 mgL⁻¹(data not shown). The removal of ammonia in AB was considerably more than CK effluent ($p < 0.05$). This removal ability increased when desalter effluent was in the mixotrophic condition ($p < 0.05$). While the high ammonia content did not inhibit the growth rate of some microalgae, the species from *Chlorella* and *Scenedesmus* exhibited high tolerances to ammonia levels varying in the broad range 30 to 300 mgL⁻¹ of ammonia-N. In addition, ammonia may be a preferable source of nitrogen because its assimilation does not require an electron donor and energy for the reduction in contrast to nitrate-N. The improvement from the enrichment was more evident for the secondary effluent since it had a lower original nutrient content compared to the primary effluent.²⁴³

Importantly, algal growth was associated with a significant reduction in the concentration of nitrogen and phosphorus, which indicates algae's potential in phycoremediation applications. The amount of biological phosphorus (P) removal is dictated mostly by the

final concentration of algal biomass. In this study, 90% of P was removed in the AV brine in four conditions (AVH, AVM, AVBH, and AVBM) by microalgae. Indeed, the phosphorus may be another limiting nutrient for algal cultivation in the desalter effluent according to P concentrations displayed in Table 5-1.

Depending on substrate availability, algal growth can either be enhanced or suppressed by the presence of NH_4^{268} . At the lower end of the availability spectrum, NH_4 is frequently reported as the preferred N source of most algae due to its superior uptake kinetics, whereas at the higher end of the available range, NH_4 has been shown to inhibit growth at concentrations exceeding $0.1 \text{ mmol-N L}^{-1}$ and suppress algal growth, with the resulting toxic effects not easily alleviated.²⁶⁹

Response in terms of ammonia removal under the three main factors of nutrient (BBM), light, and desalter effluent type were investigated through ANOVA (Table 5-5). The Model *F* value of 21.26 implies the model was significant. There is only a 0.01% chance that an *F* value this large could occur due to noise. *P* values less than 0.05 indicate that model terms were significant. In this case, types of desalter effluent (Ç) and interaction between BBM-Desalter (βÇ) are significant model terms. Values greater than 0.1 indicate the model terms are not significant. The lack of fit *F* value of 0.02 implies the lack of fit is not significant relative to the pure error. There is a 99.91% chance that a lack of fit *F* value this large could occur due to noise. The *p*-value of lack of fit is > 0.05 (not significant) means that the model fits well. The Predicted R^2 of 0.72 is in reasonable agreement regression model predicts responses for new observations. Adeq precision measures the signal to noise ratio. The ratio of 11.14 indicates an adequate signal. This model can be used to navigate the design space.

The wastewater nitrogen content was represented mostly by ammonia in desalter effluents, and mixed effluents contained both nitrates and ammonia (Figure 5-5). Remarkably, the $\text{NH}_3\text{-N}$ was removed in all cultures including desalter in modes CK, AV, CKB, AVB, and the mixed culture of AV + CK + B. The amount of N ($\text{NH}_3\text{-N}$) assimilated by algae from the wastewater is displayed in Figure 5-5. The graph displays a removal efficiency of up to 81.4% for NH_3 present in the AV effluent in the mixotrophic condition, approximately

12.1% for $\text{NH}_3\text{-N}$ in the CK effluent, and approximately 69.1% of N in the mixture of CK + AV desalter effluent (Figure 5-5). Therefore, a significant part of the nitrogen in CK Brine effluent could be withdrawn through its assimilation by microalgae, when it is mixed with AV desalter effluent.

5.3.5 Total Phosphorous removal

The physicochemical characteristics of desalter media are summarized in Table 5-1 and compared to BBM medium ingredients. Both types of desalter CK and AV effluents are a source of N and P for limited algal growth. They are present as organic nitrogen, ammonia or nitrate, and orthophosphate. However, the contents of N and P in CK and AV are lower than in BBM. Some components in CK are less than AV (Table 5-1).

The amount of phosphorous and carbon source is limiting factors for microalgae growth in desalter effluent. The N to P ratios are more than the suggested optimal range of 4.5 to 14 for microalgae,²⁴³ reflecting a potential P limitation. Moreover, CK effluent is even more deficient in P. Furthermore, both types of wastewater are richer in S, Mg, Ca, Fe, and Mn than BBM, but trace elements such as B, Zn, Mo, Co, and Cu exist in higher concentrations.

Nitrogen and phosphorus are essential nutrients for algal growth. As expected, the concentrations of both nitrogen and phosphorus dropped because of algal growth. The removal of orthophosphate-P for the selected cultures is depicted in Figure 5-5. In general, the higher ratios of phosphorus removal (approximately 100%) corresponded to better performing algal cultures with high biomass density at the end of cultivation.

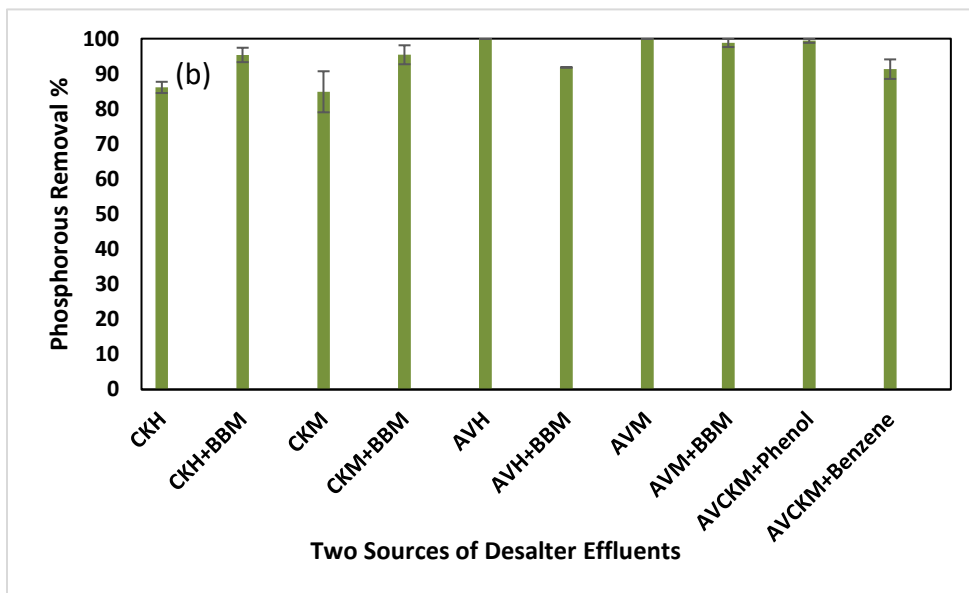
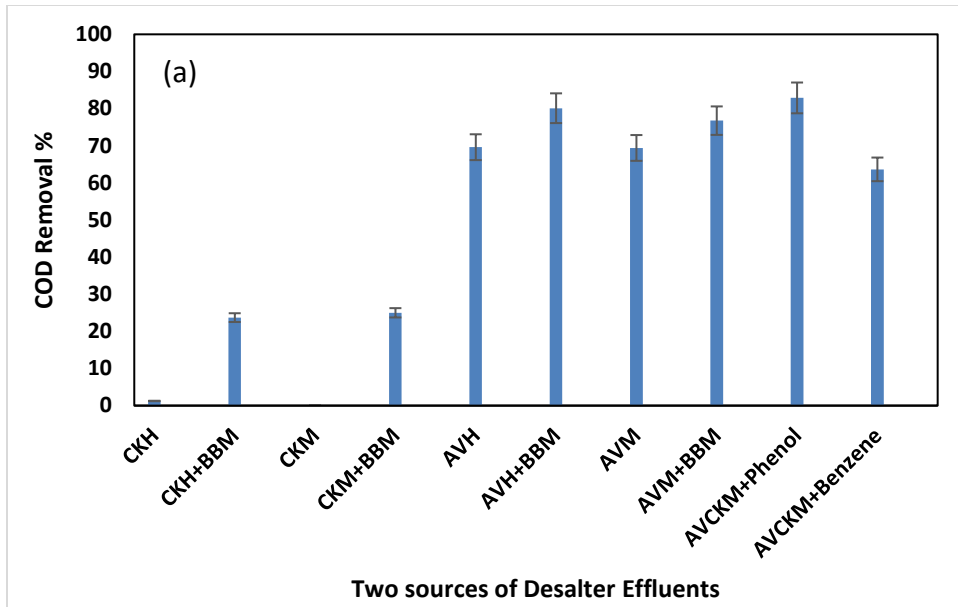
The estimated amount of P assimilated by microalgae assuming the biomass content in the range of 1% to 1.2% ash-free dry weight,²⁴³ as shown in Figure 5-4. These values correspond to the removal of up to 86.9% to 100% of P present in both types of desalter (Figure 5-5). Therefore, a significant part of the P in the AV and CK media could be taken up by microalgae.

Table 5-5 represents the ANOVA of total phosphorus removal in desalter effluent. In this case types of desalter effluent (ζ), the interaction of BBM and desalter effluent (Factors $\acute{A}*\zeta$) are significant model terms.

Table 5-5: ANOVA for quality parameters of wastewater treatment and Lipid content of P.kesslery biomass in desalter effluent in different types, nutrient concentration and light

Response	COD		NH3		Phosphorous		Biomass		Lipid content	
	F value	P value	F value	P value	F value	P value	F value	P value	F value	P value
Model	232.97	<0.0001	21.26	<0.0001	9.01	0.0018	58.98	<0.0001	13.81	0.0003
\acute{A} (BBM/0)	33.83	<0.0001	—	—	—	—	—	—	—	—
β (H/M)	—	—	—	—	—	—	—	—	—	—
ζ (AV/CK)	432.11	<0.0001	24.52	0.0003	22.34	0.0006	175.36	<0.0001	13.17	0.0092
$\acute{A} * \beta$	—	—	—	—	—	—	—	—	23	0.0005
$\acute{A} * \zeta$	—	—	—	—	14.34	0.003	—	—	31.79	0.0003

$\beta * \zeta$	-----	-----	38.23	0.0001	-----	-----	-----	-----	-----	-----
Lack of fit	1.05	0.452 9	0.81	0.5524	2.86	0.1042	0.25	0.9460	3.06	0.103
R²	0.97		0.84		0.77		0.94		0.87	
Adjusted R²	0.97		0.80		0.68		0.93		0.81	
Predicted R²	0.96		0.72		0.51		0.89		0.68	
Adeq Precision	30.72		11.13		8.79		14.53		12.28	



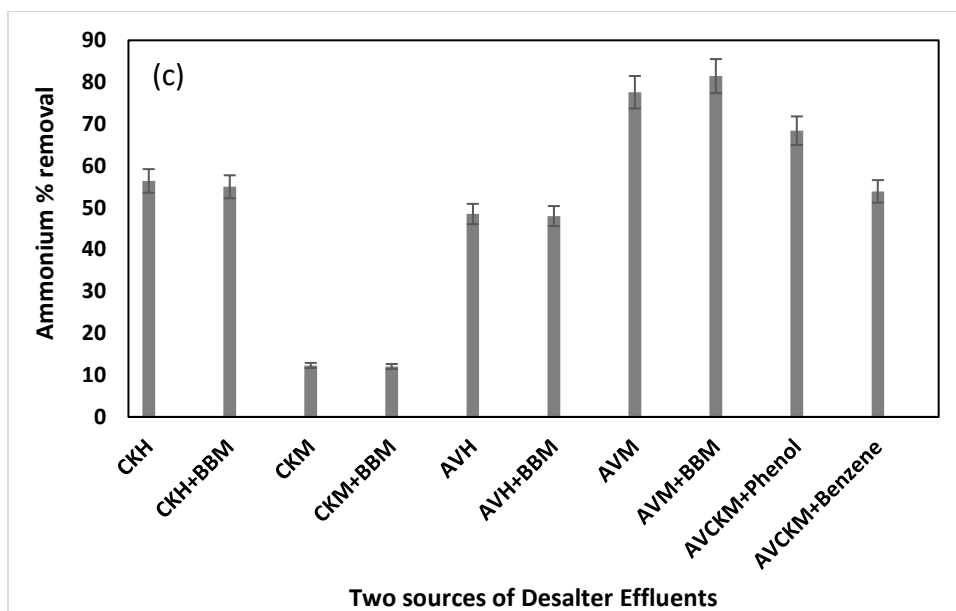


Figure 5-5: Percent removal of a. COD removal, b. Phosphorous removal, c. Ammonium removal in two different desalter effluents in 12 days culture

5.3.6 Analysis of Phenol and Benzene removal

First, the effect of benzene on the growth of *Parachlorella kessleri* in simulated desalter effluent was monitored. Due to the volatility of benzene, the control sample contained simulated desalter effluent with benzene and no microalgae were used to compare the concentration of benzene in the presence of microalgae and without algae. This method aimed to determine whether the reduction of benzene was due to volatilization or degradation by microalgae. Figure 5-6 depicts the growth of *P. kessleri* in simulated desalter effluent in the presence of Benzene for 4 days. The inhibition of *P. kessleri* growth was observed after 3 days. The initial concentration of benzene was about 28 mg l^{-1} in simulated desalter effluent. During the biodegradation experiments, the concentration of Benzene in the mixture was monitored by cell counting daily for 4 days. The number of cells grew until the end of 3 days; then, it attained a stationary phase between Days 3 and 4. Eventually, the number of cells decreased due to growth inhibition. The concentration

of benzene in simulated desalter effluent was detected using Boczkaj's extraction method²⁵⁴, and gas chromatography (GC). The results of the reduction of benzene due to biodegradation are demonstrated in the right axis of Figure 5-6. All the values are represented as means plus standard deviations.

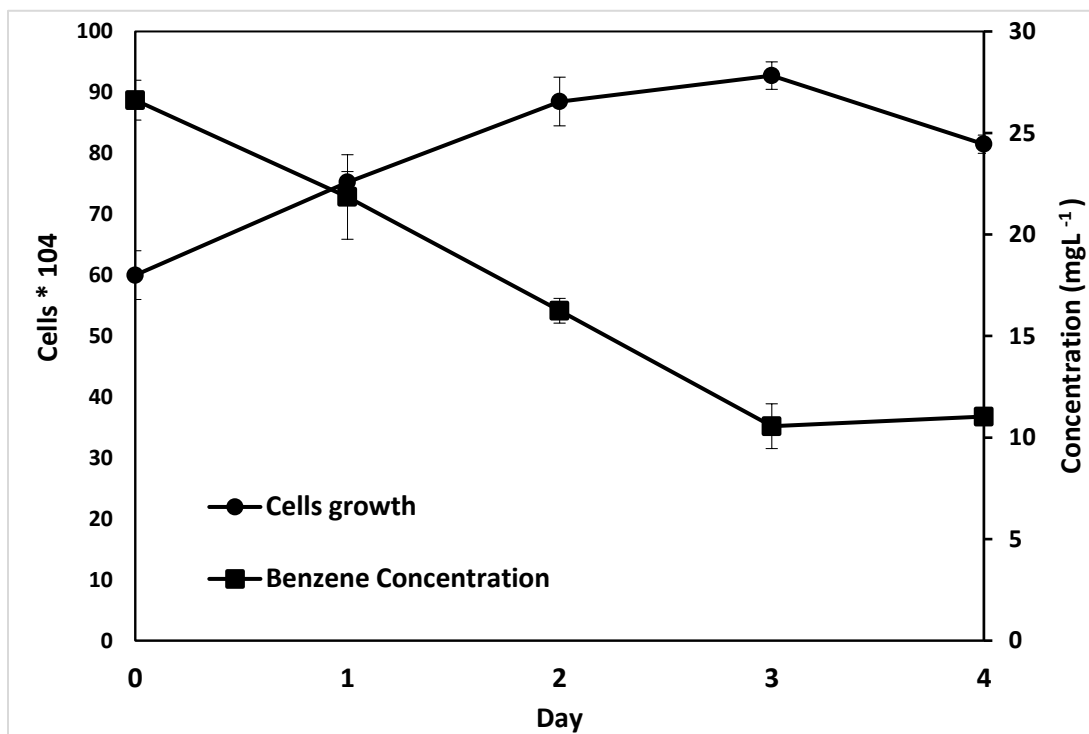


Figure 5-6: ●, Mixotrophic growth of *Parachlorella kessleri* (*P. kessleri*) in simulated desalter effluent containing Benzene

Since the biological test was conducted in a completely closed system, and benzene was the only carbon source, removal of benzene was caused exclusively by *P. kessleri*. It has been reported that this microalga in mineral media with initial benzene, toluene, ethylbenzene, and xylene concentrations of 100 $\mu\text{g L}^{-1}$ each, and without high concentration of chloride sodium was degraded during first 2 days, and then displayed growth inhibition after 2 days.²⁴⁶ *P. kessleri* in media with a salt concentration of 1000 mgL^{-1} (1gL^{-1}) was able to experience more growth, and the microalgae were inhibited on Day 4. Salt does not affect *P. Kessleri* growth negatively; it instead enlarges its cell size.²⁴⁷

Microalga changes its metabolism flexibility in order to adjust in the presence of the salt, and it also alters molecular function to tolerate high salt exposure.²⁷⁰

Results revealed that 51% of benzene was degraded within 3 days at a degradation rate of $4.1 \text{ mgL}^{-1} \text{ d}^{-1}$ and specific growth rate of 0.146 d^{-1} . Some species of algae are capable of heterotrophic growth in organic carbon sources. It was reported that microalgae can rarely complete degradation of aromatic pollutants.²⁷¹ One way of investigating the biodegradation of organic pollutants by algae is to encourage algal cells to grow in the presence of the pollutant.

Optimization of benzene biodegradation in laboratory conditions provides an opportunity to observe or determine the consortia capable of biodegrading benzene. The only carbon source in media was benzene. The maximum degradation of 51% was achieved after 3 days. Microalgae like *Chlamydomonas* spp., *Chlorella* spp., *Cylindrotheca* sp., *Dunaliella* sp., *Euglena gracilis*, *Scenedesmus obliquus*, and *Selenastrum capricornutum* demonstrate that algae are indeed capable of contributing to the degradation of environmental pollutants, either by directly transforming the pollutant or by enhancing the degradation potential of the microbial community present.²⁷¹ Utilization of the remarkable potential of algae, *P. Kessleri*, to accumulate pollutants from desalter effluent presents a novel biological method of clearing the environment of toxic elemental and organic pollutants from desalter effluent.

To ensure phenol and benzene in real desalter effluent can be degraded and removed, the experiment displayed in Table 5-3 was run. Runs 9 and 10 monitored the growth of cells and the quality of effluent after 12 days of treatment by *P. kessleri*. The number of cells in the mixture of desalter effluent when benzene concentration was 35 mgL^{-1} increased two-fold after 4 days, and then attained a stationary phase, where further growth was inhibited. Figure 5-5 shows the COD, ammonia and phosphorous removal rates were 91.3%, 69.1%, 7%, 63.6%, respectively. These results confirmed that microalga metabolism was able to remove benzene and other contaminants. When phenol concentration was 60 mgL^{-1} in a mixture of AV + CK brine desalter effluent microalgae cells grew more than four-fold than the initial cell concentration. Phenol does not inhibit its growth, and *P. kessleri* could

remove P, ammonia, and COD at rates of 99.4%, 68.4%, and, 82.3%, respectively. Interestingly, when the media is a mixture of CK and AV + BBM, there is positive nitrate reduction after 12 days of microalga growth.

Future studies can investigate the degradation of toluene, xylene and ethyl benzene in desalter effluent. The complete degradation of pollutants under these conditions usually involves the combined actions of two or more microorganisms. Under environmental conditions, the combined action of microalgae, *P. kessleri* and other microorganisms (*Debariomycys hansenii*) might be a rather important process for the elimination of undesired compounds (phenol, alkane, volatile compounds, ammonia and phosphorous) from desalter effluent and other wastewater with similar characteristics. The above analysis and results demonstrate that this species of microalgae can degrade and treat both desalter effluent in salt concentrations that are typical of crude oil in Calgary, Alberta. The results for the degradation of phenol and benzene in high metal ions in desalter effluent also suggests that they are capable of biotransforming some of these environmental pollutants.

5.3.7 Lipid content

In the present study, lipid production of *P. kessleri* in desalter effluent under different conditions in terms of the absence or limitation of light and nutrients was tested. Biomass accumulated as microalgae removed pollutant from the desalter effluent. Microalgal biomass typically contained a large share of carbohydrates, proteins, and lipids, which could be used as feedstock for different products. As shown in Figure 5-7, a high proportion of lipid was detected when *P. kessleri* was inoculated in different conditions of desalter affluent cultures. The lipid content in AV desalter effluent indicated that *P. kessleri* grew better in AV than the other tested microalgae (Figure 5-7).

Lipid content highly depends on the type of desalter. Lipid content in AV was much higher than CK ($p < 005$). During the photosynthetic processes, after about 2 weeks, microalgae

accumulate significant quantities of lipids (up to 70% of DW) in AV desalter effluent. Figure 5-7 shows a slight difference in lipid accumulation between AV in heterotrophic and mixotrophic conditions ($p < 0.05$) or for no supplement media or BBM ($p < 0.05$). The same applies to CK. These can be commercially processed into biofuels, particularly biodiesel. However, microalgal lipids are valuable not only from the viewpoint of renewable energy, but they can also be used to produce biochemicals, nutraceuticals, cosmetics, or food additives. Several studies have demonstrated that it is possible to control cell metabolism to yield a high content of energy-rich compounds, either starch and/or lipids.²⁷²

Table 5-5 presents ANOVA for Lipid content in different desalter effluents, light, and nutrient conditions. The effects of four variables at two levels (2^4) were tested based on the experiment in Table 5-2. The model response of lipid content is described in Table 5-5. The model F value of 13.81 implies the model is significant. There is only a 0.03% chance that an F value this large could occur due to noise. P values less than 0.05 indicate model terms are significant. It means the result cannot be attributed to chance. In this case, desalter effluent (C), the interaction of BBM-desalter effluent (A*C), and light-desalter effluent (B*C) are significant model terms. The lack of fit F value of 2.32 implies the lack of fit is not significant relative to the pure error. There is a 16.09% chance that a lack of fit F value this large could occur due to noise. It means the model fits well. The predicted R^2 of 0.68 is in reasonable agreement and the regression model predicts responses for new observations. Adeq Precision ratio of 12.28 indicates an adequate signal.

In general, microalgae produce lipids containing fatty acids with chains ranging from 12 to 22 carbons and up to 6 unsaturations.²⁴⁵ Microalgae can accumulate substantial amounts of lipids (approximately 5% to 50% of dry weight).²⁴⁹ Lipids can be used as a source for biofuels, as building blocks in the chemical industry and edible oils for the food and health market. Several species of microalgae can be induced to produce specific lipids and fatty acids through simple adjustment of the physical and chemical properties of the culture medium. Microalgae *P. kessleri* CCALA 255 is characterized by high biomass and lipid productivity.¹⁷⁷ The maximum lipid content of *P. kessleri* in this study was over 70% of dry weight.

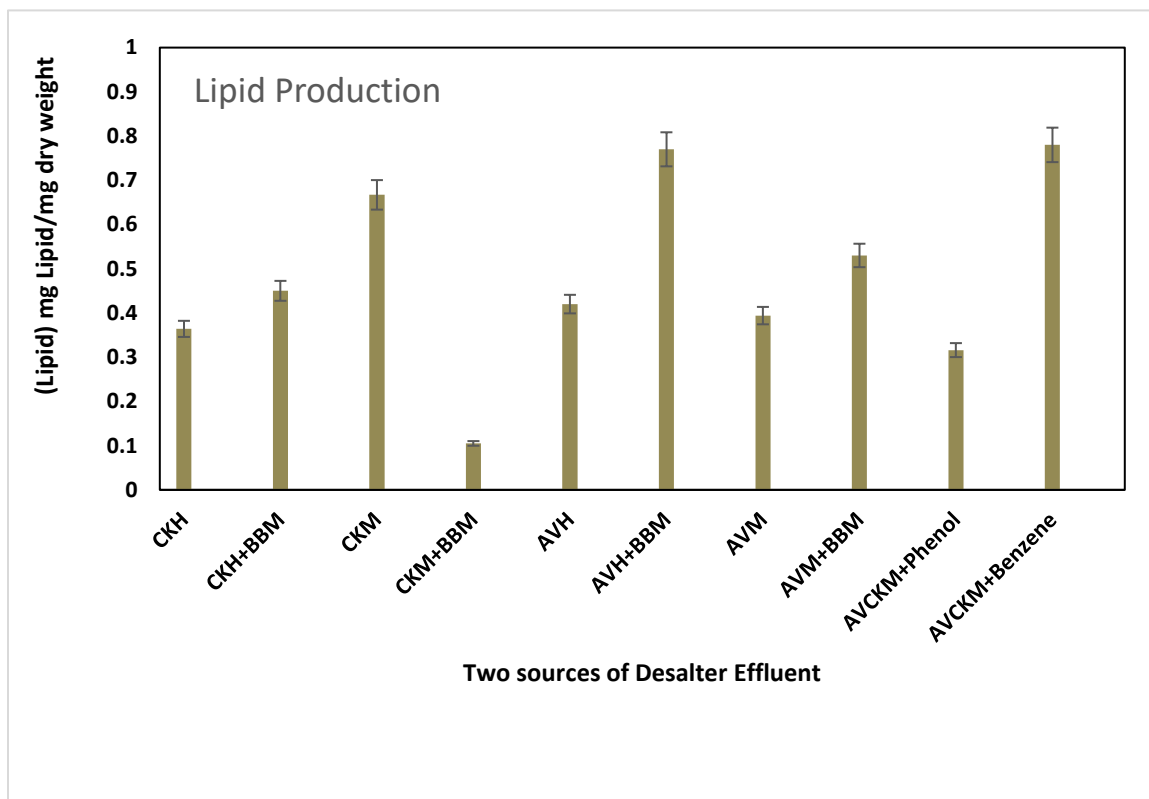


Figure 5-7: Lipid content biomass *P. kessleri* after 12 days growth in desalter effluent in different conditions

5.3.8 Effect of salt in Biomass and lipid production of *Parachlorella kessleri*

Parachlorella kessleri, a unicellular green alga belonging to the class *Trebouxiophyceae*, achieves very high biomass, lipid, and starch productivity levels.¹⁶¹ Some microalgae are salt-resistant strains that grow well even in high salinity after long-term and continuous cultivation.²⁷³ The neutral lipid production in *P. kessleri* was greatly improved under

0.35M salt concentration, as compared to that under untreated culture. According to literature, the maximum neutral lipid content (36.13% biomass) was obtained after 12 days cultivation, which was 1.31-fold higher than that of untreated culture (15.63% biomass). These results suggested that salt induced cell size.²⁴⁷ The biomass concentration of *P. kessleri* under 0.35M salt stress after 7 days cultivation was the same as that under normal condition (0.89 g L⁻¹). Similar behavior has been observed in *Scenedesmus* sp.²⁷⁴ This microalga efficiently adapted to 100% seawater salinity and enhanced its lipid content. In saline media, microalga efficiently modified its metabolic flexibility to adjust to the salinity-induced stress. Some microorganisms evolve excess salts through salt glands. Salt glands shape the molecule function and contribute to salt tolerance.²⁷⁰ Salt treatment led to a significant increase in ploidy levels. The analysis highlighted salinity-induced changes in genes involved in DNA replication, cell cycle, and so on. The increase in cell size and ploidy under salinity stress may contribute to salt tolerance by increasing the storage capacity for sodium sequestration and higher metabolic activity driving rapid cell enlargement.²⁷⁵ On the one hand, some marine microalgal strains that could grow in brackish water or seawater have been considered as potential bioenergy producers due to their characteristics of high salt tolerance and high lipid content. *Chlamydomonas* sp. JSC4, *Chlorella sorokiniana*, and *Dunaliella tertiolecta* ATCC30929 have been reported to produce lipid content of 59.4%, 57.7%, and 67.0% w/w of dry weight, respectively. On the other hand, freshwater microalgae that can grow in both the absence and presence of salts are also used as an alternative feedstock for producing bioenergy. For example, *Scenedesmus* sp. IITRIND2 cultivated under saline conditions accumulated lipids in quantities that ranged between 38.9% and 51.8% w/w of dry weight²⁴⁷

In recent years, interest in microalgae oil for animal feed and human food industries, as well as for sustainable biofuel production has increased.²⁴⁵ These research results demonstrated that salt-induced cell size increase was an effective strategy for the enhancement of oil production, microalgae harvesting, and oil extraction. Cells may cause an increase in neutral lipid content, thereby contributing to oil production. Various efforts are being made for cost-effective production of algal oil, including enhancing lipid

concentrations by using environmental stress factors and developing methods of microalgae harvesting or a combination of these. Stressful environmental conditions, such as unfavorable light intensity, temperature, high salinity, and nutrient limitation generally lead to lipid accumulation^{247,276–280} in microalgae. Among these, salt stress is of central attention. Besides enhancing lipid accumulation, it can also reduce the contamination risk and dependence on freshwater reserves.

5.3.9 Possibility of Lipid production, harvesting and extraction

Industrial scale

P. kessleri is a green alga with cells capable of utilizing organic carbon sources such as glucose²⁸¹, ethanol, and glycerol.²⁸² This makes *P. kessleri* a great candidate for photoheterotrophic and mixotrophic cultivation and offers great potential for the production of microalgal renewable biomass for biodiesel production and for different applications.²⁸³ It is important to reduce the cost of microalgal biomass production. Under mixotrophic conditions based on wastewater media, microalgae may provide flexibility to improve the economics of production, while generating valuable products. Lipid content can be increased by nitrogen or phosphate limitation, high salt concentrations, high iron concentrations or growth under heterotrophic or mixotrophic culture conditions. The microalga *P. kessleri* strain CCALA 255 is characterized by a high growth rate, tolerance to high temperatures, resistance to shear stress, poor adhesion to bioreactor surfaces, and a low tendency to form aggregates; this was previously tested in a large-scale thin-layer bioreactor to simulate the industrial production of microalgal lipid-rich biomass²⁸⁴. These are positive characteristics for its use in large-scale production bioreactors, with a potential for biofuel production. Under optimal conditions, the strain is characterized by energy storage in the form of lipids. If untreated, the cultures propagate rapidly, producing large amounts of biomass in a relatively short period of time. The cells contained negligible lipid storage (1% to 10% of DW) but it was possible to induce hyperproduction of storage lipids in *P. kessleri* biomass using various methods,²⁷² while microalgae can grow in seawater or wastewater and microalgal oil can exceed 50–60% of dry cell weight.²⁸⁵

These microorganisms can produce and accumulate large quantities of triglycerides (TAGs) that can be transformed into biodiesel. However, the recovery of the valuable fractions produced by the microalgae through a low-cost wet pathway necessitates the development of new combined processes integrating culture, harvesting, and several biorefining steps, among which cell disruption, centrifugation, and molecular separation through membrane processes or solvent extraction. Some microalgae are remarkable for their high oil productivity. For instance, *Botryococcus braunii*, *Schizochytrium sp.*, *Nannochloropsis sp.* and *P. kessleri* have been reported to produce lipids in quantities that ranged between 25% and 75%, 50% and 77%, 31% and 68%, and 41% and 65% w/w of dry weight, respectively.²⁴⁵ Extensive research has demonstrated that *P. kessleri* and *Chlamydomonas reinhardtii* increased their TAG production up to seven-fold and fifteen-fold, respectively in response to nitrogen deprivation. *P. kessleri* also has characteristics of interest for photobioreactor cultivation and cellular pretreatment for lipid extraction (high growth rate and low levels of biofilm and aggregate formation).²⁴⁵

Today, numerous studies on microalgal biodiesel production are available; however, none of those illustrate a detailed step-wise description with the pros and cons of the upstream and downstream processes of biodiesel production from microalgae. Specifically, harvesting and drying constitute more than 50% of the total production costs²⁸⁵; however, there are quite fewer detailed study reports available. In this study, lab-scale lipid extraction analysis was attempted. Design and cost analysis on an industrial scale should be considered for future research on isolation and screening of *P. kessleri* microalgae, microalgal large scale cultivation, biomass harvesting, drying, lipid extraction, and biodiesel production.

Microalgae can be harvested through many methods, including sedimentation, flocculation, flotation, centrifugation, and filtration. Self-flocculation is one of the most convenient strategies for low-cost harvesting of microalgae because it requires no extra investment in the cultivation of microalgae and purification of bio flocculants. Energy consumption of sedimentation harvesting is also generally low. However, sedimentation has not been widely used for separation of the microalgae due to their density and small size. Two separate studies by Arora and Kato in 2017 reported that salt stress induced an

increase in cell size. It is possible that the larger cells could contribute to settlement harvesting of microalgae.^{273,274} To further lower the unit cost of microalgae oil, high lipid production in association with industrial waste as sources of nutrients or developing high-value co-products like biofuel appear promising. *P. kessleri* is known to accumulate starch and lipid. It also has characteristics of interest for a semi-industrial scale in outdoor photobioreactors and cellular pretreatment for lipid extraction. This microalga is therefore considered as one of the most promising potential feedstocks for biofuel production.^{161,245}

The sedimentation efficiency of *P. kessleri* cultivated under normal conditions was less than 15%, while the sedimentation efficiency of microalgae with 0.35M NaCl was greatly improved. A salt-induced increase in cell size can contribute to improvement in sedimentation efficiency. Both sedimentation and flocculation can simplify the dewatering process. Flocculants are usually added to induce flocculation. Self-flocculation of algal cells without flocculants addition is economical.²⁴⁷

5.4 Conclusion

P. kessleri being able to grow in desalter effluent suggests that selected algae possess certain traits that allows them to be good candidates for cultivation in wastewater. The growth of microalgae highly depends on the COD and phosphorus concentration. Supplemented media rich in phosphorous of **CK + BBM** does not change the algal growth rate and final biomass density in the culture in comparison to growth of *P. kessleri* in desalter without BBM. The biological effect of BBM supplementation was especially prominent when added into a mixture of two types of effluent due to its low nutrient content due to it having a high carbon level from the addition of phenol and the high COD of AV. However, the cultivation of microalgae in desalter effluent in mixotrophic conditions may be a more favorable approach from an economical and sustainability perspective since this approach can eliminate costly and energy-intensive biological treatment steps prior to algal cultivation.

Parachlorella kessleri grown in desalter effluents display a higher tolerance to salt, metals, toxic hydrocarbons and competitiveness for resources of these species. Results confirmed that *P. kessleri* can grow in desalter effluent and in high salinity conditions. This microalga can produce biomass with enlarged cells for biodiesel and settling in industrial scale operations, which may contribute to a direct reduction of costs.

Possible reasons for the limited performance of biomass production in different conditions may be phosphorous limitation and high ammonia nitrogen concentration due to nitrification that can be resolved by adjusting pH, adding a supplement or mixing different desalter effluents. *Parachlorella kessleri* can degrade phenol and remove benzene in simulated desalter effluent. These properties make this microalga a unique microorganism; not only can it grow in the presence of toxic chemicals like phenol and Benzene, but it is also a halotolerant microalga that can produce biomass and accumulate a high content of lipids. Therefore, the microalgae–water mixture can be directly discharged in desalter effluent to provide both clean water, biomass for biofuel production, and irrigation which is both economical and feasible for the petroleum industry. Quality parameters of desalter effluent after treatment by *P. kessleri* falls within the range of water quality standards for Ontario effluent quality guidelines for petroleum refineries.⁵⁴

Furthermore, it is important to note that application of desalter effluent has a critical economical advantage; the cultivation of algae in the desalter effluent which contains harmful nutrients does not require capital and energy-intensive biological preliminary treatment. Therefore, the cultivation of robust microalgae in desalter effluent media is likely to be the most favorable processing approach from an economical and sustainability perspective if the applied alga possesses critical characteristics required for robust growth in wastewater.

Chapter 6

6 Continuous cultivation of *Debaryomyces hansenii* (Laf-3 10 U) at Varying Dilution Rates on Dodecane

6.1 Introduction

The desalter unit is installed in the first stage of the petroleum refinery process to remove the salt present in the incoming crude oil. Crude oil desalting is necessary to avoid corrosion, rust, and deposition in the refinery process and plant equipment, including heat exchangers, pipes, pumps, distillation columns etc. The salt dissolved in the water, along with impurities^{4,5}, is called desalter effluent and is sent to wastewater treatment plant for further treatment. The addition of this salt containing effluent in high doses may affect the biological treatment.

Several approaches have been reported in literature for desalter treatment¹²⁻¹⁹. Many such approaches such as membrane require high maintenance costs, replacement of spare parts and high energy consumption. In addition, Physico-chemical methods are capable of removing contamination but not eliminating it^{58,84,85,104,105}. Thus a need for alternative cost effective solutions is desirable.

Debaryomyces hansenii is a halotolerant yeast which has been shown to effectively metabolize several hydrocarbons. In particular, the application of the yeast in treatment of challenging wastewater streams such as desalter effluent has significant potential. This yeast can tolerate high concentrations of salt (e.g. NaCl, and KCl) up to 24% (w/v)¹⁵⁰ and

is one of the lipid-accumulating yeasts¹³⁷. The yeast is found in salty food, blue cheese and brines and has both high respiratory and low fermentative activity^{228,286}. The yeast was previously shown to remove phenol (aromatic group)⁵² and dodecane (a chain hydrocarbon and an alkane)²⁴. Previous studies show that high substrate concentrations are inhibitory for the yeast cultivation, therefore continuous cultivation at steady state (CSTR) may be an effective way to control the specific growth rates and avoid substrate inhibition.

There are only a limited studies involving the bioremediation of petroleum refinery wastewater by yeast²⁰² and bacteria using CSTRs^{227,287–293}.

In this study, the cultivation of *D. hansenii* on dodecane as a substrate was investigated in a laboratory scale CSTR under different dilution rates to find out optimum substrate removal. The degradation kinetics were modelled and kinetics were determined.

6.1.1 Growth kinetic modeling in CSTR

The rate of cell production (dX/dt) is proportional to the cell concentration (X) as is shown in Equation (6-1):

$$\frac{dX}{dt} = \mu_{\text{net}}X \quad (6-1)$$

where μ is the specific growth rate.

In the CSTR setup, a substrate solution (dodecane the carbon source) is pumped continuously to the reactor; culture media is withdrawn from the bioreactor with exactly the same flow rate. Therefore, under steady-state conditions, all of the parameters of the process (volume, concentrations of substrate, product and biomass, reaction rate etc.) remain the same and do not change in time. In 1949, Jaques Monod proposed a relationship between μ and S ²⁹⁴. He has shown experimentally that this relationship is similar to the

relationship between the reaction rate and substrate concentration in enzyme kinetics (Michaelis–Menten kinetics). The Monod equation is shown in Equation 6-2.

$$\mu_{\text{net}} = \frac{\mu_{\text{max}} S}{K_s + S} \quad (6-2)$$

Where the μ_{max} is maximum specific growth rate and K_s is the saturation constant and S is dodecane concentration.

The continuous stirred tank reactor (CSTR) used for aerobic respiration and microbial fermentations is also called chemostat. A schematic diagram of such a reactor is shown in Figure 6-1.

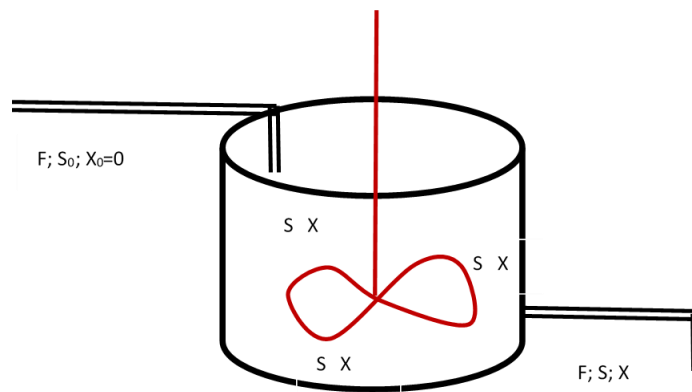


Figure 6-1: Schematic of continuous bioreactor

The material balance of biomass X can be written as:

$$V_r \frac{dX}{dt} = FX_0 - FX + V_r \mu X \quad (6-3)$$

V_r is the volume of the reactor that is constant. Considering that the inlet flow usually contains no microorganisms ($X_0=0$), Equation 6-3 can be rearranged that as equation 6-4:

$$\frac{dX}{dt} = \mu_{\text{net}}X - DX \quad (6-4)$$

Therefore, under steady-state conditions when $dX/dt=0$

$$D = \mu_{\text{net}} \quad (6-5)$$

Combining Equations 6-2 (Monod) and 6-5, we have

$$\mu_{\text{net}} = D = \frac{\mu_{\text{max}} S}{K_s + S} \quad (6-6)$$

where μ_{net} is specific growth rate, μ_{max} is maximum specific growth rate in absence of substrate limitation, S is the concentration of substrate in the reactor (which equals the concentration of substrate in the liquid leaving the reactor) under steady state conditions, K_s is substrate concentration which allows the organism to grow at $0.5 \mu_{\text{max}}$.

The substrate and product concentrations can be related through the yield coefficient ($Y_{x/s}$) as:

$$Y_{x/s} = \frac{X - X_0}{S_0 - S} = \frac{X}{S_0 - S} \quad (6-7)$$

Combining equations 6-6 and 6-7, the material balance of substrate can be obtained:

$$D(S_0 - S) = \frac{X}{Y_{x/s}} \frac{\mu_{\max} S}{K_s + S} \quad (6-8)$$

Equation 6-8 can readily be solved for X and S to yield:

$$X = Y_{x/s} \left(S_0 - \frac{DK_s}{\mu_{\max} - D} \right) \quad (6-9)$$

And

$$S = \frac{D K_s}{\mu_{\max} - D} \quad (6-10)$$

The maximum specific rate of *D.hansenii* in SDE when dodecane is the only hydrocarbon, was obtained from previous experiment in chapter 4 with batch bioreactor, μ_{\max} is equal 0.085 h⁻¹.

$$\mu_{\max} = \frac{D(K_s + S)}{S} \quad (6-11)$$

To find the relationships of S vs. D, K_s is required to be calculated. It can be seen that cell concentration decreases with the increase of D (Eq 6.9) and reaches zero at washout. At

this dilution rate all the microorganisms are washed out and therefore, there is no biochemical reaction. Therefore, the concentration of substrate in the reactor equals that of the feed (S_0)^{295,296}.

$$\mu_{\text{net}} = D = \frac{\mu_{\text{max}} S}{(K_s + S)} \quad (6-12)$$

The CSTR is a powerful tool for the study of microbial process and allows control for specific growth rate by controlling the dilution rate. Microorganisms in the continuous reactor are almost always in exponential phase of growth. The change of the flow rate of substrate solution results in the change of dilution rate (D) since $D=F/V_r$. If dilution rate is changed and the substrate concentration in the reactor is measured as a function of dilution rate, Equation 6-6 can be used to determine the kinetic constants μ_{max} and K_s . A plot similar to that of Lineweaver _Burk can be used to calculate the kinetic constants (Figure 6-3).

In addition the Monod model, a relationship between dilution rate and COD could also be obtained by using inhibitory models such as Haldane, Aiba and Edwards models. The inhibitory growth kinetic equations of Andrews²⁹⁷, Aiba¹⁹⁴ and unstructured mathematical model Edward¹⁹⁵ as given by the equation 1, 2 and respectively as follows:

$$\mu = \frac{\mu_{\text{max}} S}{K_s + S + \frac{S^2}{K_I}} \quad (6-13)$$

$$\mu = \frac{\mu_{\text{max}} \frac{S}{K_I}}{K_s + S} \quad (6-14)$$

$$\mu = \mu_{max} \left[e^{\frac{-S}{K_I}} - e^{\frac{-S}{K_S}} \right] \quad (6-15)$$

where K_S , K_I , μ , μ_{max} , and S are the half saturation constant (mg L^{-1}) (substrate-affinity constant), substrate inhibition constant (mg L^{-1}), specific growth rate (h^{-1}), maximum specific growth rate (h^{-1}), and substrate concentration (mg L^{-1}), respectively.

Although dodecane concentration is not high in this research and inhibition models are applied for high substrate concentrations, the experimental data in inhibition models were replaced to compare with Monod model Aiba, Edwards and Haldane models were used and discussed. These three model equations were discussed in degradation of phenol in previous study by Azimian *et al.* in 2018⁵².

6.2 Materials and methods

6.2.1 Materials

The Synthetic Desalter Effluent (SDE) was derived from a mineral media solution with equivalent properties of real desalter effluent, with dodecane the only yeast-degradable carbon source. Tween 20 (non-ionic surfactant) was added to dissolve the nonpolar hydrocarbon dodecane into the aqueous medium of SDE to help yeast access this carbon source. Synthetic desalter components in the mineral media solution²¹⁰ is described in Table 6-1.

6.2.1.1 Chemicals of synthetic desalter growth medium

All chemicals used in this study were purchased from Sigma Aldrich (Oakville, Canada) as analytical grade. The Synthetic Desalter Effluent in 1 L distilled water was prepared as described in Table 6-1. The pH of the growth media was adjusted to between 6 and 6.5. All growth media were autoclaved at 121°C for 20 min prior to yeast cultivation. Dodecane was added to SDE as a petroleum hydrocarbon representative at concentrations of 750mg.L⁻¹. The theoretical oxygen demand (ThOD) for the oxidation of 1 g of dodecane is 3.43 g (adapted from Pitter and Chudoba, 1990). The equivalent of ThOD for dodecane (750 mgL⁻¹) is 2610 mgL⁻¹; this is within the range of the COD in Imperial Oil desalter effluent. Total free hydrocarbon content, including dodecane, in typical desalter effluent has been reported as high as 1,000 mgL⁻¹ ^{38,211}.

Table 6-1: Phase 1 of synthetic desalter effluent components with Dodecane

Mineral Media component	Concentration in 1 liter distilled water
KH ₂ PO ₄	1g
K ₂ HPO ₄	1g
(NH ₄) ₂ SO ₄	1g
MgSO ₄	0.2g
FeCl ₃	0.05g
CaCl ₂	0.02g
NaCl	1 g
FeCl ₃ , CaCl ₂ , NaCl	0.05g, 0.02g, 1 g
Tween 20	1 ml
Dodecane	750mg

6.2.1.2 Yeast preparation and experiments

Debaryomyces hansenii SWING YEAST LAF-3 (Parmalat Inc., London, Canada) was used for all experiments. Pre-cultivation of fresh and sterilized yeast extract peptone dextrose (YEED) agar slants was conducted, and the cultures were then incubated at 25°C and 180 rpm on a rotary shaker (VWR, Mississauga, ON, Canada) for 24 h. Growth in liquid media was facilitated by 50 mL of sterilized malt extract medium. Optical density (absorbance percentage) at a wavelength of 600 nm was measured every four hours on an Evolution™ 60S UV-visible spectrophotometer (Thermo Fisher Scientific) during the hours of incubation.

Once the cultures reached the late exponential phase, the *D. hansenii* cells were added to SDE in 250 mL flasks with a suspended yeast cell concentration of 1% v/v (1 mL *D. hansenii* inoculum in 100 mL of desalter effluent) and incubated at 25°C in a rotary shaker set to 180 rpm for three days.

6.2.1.3 CSTR bioreactor

The biodegradation of hydrocarbons was studied in a bioreactor (shown in Figure 6-2) with total volume of 1000 ml and working volume of 500 ml for continuous experiments. The reactor is Wheaton™ Celstir™ Spinner Flask. Aeration was provided by impeller and injection from the top of reactor for yeast growth. The bioreactor was fed continuously with SDE contains dodecane as a sole carbon source.

The reactor was inoculated with 250 mL of precultured (enriched culture), *D.hansenii*, yeast suspension and filled with SDE. The continuous feed was started at dilution rates (D) in the range 0.007-0.045 h⁻¹. Synthetic desalter effluent was supplied at the bottom of the reactor by means of a mini and ultra-pump variable flow (VWR, 120 mL to 2.2 Lmin⁻¹). Sterile air was passed into the continuous reactor and storage feed tank the temperature was maintained at 25 °C. The sampling for optical density and Chemical Oxygen Demand

(COD) measurement were carried out once a day from reactor using sterile syringe. The monitoring of the reactor is by analysis of COD and biomass (optical density).

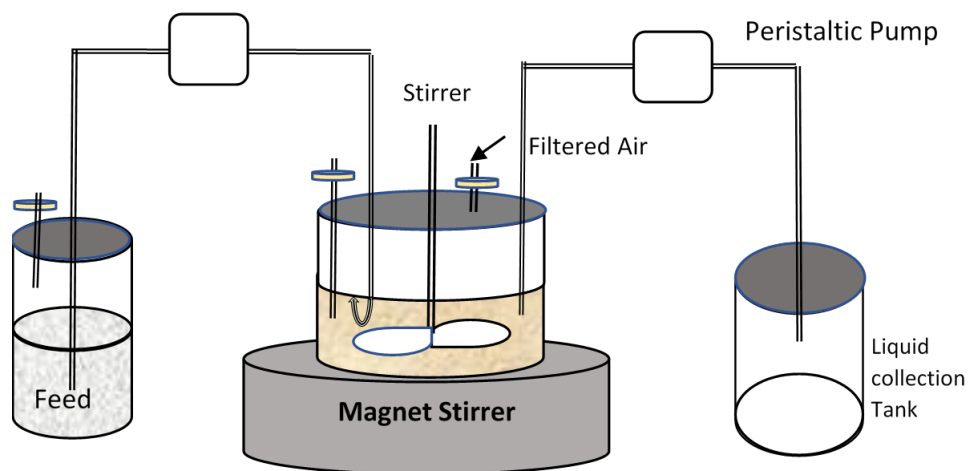


Figure 6-2: Schematic of continuous reactor for dodecane removal from SDE

pH of the culture medium was controlled at 6.5 ± 0.3 .

6.2.2 Analytical methods

Organic carbon (dodecane) concentration was measured by assessing COD. SDE, mineral media (MM) and surfactant (Tween 20), were maintained at the same concentrations for all runs of all experiments, with dodecane concentration as the only variable.

6.2.2.1 Cell concentration

Yeast (*D. hansenii*) is a unicellular microorganism, and growth (cell concentration) was measured using the optical density (OD) of the cell culture by measuring absorbances at 600 nm.

6.2.2.2 Chemical oxygen demand (COD)

The strong linear relationship between total organic carbon (TOC) and COD indicates that a COD assay can reliably replace the TOC test normally used in the evaluation of specific wastewater and treatments²¹². Amounts of consumed dodecane were evaluated by measuring reductions in COD after five days using Equation 6-16

$$COD_{Total} = COD_{MM} + COD_D + COD_T \quad (6-16)$$

where COD_X denotes the COD of component X, MM represents mineral media, T represents Tween 20 and D represents dodecane.

Equation 6-17 illustrates that COD_{Total} has linear regression with the TOD of Tween 20 (T) and dodecane (D)

$$COD_{Total} = \alpha TOD_{\tau+D} + \delta \quad (6-17)$$

where α is the slope and δ is the intercept of the straight line.

Equation 6-18 similarly illustrates that COD_{Total} has linear regression with the TOD of Tween 20 (T) and dodecane

$$COD_{Total} = \alpha D + \beta \quad (6-18)$$

where α is the slope and β is the intercept of the straight line.

Tween 20 is not degradable by yeast, so amounts thereof at the first (i) and final (f) days remained constant

$$[COD_{Total(i)} - COD_{Total(f)}] = \alpha\beta [D_{(i)} - D_{(f)}] = \Delta D \quad (6-19)$$

As the actual desalter effluent is represented in the COD values (due to a range of carbon sources), COD measurements were also used for the SDE. For experimental determinations of COD, the microbial culture samples from the shaker flasks were centrifuged with an IEC Micromax (Hyland Scientific Company, WA, USA) at 1,0000 rpm for 45 min. The supernatant was then filtered using sterile 0.2-micron cellulose acetate membrane syringe filters (VWR) to remove any remaining cells. COD analysis of the filtrated SDE was conducted with a Hach 8000 (Hach Inc., Loveland, USA).

6.2.2.3 n-dodecane removal measurement

Dodecane removal was evaluated using Equation 6-19 and the following formula

$$\Delta COD\% = \frac{(COD_{Total(i)} - COD_{Total(f)})}{COD_{(Total)i}} \times 100 \quad (6-20)$$

Here COD_i is the initial dodecane concentration before adding yeast and COD_f is the final dodecane concentration at the end of the experiment.

6.2.2.4 Modeling the kinetics of synthetic desalter effluent

Michaelis–Menten kinetics is a models of enzyme kinetics and equation is based on theoretical considerations while the Monod equation is empirical. The use of Michaelis - Menten kinetics was particularly attractive to researchers studying nutrient relationships, since two parameters were needed to define the nutrient acquisition and growth potential

of a particular of microorganism²⁹⁸. Michaelis–Menten can apply for microorganism growth kinetics under steady state condition²⁹⁹.

Because it is difficult to accurately determine the μ_{\max} by examining a rectangular hyperbola, it is also difficult to establish the value of the K_s in this way. The Lineweaver-Burk plot is the most commonly used linear plot for enzyme kinetic analysis (Figure 6-3). Today enzyme kinetic constants are determined by fitting experimental data to rate equations by computer. when linear data are desired, the reciprocal of the Michaelis-Menten equation (Lineweaver-Burk) plot is obtained (figure 6-3) for illustrative purposes based on kinetic constants^{300,301}. The equation for these linear constructs is obtained by inverting Monod equation 6-2:

$$\frac{1}{\mu} = \frac{K_s}{\mu_{\max}} \frac{1}{S} + \frac{1}{\mu_{\max}} \quad (6-21)$$

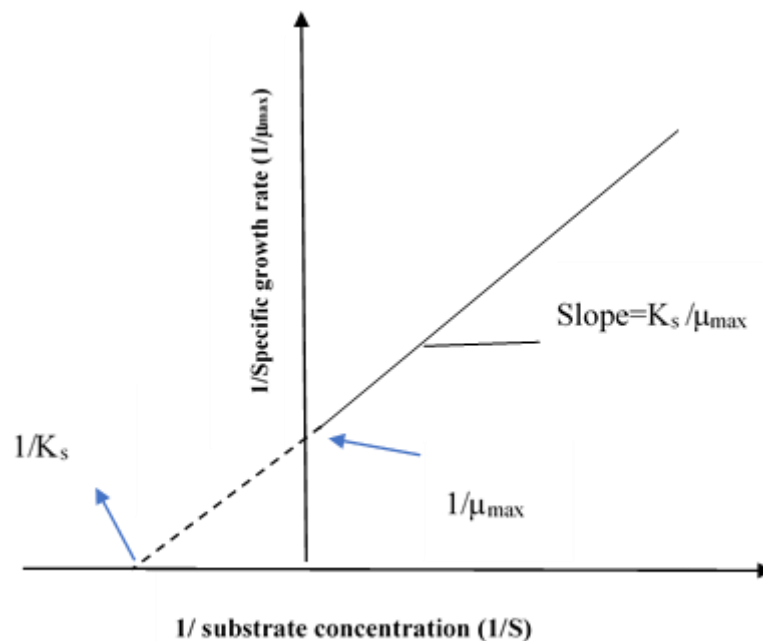


Figure 6-3: A Lineweaver-Burk plot of $1/\mu$ against $1/s$ ²⁹⁸

The Monod equation explains the growth of *D.hansenii* and the utilization of substrate in SDE as it was shown in equation 10. The substrate is not high concentration so the maximum specific growth rate and saturated constant can be obtained from Lineweaver-Burk plot.

6.3 Results and Discussion

6.3.1 Effect of dilution rate (DR)

Dodecane concentration is one of the important parameters monitored to improve the removal efficiency of the treatment system. Table 6-3 shows operation parameters, steady state data and dodecane removal by COD was determined throughout the SDE. The system attained an overall hydrocarbon removal efficiency of 95%. The bioreactor efficiency decreased by increasing at D of 0.45 h^{-1} . The dodecane concentration in SDT was equivalent of initial COD 2793 mgL^{-1} at the beginning and decreased to 136 mgL^{-1} after reaching to steady state at dilution rate of 0.07 h^{-1} in CSTR. Yeast, *D. hansenii*, effectively mineralized dodecane as demonstrated by reduction in COD, indicating that *D. hansenii* play an important role in dodecane break down. Dilution rate of SDE helped control organic loading rate in continues bioreactor. Removal efficiency was observed in the range of 80.96 – 95.14% in D range between 0.007 and 0.026 h^{-1} . However, dilution rate of 0.007 h^{-1} is the best parameter, to be considered for CSTR design due to fluctuating of organic load in different situation, therefore higher hydrocarbon load can be mineralized and significantly reduced at D of 0.007 h^{-1} . Maximum growth rate of yeast, *D. hansenii*, was attained during the treatment of SDE in batch reactor with maximum COD of 61%. This value increased in CSTR when the range of substrate (dodecane) is lower than 750 mgL^{-1} at D 0.007 h^{-1} .

Table 6-2 : Operational parameters and steady state data and COD removal in CSTR with yeast *D.hansenii*

Day	Flow- rate (mL h ⁻¹)	D< ($\mu_{\max}=0.085$) (h ⁻¹)	S (COD _f) (mgL ⁻¹)	1/D (h)	COD % removal
10	3.5	0.007	136±2	142.86	95.14
17	13	0.026	618.7±5	38.46	85.05
24	15.5	0.031	733±6	32.26	80.96
30	17.5	0.035	1000±8	28.57	71.43
37	22.5	0.045	2793 ±20	22.22	7.37

The effect of D on the removal of dodecane was studied. Dodecane and other components of desalter effluent were kept constant. The initial dodecane concentration is 750 mgL⁻¹. Effect of different dilution rate on the COD removal and cells concentration is shown in Figure 6-4. The change in biodegradation and mineralization of dodecane at different dilution rate is shown as COD in blue line. Cell concentration of SDE recorded when there was only slightly fluctuation in optical density at each D as it is shown in red line. When the D was adjusted to 0.007 h⁻¹, the cell concentration gradually increased to 0.496 and the removal efficiency has been observed. The bioreactor showed greater than 95% removal of COD (equivalent of 100% removal dodecane) at 142.86 h. However, further increase in dilution rate to 0.026 leads to gradually decrease in biodegradation rate to 85.05 % (COD %). At dilution rate of 0.045 h⁻¹, the biodegradation rate was drastic decreased, and cell concentration was diluted to 0.293 with COD removal of 7.4%. The optimum D can be designed in CSTR, when SDE contains COD of 750mgL⁻¹(THOD of dodecane is 2610 mgL⁻¹ < COD_(Dodecane +SDE) of 2793 mgL⁻¹).

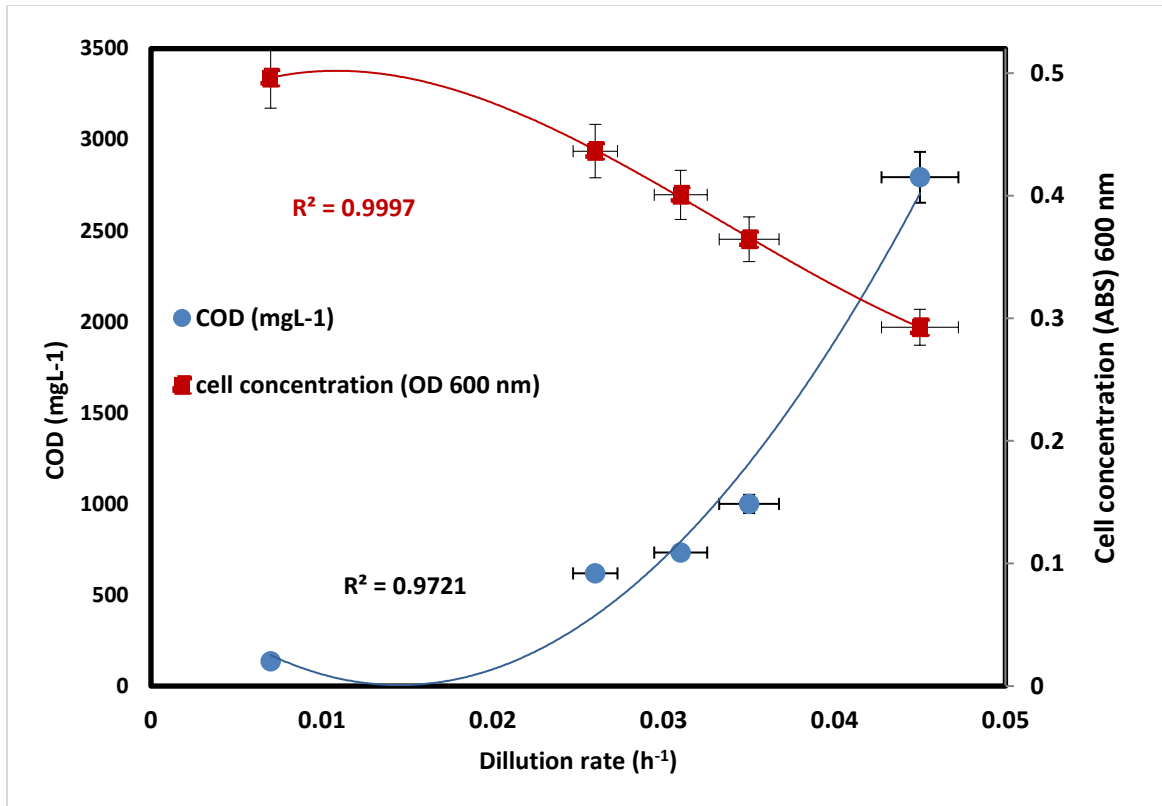


Figure 6-4: Steady-state values of the concentrations of dodecane (■), and CO
D removal (●) for different dilution rate using *D.hansenii* in CSTR

The biodegradation rate was gradually increased to 95% at steady state when dilution rate was increased to 0.07 h^{-1} . Table 6-3 summarizes the change in COD removal and dilution rate and initial substrate concentration of 750 mgL^{-1} . The D was based on the flow rate of the effluent passing through the pump to the bioreactor. Two dilution rates, 0.007 and 0.026 h^{-1} , were given high percentage COD removal. But D of 0.007 (142.9 h) is recommended for CSTR in pre-treatment phase due to fluctuating the amount of organic carbon load in desalter effluent.

Figure 6-5 shows the change in cell concentration with time at five different dilution rates 0.07 , 0.026 , 0.031 , 0.035 and 0.045 h^{-1} at initial COD 2793 mg. l^{-1} in steady state. In the presence of dodecane the cell concentration of *D.hansenii* decreased as the dilution rate increased. At 0.045 h^{-1} dilution rate which is lowest growth of yeast with cells

concentration about 0.292 ± 0.008 (OD_{600}) and no significant removal of COD was obtained under steady state condition, which clearly indicates the cell is wash out condition. This is also supported by incomplete utilization of dodecane by *D.hansenii* under steady state condition. Although, at dilution rate of 0.035 h^{-1} , 0.031 h^{-1} and 0.026 h^{-1} (longer residence time) the cell concentrations were found to be 0.364 ± 0.01 , 0.382 ± 0.02 and 0.401 ± 0.01 respectively, but dodecane still remain unutilized. This indicates further reducing of dilution rate, enhanced the COD removal and consequently complete dodecane utilization through biomass growth. Thus, at a dilution rate 0.007 h^{-1} the dodecane was found to be completely utilized and the maximum cell concentration at Absorbance of 600 nm was observed to be 506 ± 0.3 .

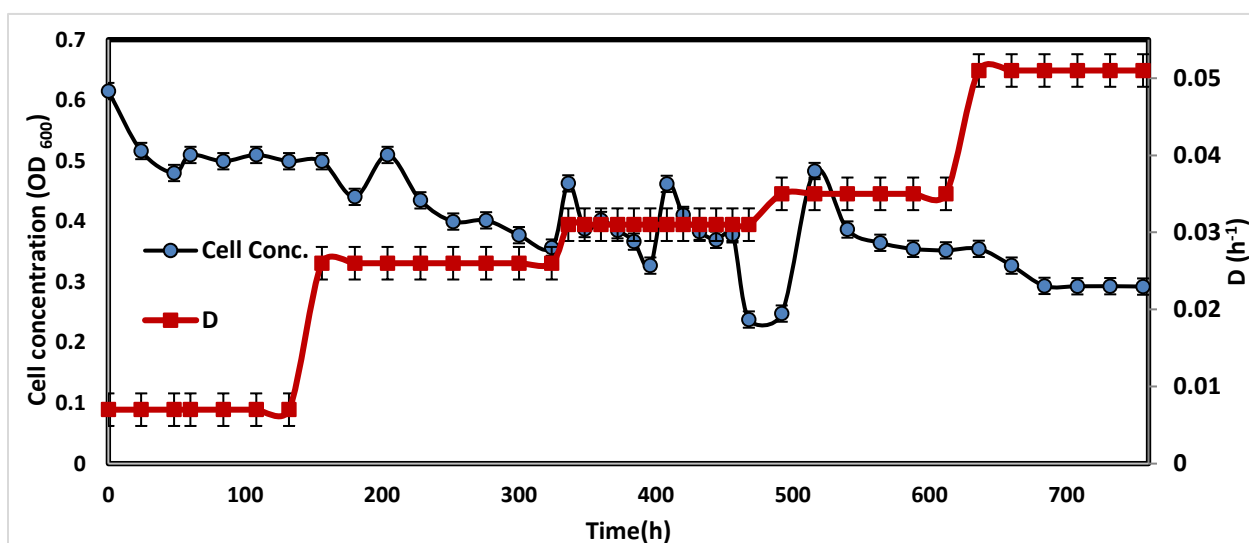


Figure 6-5: The change of cell concentration in SDE at different dilution rates during the continuous operation

As dodecane was completely utilized at this dilution rate, A maximum COD removal (95%) was observed from 2793 to 136 mgL^{-1} . by operating the process in decreasing D from 0.045, 0.035, 0.031, 0.026 and 0.007 h^{-1} the dodecane was completely utilized by reducing COD from 2793, 1000, 7333, 618.7 and 136 mgL^{-1} respectively (Figure 6-6). As dodecane (equivalent to COD) was completely utilized at 0.007 h^{-1} , further studies were not carried out at a dilution rate lower than 0.007 h^{-1} .

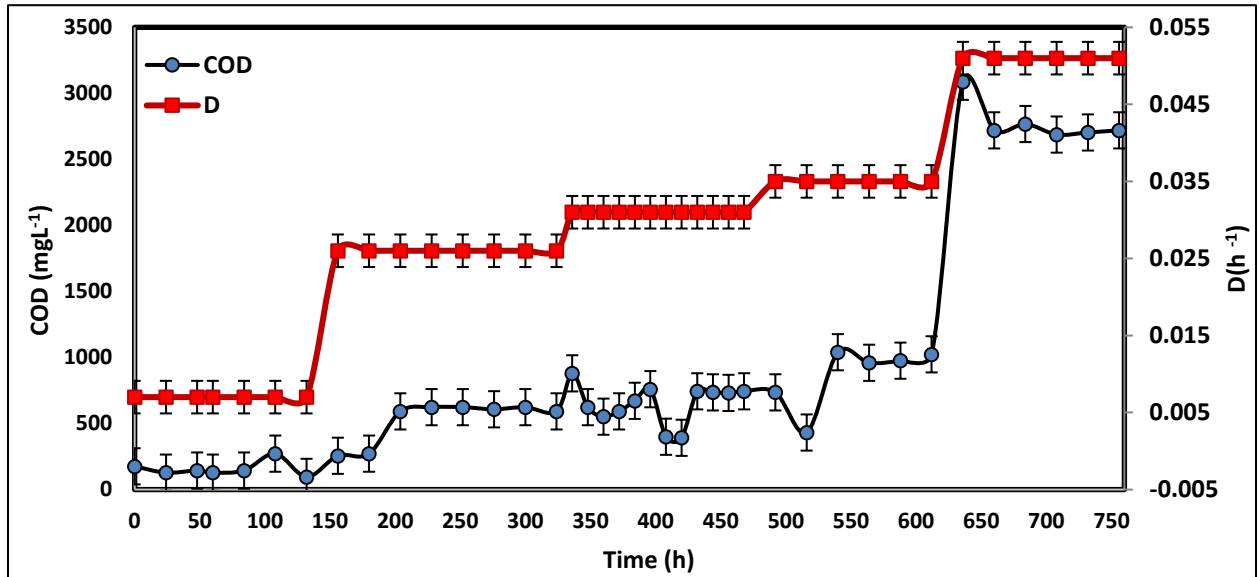


Figure 6-6: Dodecane concentration equivalent with COD in SDE as function of time during biodegradation in aerobic bioreactor CSTR

6.3.2 Growth kinetic modeling

The substrate is not high enough to inhibit growth of *D.hansenii*. Therefore, the growth of cells in different dilution rate follows of Monod equation (as shown in Figure 6-7 a). To measure maximum growth rate and K_s , we used the experimental data in the Lineweaver–Burk plot. This plot linearizes the hyperbolic curved relationship, and the line produced is easy to extrapolate, allowing evaluation of $D_{\max}=\mu_{\max}$ and K_s . We obtained only the five data points from complete cure of substrate vs D ; we would have difficulty estimating D_{\max} from a direct plot as shown in Figure 6-7. a.

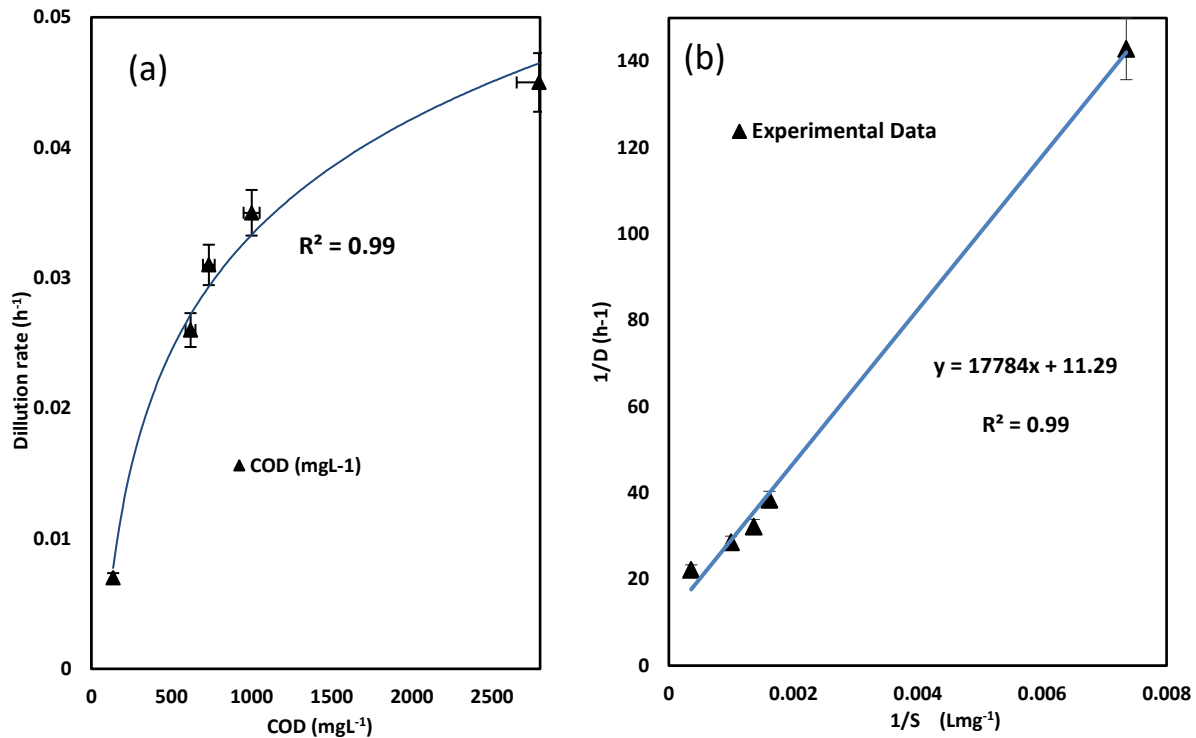


Figure 6-7: (a) Relationship between substrate concentration and the rate of growth rate reaction (b) Lineweaver–Burk plot of the same kinetic data

As shown in Figure 6-7.b, if these five points are plotted on a graph of $1/D$ against $1/S(\text{COD})$, the data are linearized, and the line can be easily extrapolated to the left to provide intercepts on both the y -axis and the x -axis, from which μ_{\max} and K_s , respectively, can be evaluated.

$$\frac{1}{\mu} = 17784.2 \frac{1}{S} + 11.29 \quad (6-22)$$

Based on experimental data and the model in equation 6-22 and 6-23, μ_{\max} is 0.085 h^{-1} , $K_{S(\text{Lineweaver-Burk})} = 1575.2 \text{ mgL}^{-1}$, μ_{\max} and K_s can be applied as the saturation constant of the Monod equation.

Therefore, the kinetic model for SDE when dodecane presents alkane and chain hydrocarbon in range of concentration around 750 mgL^{-1} and less is in equation 20:

$$S = \frac{1575.2 D}{0.08 - D} \quad (6-23)$$

Next, the experimental data were compared with inhibitions equations 6-13, 6-14, and 6-15. The values, μ_{\max} , K_s and K_I were calculated by the method of least square in MATLAB Program Software and compared with Monod model. Figure 6-8 demonstrates the effect of dilution rate on COD removal using *D.hansenii*. The dilution rate could reach at 0.007 h^{-1} . Then, the rate begins to increase exponentially with COD (dodecane removal) until the value reaches close to initial COD in SDE, where the D is the highest at 0.045 h^{-1} with cell concentration of 0.293. Further increase in dilution rate, decreases the rate of substrate removal and growth, implying that the dilution rate stage has taken place during the process. When D increases (close to μ_{\max}), this adverse effect on *D.hansenii* growth and depresses substrate degradation. There is not enough time for yeast to metabolize dodecane in SDE.

The observed relationship between D and COD discussed in Figure 6-5 was further used to compare the kinetic parameters of Monod, Aiba, Edwards and Haldane models to each other. At the first glance, it seems the Monod is less fit with the experimental data. As shown in the Figure 6-8, the Monod equation could not estimate the experimental data well, with a coefficient of determination, RMSE 0.0013. When we observe other kinetics constants in Table 6-3, it helps us to analyze profoundly and chose the right model. The kinetic parameters, using five experimental data points, were obtained as 0.085 h^{-1} and 1575.2 mgL^{-1} for μ_{\max} and K_s , respectively. On the other hand, in this study, dodecane (750 mgL^{-1}) is not beyond its saturation value. The identical curves were demonstrated by the Aiba, Edwards and Haldane models. It shows the better agreements between the experimental and the simulated data were obtained by these models compared with that of Monod in Figure 6-8. However, Table 6-3 displays the constant inhibition (K_I) in the growth kinetics of Aiba, Edward and Haldane models are less than constant saturation, K_s .

In addition, Aiba model with μ_{\max} 0.27 h^{-1} cannot be accepted due to literature report about *D.hansenii* specific growth rate. Previously Prista et al.¹⁹³ described the specific growth rate of *D. hansenii* in the presence of different salts between 0 and 0.6 M NaCl is in the range of 0.02 to 0.22 h^{-1} . With similar reason Edward model cannot be accepted. The values of μ_{\max} , K_S and K_I were selected as 0.097 h^{-1} , 2467 mgL^{-1} and 2410 mgL^{-1} , respectively, for the Edwards model, which are less than those obtained by the Andrew (Haldane) model 0.137 h^{-1} , 2464.5 mg^{-1} and 2410.5 mgL^{-1} , respectively. It was observed that. The value of K_S is larger than K_I in all inhibitions mathematical models that demonstrates the substrate concentration and dilution rates in experimental data are not within the range to inhibit the growth of cells. The parameter values, however, were comparable with previous research was carried out by authors for optimization of dodecane removal in wide range between 0.3 to 30 gL^{-1} in batch reactor with 7 experimental data points and the models showed Aiba model with μ_{\max} of 0.085 h^{-1} was the best fit in batch system. While this study was evaluated five experimental data at five different D in CSTR and this experiment was investigated for substrate concentration of 750 mgL^{-1} and less. We might obtain more accurate RMSE for Monod model with running extra D (more than 5 experimental data) between 0.01 and 0.045 h^{-1} . On the other hand, experimental data shows exponential phase with no inhibition. Therefore, the Monod model is the most realistic simulates the experimental data and is an appropriate kinetic model to represent the growth of the *D. hansenii* CSTR at steady state.

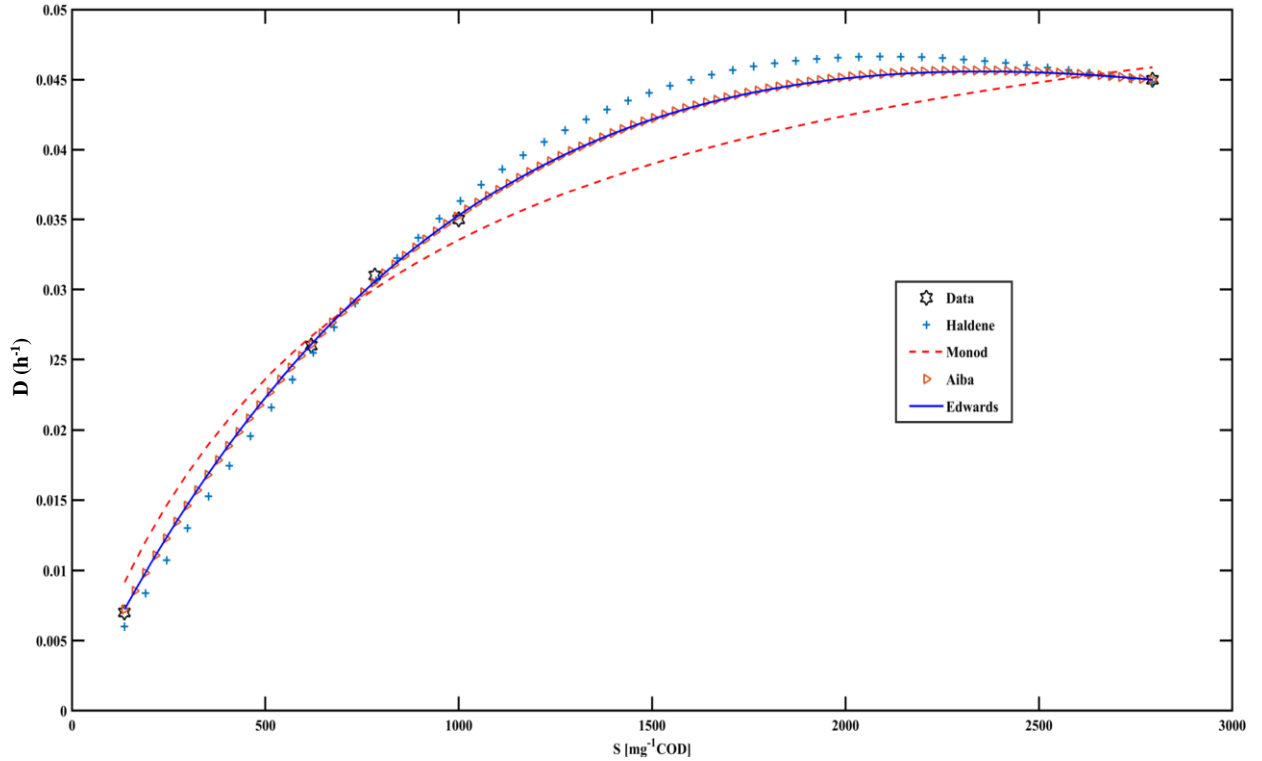


Figure 6-8: The effect of COD (Dodecane load) using *D.hansenii* on different dilution rates. The curves refer to the simulated data using the Monod, Aiba, Edwards and Haldane models, equations 6-13,14 and 15, (The line represents different kinetic models using least squares non-linear regression and exponential curve fitting (MATLABTM)).

Table 6-3: Summary of the kinetic parameters used in the modeling of *D.hansenii* dilution rate using Monod, Aiba, Edwards and Haldane models

Kinetic Model	μ_{\max} (h^{-1})	K_s (mgL^{-1})	K_i (mgL^{-1})	RSME
Aiba	0.2748	4837	34711	0.0002617
Edward	0.0970	2467	2410.5	0.0002584
Andrew (Haldane)	0.1368	2464.5	2410.5	0.0008
Monod	0.085	1575.2	—	0.0013

The result of this study was compared with the most similar wastewater with desalter effluent. The result of biodegradation of low molecular weight in refinery wastewater under saline condition in Saudi Arabia by halophilic bacteria consortium in CSTR system was reported in 2018. 94% COD removal was obtained after 12 days, when initial concentration of polycyclic aromatic hydrocarbon (PHAs) was 100 mgL^{-1} and NaCl concentration of 40 gL^{-1} ²⁸⁸. Another study the petrochemical wastewater with initial COD of 1025 mgL^{-1} was removed up to 93% using biosurfactant rhamnolipid in continuous bioreactor within 21 and 25 days. While in our study COD removal of 95% at initial COD of 2793 mgL^{-1} was achieved²²⁷. The petroleum hydrocarbons with n-alkane of C10–C35 were strongly degraded (COD removal of 97%) after 200 days by the microbial consortium in continuous aerobic treatment in the CSTR³⁰². There is only one study using microbial consortium in CSTR mode. This yeast is capable degrader of hydrocarbon can be added to biological treatment of desalter effluent in continuous reactor.

6.3.3 Design of CSTR

Refinery operations may process about 120,000 bpd (barrel per day) crude oil. The oil residence time is approximately 1 h in each of the desalter vessels for this 60,000 bpd ($9540000 \text{ Lit day}^{-1}$) application. A brine-settling tank is also utilized to maximize oil recovery from the brine effluent³⁰³.

Based on the volume of desalter effluent and required optimum resident time for the yeast to grow and remove hydrocarbon and reduce COD, the capacity of the continuous reactors can be calculated and designed in the pre-treatment line. First, we studied the removal of COD in different dilution rates on the lab scale. An optimum dilution rate for COD removal of SDE using halotolerant microorganism, *D.hansenii*, can lead us to design volume of the continues stirred tank reactor (CSTR) to remove COD (oil and aliphatic compound) when initial dodecane concentration is about 750 mgL^{-1} with surfactant for improving miscibility of dodecane in aqueous phase.

Three parameters affecting CSTR functionality; these are flow rate (Q), residence time (RT) and, dilution rate (DR).

Desalting units remove contaminants from crude oil by washing with water at a ratio of 2-8% v/ v of crude oil^{5 38}. If the volume of water for desalting is 2% of volume of crude oil, The flow rate of desalter effluent is 0.08 *9540000 Lit day⁻¹.

$$Q = 0.02 \times 9540000 (\text{Lit. day}^{-1}) \times \frac{\text{day}}{24 \text{ h}} \times \frac{\text{m}^3}{\text{Lit}} = 7.95 \text{ m}^3 \text{h}^{-1}$$

The dilution rate equals the flow rate divided by the reactor volume.

$$D = \frac{Q}{V} \quad (6-24)$$

$$V = \frac{7.95 \text{ m}^3 \text{h}^{-1}}{0.026 \text{h}^{-1}} = 305.7 \text{ m}^3$$

The volume of CSTR (V) is total volume of Equalization tank and flotation tank in pre-treatment module. It can be divided to two bioreactors with equal volume:

$$V_{\text{Equalization}} = V_{\text{Flotation}} = \frac{4542.86}{2} = 152.8 \text{ m}^3$$

The dimension of CSTR can be defined based on limitation and specifications of a petroleum refinery. If another microorganism such as microalgae is added to the pre-treatment for further treatment, the candidate dilution rate is appropriate for fast growth microalgae.

The biomass produced from yeast *D.hansenii*, can be harvested and extract lipid for biofuel production. Lipid content increase when *D.hansenii* is grown in high NaCl concentration

6.4 Conclusions

A continuous bioreactor was studied for removal of dodecane in SDE using halotolerant *D.hansenii*. The result demonstrated that different DR at one specific wastewater (all of the components of SDE were kept constant when DR changed) have a profound effect on dodecane removal efficiency. The CSTR showed an excellent removal efficiency for dodecane removal with COD removal of 95% (99.9% removal dodecane). The optimum D for bioreactor was found to be 0.007 h^{-1} and below of maximum growth rate that the wash out of the yeast *D.hansenii* was observed. Effect of salt in SDE does not change the removal efficiency; however, the literature reported *D.hansenii* grows more when salt concentration increases^{137,229–232,234}. The initial substrate concentration of 750 mgL^{-1} of dodecane was efficiently removed up to 99.9% (COD 95.5%) at D of 0.007. The stability and efficiency showed by *D.hansenii* for different D and typical hydrocarbon concentration (Dodecane) indicate its suitability for bioremediation of desalter effluent in the continuous bioreactor.

Chapter 7

7 Conclusions and Recommendations

The transfer of high concentration of salt from the desalter unit to petroleum refinery effluent is a serious challenge in this industry. The quality of wastewater treatment may not meet the environmental standard guidelines due to compositions and characteristics of desalter effluent. The stringent environmental regulations to prevent toxic hydrocarbons emissions into the environment have obliged refineries to lower and ultimately totally remove pollutants in discharged treated wastewater from petroleum refinery plants. Adjustment of operational and environmental parameters in petroleum refinery wastewater treatment plants are currently used to minimize the transferred load of a shock to the system. Separation techniques, which is currently used in refineries for desalination, is prohibitively expensive. Many of the current facilities are not able to desalinate salt and remove metal ions compounds, because, higher temperature and pressure are required. In addition, other approaches such as membrane technologies, nanofiltration, dehydration, absorption do not eliminate contaminants. The challenges for desalination have provided an inevitable necessity to develop other alternative cost-effective treatment methods.

In this research, the bioremediation of desalter effluent in the presence of high salt using halotolerant and robust yeast strain *Debaryomyces hansenii* (LAF-3 10 u) and microalgae strain *Parachlorella kessleri* was investigated. The following are the main conclusions of this study:

- Growth of *D. hansenii* with phenol was studied in simulated desalter effluent at a salt concentration of 1 gL^{-1} . At lower COD, when phenol is the only carbon source, *D. hansenii* could be assimilated. Phenol, as the sole carbon source, inhibited growth at COD of 1200 mgL^{-1} . Phenol inhibition followed a substrate inhibition model (Edward model) and kinetic constant of 0.21 h^{-1} , 633.95 mgL^{-1} , and 1263.6 mgL^{-1} for μ_{\max} , K_S , and K_I , respectively were obtained.. Presence of salt, metal ions with phenol significantly compounded the inhibition and decreased the value of the

observed μ_{max} in particular when the Phenol concentration was more than 1200 mgL⁻¹. This yeast was growing in real desalter effluent. and the COD removal in real desalter effluent wastewater was about 1.3-8 times higher than that obtained in simulated desalter effluent containing phenol as the only carbon substrate.

- *D.hansenii* was also shown to metabolize dodecane in the presence of Tween 20 non-ionic surfactant. A factorial design was used to study the effects of temperature, substrate concentration (n-dodecane), initial pH, and salt (NaCl) concentrations. Yield (COD removal) is dependent on the effect of pH, Temperature. From the performed experiments it was concluded that higher temperatures at low pH at the presence of nonionic surfactant had a negative effect on biodegradation. *D.hansenii* can remove high substrate at high pH and low temperature in a wide range of salt concentrations. The best dodecane removal was obtained at temperature of 20 °C, pH of 9, salt concentration (NaCl concentration of 1000m gL⁻¹) to get 100% removal in both dodecane concentrations of 150 and 750 gL⁻¹. Low pH at high temperature postponed dodecane removal in further time.
- Biodegradation in two types of desalter effluent of AV Brine and CK Brine was carried out in photobioreactor using *Parachlorella kessleri* a robust microalga at different conditions of both heterotrophic or heterotrophic and, with supplement media or no supplement media. It was observed that the strain could acquire adaptability with AV brine, and it could start growth with no lag time.
- The use of BBM as a supplemented media for biodegradation of contaminants in desalter effluent has shown the potential to eliminate ammonia, phosphorous and COD in AV brine is much higher than CK brine due to COD level. After 12 days, the biodegradation in the presence of BBM is, however, lower than when microalgae grow in AV Brine only. But the quality of effluent treatment results is as similar to the one when BBM was not added to AV Brine. Microalgae could not grow well in CK effluent even with BBM due to low range of COD.

- Growth of strain *P.kessleri* in CK brine did not change significantly in both heterotrophic and mixotrophic when the growth of microalgae and quality of effluent treatment were evaluated between mixotrophic and heterotrophic. Mixing two types of desalter effluent was favorable media for *P.kessleri* to remove the maximum COD removal up to 82.9%. To sum up the result of COD final in AV brine shows, *P.kessleri* can reduce COD in the range of environmental guideline of Canada to be discharged while it has the advantage of being tolerated in high salt, remove phenol and Benzene. Benzene was removed up to 51% in the closed photobioreactor system
- Growth of *D.hansenii* in CSTR in different dilution rates gives a model to predict the dilution rate regarding hydrocarbon concentration in desalter effluent. Growth and hydrocarbon removal at different dilution rate of desalter effluent using *D.hansenii* was studied , then CSTR can be designed based on optimum dilution rate that remove high COD percentage. Furthermore, the study can be developed in high substrate (Hydrocarbon) concentration to find an inhibition kinetics model. In current study the Monod model was fit with experimental data.

7.1 Recommendation

The current research on biotreatment of desalter effluent by halotolerant yeast and robust microalgae *Parachlorella kessleri* is still in early phases. Bioremediation and Phycoremediation of desalter effluent are completely a brand-new approach and no information regarding its interactions and biocompatibility are available in the literature. Collective research in different disciplines is required to understand many of the missing parts in this field. The present research is considered the first step in this field and the

following points are recommended to improve the bioremediation of desalter effluent by halotolerant yeast and robust microalgae.

Biodegradation of desalter effluent using *D.hansenii* and *P.kessleri* was limited to petroleum refinery effluent in Sarnia, ON, Canada. Due to the versatility of both microorganisms, other types of effluent might show better biocompatibility. Future studies should concentrate on mixtures of substrates. Other microorganisms can also be investigated.

Too much ammonia can inhibit biomass growth. Other sources of wastewater mixed with desalted effluent can be investigated. A balance between supplement media and requirement of microorganism for optimum degradation and optimum removal in bioreactor must be developed. Growth of *P.kessleri* is highly dependent on COD and Phosphorous concentrations, and pollutant removal. Desalter effluent can be mixed and dilute by other types of effluent inside of petroleum refinery or external industrial effluent which are nearby.

Biodegradation requires optimization. This process due to microorganism activity is slow; therefore, one run at a time cannot be a decent approach for optimization studies. It is recommended several identical photobioreactors be designed so that various changes can be studied when the reactors are running in parallel.

In the central composite design studies, it was concluded that salt concentration does not have any effect on COD removal. Salt presence in the reactor is the function of desalting unit operation and crude oil properties. To find the best setting point for salt presence based on environmental and operation parameters, Temperature, initial pH, and hydrocarbon concentration, can considerably increase hydrocarbon removal yield.

The full factorial design showed a positive effect on dodecane concentration, temperature, salt and initial pH on hydrocarbon removal using halotolerant yeast after 5 days. This research dodecane concentration from 150 to 750 mgL⁻¹ and NaCl between 1 and 5 gL⁻¹ were examined. It should be investigated in higher dodecane and salt concentration with the same period of 5 days.

Environmental impacts of volatile organic compounds are fully known. To do the optimization study on degradation of Benzene in a closed system, a balance between required oxygen and carbon dioxide must be developed. Using consortium microorganism, *D.hansenii* and *P.kessleri* required to be designed in a photobioreactor.

Growth of *D.hansenii* and *P.kessleri* depend on oxygen. *D.hansenii* has high aerobic metabolism. This captures oxygen and produces CO₂. On the other hand, microalgae required CO₂ to do chemical photosynthesis reaction by taking CO₂ and introducing O₂. It is recommended to maximize Benzene degradation and contaminant removal, the relationship between the cell concentration and the required O₂ and CO₂ is developed. Based on this calculation, a model of contamination removal is designed which is a function of microalgae and yeast cells concentration and the characteristics of media.

This is recommended to study oxygen and CO₂ production be developed in three phases salt content, hydrocarbon content (COD) and microbial metabolism. Then the microorganism concentrations can be designed at the presence of different salt concentration for optimum hydrocarbon removal.

D.hansenii and *P.kessleri* have the high content of lipids, part of biomass can be used for bioremediation of desalter effluent and they do not need to be purchased regularly. If the amount of biomass was considerable, harvesting the biomass and producing biofuel from *D.hansenii* and *P.kessleri* is recommended for development of bioremediation process.

Scale up in larger bioreactors is recommended to develop processes for industrial applications.

Other halotolerant yeasts and microalgae could be explored.

References

1. Dadari S, Rahimi M, Zinadini S. Crude oil desalter effluent treatment using high flux synthetic nanocomposite NF membrane-optimization by response surface methodology. *Desalination*. 2016;377:34-46. doi:10.1016/j.desal.2015.09.005.
2. Juárez ÁB, Vélez CG, Iñiguez AR, et al. A *Parachlorella kessleri* (Trebouxiophyceae, Chlorophyta) strain from an extremely acidic geothermal pond in Argentina. *Phycologia*. 2011;50(4):413-421. doi:10.2216/10-79.1.
3. Pérez-Bibbins B, Salgado JM, Torrado A, Aguilar-Uscanga MG, Domínguez JM. Culture parameters affecting xylitol production by *Debaryomyces hansenii* immobilized in alginate beads. *Process Biochem*. 2013;48(3):387-397. doi:10.1016/j.procbio.2013.01.006.
4. Pereira J, Velasquez I, Blanco R, Sanchez M, Pernalet C, Canelón C. Crude Oil Desalting Process. *Adv Petrochemicals*. 2015;(November 2016). doi:10.5772/61274.
5. Pak A, Mohammadi T. Wastewater treatment of desalting units. 2008;222:249-254. doi:10.1016/j.desal.2007.01.166.
6. Nasehi S, Sarraf MJ, Fazaelpoor MH. Study of Crude Oil Desalting Process in Refinery. 2018:29-33.
7. Meidanshahi V, Jahanmiri A, Rahimpour MR. Modeling and Optimization of Two Stage AC Electrostatic Desalter. *Sep Sci Technol*. 2012. doi:10.1080/01496395.2011.614316.
8. Fahim MA, Alsahhaf TA, Elkilani A. *Fundamentals of Petroleum Refining*.; 2010. doi:10.1016/C2009-0-16348-1.
9. Norouzbahari S, Roostaazad R, Hesampour M. Crude oil desalter effluent

- treatment by a hybrid UF / RO membrane separation process. *DES*. 2009;238(1-3):174-182. doi:10.1016/j.desal.2008.01.045.
10. Basu S. Impact of Opportunity Crudes on Desalter Operation and Wastewater Treatment Performance in a Refinery. *Proc Water Environ Fed*. 2017. doi:10.2175/193864717822154084.
 11. Street V, Street V. Process design , simulation and integration of a new desalter in the crude distillation unit of a refinery Mazda Biglari * Shahrokh Ilkhaani Ibrahim Alhajri Ali Lohi. 2010;3(4):350-361.
 12. YE G, LÜ X, PENG F, HAN P, SHEN X. Pretreatment of Crude Oil by Ultrasonic-electric United Desalting and Dewatering. *Chinese J Chem Eng*. 2008. doi:10.1016/S1004-9541(08)60122-6.
 13. Bijani M, Khomehchi E. Optimization and treatment of wastewater of crude oil desalting unit and prediction of scale formation. 2019.
 14. Xu X, Yang J, Jiang Y, Gao J. Effects of Process Conditions on Desalting and Demetalization of Crude Oil. *Pet Sci Technol*. 2006. doi:10.1081/lft-200056651.
 15. Daage, Michel; Barroeta, Magaly C.; Albert, Brian D.; Yeganeh, Mohsen S.; Sullivan, Andrew P.; Simonetty, Jose X.; Wolfe CJ. Patent Issued for Petroleum Crude Oil Desalting Process And Unit (USPTO 10,077,405). 2018:p1466. <https://link.galegroup.com/apps/doc/A556402539/AONE?u=lond95336&sid=AO NE&xid=f7a12ff9>.
 16. Cunha REP, Fortuny M, Dariva C, Santos AF. Mathematical modeling of the destabilization of crude oil emulsions using population balance equation. *Ind Eng Chem Res*. 2008. doi:10.1021/ie800391v.
 17. Chiesa M. Electrocoalescence modeling: an engineering approach. *15th Australas Fluid Mech Conf* 2004.
 18. Melheim JA, Chiesa M. Simulation of turbulent electrocoalescence. *Chem Eng Sci*.

2006. doi:10.1016/j.ces.2006.02.022.
19. Al-Otaibi MB, Elkamel A, Nassehi V, Abdul-Wahab SA. A computational intelligence based approach for the analysis and optimization of a crude oil desalting and dehydration process. *Energy and Fuels*. 2005. doi:10.1021/ef050132j.
 20. Popp VV, Dinulescu VD. Dehydration and Desalting of Heavy and Viscous Crude Oil Produced by In-Situ Combustion. *SPE Prod Facil*. 2007. doi:10.2118/28539-pa.
 21. Bai ZS, Wang HL. Crude oil desalting using hydrocyclones. *Chem Eng Res Des*. 2007. doi:10.1016/S0263-8762(07)73203-3.
 22. Medel A, Bustos E, Esquivel K, Godínez LA, Meas Y. Electrochemical Incineration of Phenolic Compounds from the Hydrocarbon Industry Using Boron-Doped Diamond Electrodes. *Int J Photoenergy*. 2012. doi:10.1155/2012/681875.
 23. Medel A, Méndez E, Hernández-López JL, et al. Novel Electrochemical Treatment of Spent Caustic from the Hydrocarbon Industry Using Ti/BDD. *Int J Photoenergy*. 2015. doi:10.1155/2015/829136.
 24. García-Lugo F, Medel A, Baizaval JLJ, et al. Mediated electrochemical oxidation of pollutants in crude oil desalter effluent. *Int J Electrochem Sci*. 2018. doi:10.20964/2018.01.03.
 25. Bai ZS, Wang HL. Experiments for desalting and dewatering of crude by hydrocyclones. *Shiyou Xuebao, Shiyou Jiagong/Acta Pet Sin (Petroleum Process Sect)*. 2006.
 26. Majumdar S, Guha AK, Sirkar KK. Fuel oil desalting by hydrogel hollow fiber membrane. *J Memb Sci*. 2002. doi:10.1016/S0376-7388(01)00726-8.
 27. Tirmizi NP, Raghuraman B, Wiencek J. Demulsification of Water/Oil/Solid Emulsions by Hollow-Fiber Membranes. *AIChE J*. 1996.

doi:10.1002/aic.690420508.

28. Sellami MH, Bouguettaia H, Naam R. Optimal Processing Parameters of Electrostatic Crude Oil Desalting. 2018. *حوليات العلوم و التكنولوجيا*. doi:10.12816/0042127.
29. Al-Hadhrami MN, Lappin-Scott HM, Fisher PJ. Bacterial survival and n-alkane degradation within Omani crude oil and a mousse. *Mar Pollut Bull*. 1995. doi:10.1016/0025-326X(94)00235-2.
30. Bardi L, Mattei A, Steffan S. Hydrocarbon degradation by a soil microbial population with β -cyclodextrin as surfactant to enhance bioavailability. *Enzyme Microb Technol*. 2000;27(9):709-713. doi:10.1016/S0141-0229(00)00275-1.
31. Margesin R, Gander S, Zacke G, Gounot AM, Schinner F. Hydrocarbon degradation and enzyme activities of cold-adapted bacteria and yeasts. *Extremophiles*. 2003. doi:10.1007/s00792-003-0347-2.
32. Ikeda H, Suzuki A. Empirical correlations for radiolytic degradation of n-dodecane density, viscosity and phase separation time. *J Nucl Sci Technol*. 2001;38(12):1138-1140. doi:10.1080/18811248.2001.9715148.
33. Parche S, Geißdörfer W, Hillen W. Identification and characterization of xcpR encoding a subunit of the general secretory pathway necessary for dodecane degradation in *Acinetobacter calcoaceticus* ADP1. *J Bacteriol*. 1997. doi:10.1128/jb.179.14.4631-4634.1997.
34. Gurav R, Lyu H, Ma J, Tang J, Liu Q, Zhang H. Degradation of n-alkanes and PAHs from the heavy crude oil using salt-tolerant bacterial consortia and analysis of their catabolic genes. *Environ Sci Pollut Res*. 2017;24(12):11392-11403. doi:10.1007/s11356-017-8446-2.
35. Zhang Z, Hou Z, Yang C, Ma C, Tao F, Xu P. Degradation of n-alkanes and polycyclic aromatic hydrocarbons in petroleum by a newly isolated *Pseudomonas aeruginosa* DQ8. *Bioresour Technol*. 2011;102(5):4111-4116.

doi:10.1016/j.biortech.2010.12.064.

36. Nie Y, Liang J, Fang H, Tang YQ, Wu XL. Two novel alkane hydroxylase-rubredoxin fusion genes isolated from a Dietzia bacterium and the functions of fused rubredoxin domains in long-chain n-alkane degradation. *Appl Environ Microbiol.* 2011;77(20):7279-7288. doi:10.1128/AEM.00203-11.
37. Yan N, Zhao Y, Wu D, Jia J, Wang W, Yao S. Degradation of dodecanethiol in dodecane by γ -irradiation and improvement by sensitization. *Fuel Process Technol.* 2004;85(12):1393-1402. doi:10.1016/j.fuproc.2003.09.001.
38. IPIECA. Petroleum refining water/wastewater use and management. *Ipieca.* 2010:1-60. doi:10.1016/j.apgeog.2008.08.008.
39. Wauquier J-P. Basic Principles Governing Chemical Changes. In: *Petroleum Refining, Volume 3 - Conversion Processes.* ; 2001.
40. Gurnham CF. Aqueous Wastes from Petroleum and Petrochemical plants, Milton R. Beychok, John Wiley & Sons, Inc., New York(1 967). 370 pages,\$ 12.75. *AIChE J.* 2004. doi:10.1002/aic.690140102.
41. Naseri M, Barabady J. System-Reliability Analysis by Use of Gaussian Fuzzy Fault Tree: Application in Arctic Oil and Gas Facilities. *Oil Gas Facil.* 2015. doi:10.2118/170826-pa.
42. MH S, R N. Optimization of Operating Parameters of Oil Desalting in Southern Treatment Unit (HMD/Algeria). *J Pet Environ Biotechnol.* 2016. doi:10.4172/2157-7463.1000271.
43. Pereira J, Velasquez I, Blanco R, Sanchez M, Pernalet C, Canelón C. Crude Oil Desalting Process. *Adv Petrochemicals.* 2015;(November). doi:10.5772/61274.
44. Bagajewicz M. A review of recent design procedures for water networks in refineries and process plants. *Comput Chem Eng.* 2000;24(9-10):2093-2113. doi:10.1016/S0098-1354(00)00579-2.

45. Kaldanovna G. Setting up individual indicators of economic efficiency for environmental protection in oil refineries. 2018.
46. Kamari A, Bahadori A, Mohammadi AH. On the determination of crude oil salt content: Application of robust modeling approaches. *J Taiwan Inst Chem Eng*. 2015. doi:10.1016/j.jtice.2015.03.031.
47. Aleisa RM, Akmal N. An in-situ electropolymerization based sensor for measuring salt content in crude oil. *Talanta*. 2015. doi:10.1016/j.talanta.2014.09.016.
48. Bahadori A, Zahedi G, Zendejboudi S, Jamili A. Estimation of crude oil salt content using a simple predictive tool approach. *J Pet Sci Eng*. 2012. doi:10.1016/j.petrol.2012.06.033.
49. Alshehri AK, Ricardez-Sandoval LA, Elkamel A. Designing and Testing a Chemical Demulsifier Dosage Controller in a Crude Oil Desalting Plant: An Artificial Intelligence-Based Network Approach. *Chem Eng Technol*. 2010. doi:10.1002/ceat.200900615.
50. Al-Otaibi M, Elkamel A, Al-Sahhaf T, Ahmed AS. Experimental investigation of crude oil desalting and dehydration. *Chem Eng Commun*. 2003. doi:10.1080/00986440302094.
51. Bureau JRC-I-EI. *Best Available Techniques (BAT) Reference Document for the Production of Pulp, Paper and Board - Final Draft July 2013.*; 2015. doi:10.2788/12850.
52. Azimian L, Bassi A, Mercer SM. Investigation of growth kinetics of *Debaryomyces hansenii* (LAF-3 10 U) in petroleum refinery desalter effluent. *Can J Chem Eng*. 2019. doi:10.1002/cjce.23297.
53. Gude VG. Desalination and water reuse to address global water scarcity. *Rev Environ Sci Biotechnol*. 2017;16(4):591-609. doi:10.1007/s11157-017-9449-7.
54. Industry PR. LIQUID EFFLUENT GUIDELINES FOR THE PETROLEUM

REFINING INDUSTRY, Ontario. 1977.

55. Schultz TE. Get the most out of API separators. *Chem Eng*. 2005.
56. Shammas NK, Bennett GF. Principles of Air Flotation Technology. In: *Flotation Technology*. ; 2010. doi:10.1007/978-1-60327-133-2_1.
57. Rubio J, Souza ML, Smith RW. Overview of flotation as a wastewater treatment technique. *Miner Eng*. 2002. doi:10.1016/S0892-6875(01)00216-3.
58. Cox M. *A Guide Book on the Treatment of Effluents from the Mining/Metallurgy/Paper/Platine/Textile.*; 2006.
http://elib.dlr.de/49460/1/ILE_guide_book.pdf.
59. Chen G. Electrochemical technologies in wastewater treatment. *Sep Purif Technol*. 2004. doi:10.1016/j.seppur.2003.10.006.
60. Roth HP, Ferguson PV. An integrated industrial waste water treatment system using electroflotation and reverse osmosis. *Desalination*. 1977. doi:10.1016/s0011-9164(00)82508-4.
61. De Oliveira Da Mota I, De Castro JA, De Góes Casqueira R, De Oliveira Junior AG. Study of electroflotation method for treatment of wastewater from washing soil contaminated by heavy metals. *J Mater Res Technol*. 2015.
doi:10.1016/j.jmrt.2014.11.004.
62. Kyzas GZ, Matis KA. Electroflotation process: A review. *J Mol Liq*. 2016.
doi:10.1016/j.molliq.2016.04.128.
63. Kolesnikov VA, Il'in VI, Kolesnikov A V. Electroflotation in Wastewater Treatment from Oil Products, Dyes, Surfactants, Ligands, and Biological Pollutants: A Review. *Theor Found Chem Eng*. 2019.
doi:10.1134/s0040579519010093.
64. Nonato TCM, Schöntag JM, Burgardt T, et al. Combination of electroflotation

- process and down-flow granular filtration to treat wastewater contaminated with oil. *Environ Technol (United Kingdom)*. 2018.
doi:10.1080/09593330.2017.1310306.
65. Hosny AY. Separating oil from oil-water emulsions by electroflotation technique. *Sep Technol*. 1996. doi:10.1016/0956-9618(95)00136-0.
66. Ben Mansour L, Chalbi S. Removal of oil from oil/water emulsions using electroflotation process. *J Appl Electrochem*. 2006. doi:10.1007/s10800-005-9109-4.
67. Issaoui R, Ksentini I, Kotti M, Ben Mansour L. Effect of current density and oil concentration on hydrodynamic aspects in electroflotation column during oil/water emulsion treatment. *J Water Chem Technol*. 2017.
doi:10.3103/s1063455x17030080.
68. Painmanakul P, Sastaravet P, Lersjintanakarn S, Khaodhiar S. Effect of bubble hydrodynamic and chemical dosage on treatment of oily wastewater by Induced Air Flotation (IAF) process. *Chem Eng Res Des*. 2010.
doi:10.1016/j.cherd.2009.10.009.
69. da Silva SS, Chiavone-Filho O, de Barros Neto EL, Nascimento CAO. Integration of processes induced air flotation and photo-Fenton for treatment of residual waters contaminated with xylene. *J Hazard Mater*. 2012.
doi:10.1016/j.jhazmat.2011.10.070.
70. Santander M, Rodrigues RT, Rubio J. Modified jet flotation in oil (petroleum) emulsion/water separations. *Colloids Surfaces A Physicochem Eng Asp*. 2011.
doi:10.1016/j.colsurfa.2010.12.027.
71. Li C, Wang L. Improved froth zone and collection zone recoveries of fine mineral particles in a flotation column with oscillatory air supply. *Sep Purif Technol*. 2018.
doi:10.1016/j.seppur.2017.10.054.
72. Rubio J. Modified column flotation of mineral particles. *Int J Miner Process*.

1996. doi:10.1016/S0301-7516(96)00026-9.
73. Al-Shamrani AA, James A, Xiao H. Separation of oil from water by dissolved air flotation. *Colloids Surfaces A Physicochem Eng Asp.* 2002. doi:10.1016/S0927-7757(02)00208-X.
 74. Maldonado M, Desbiens A, del Villar R. Potential use of model predictive control for optimizing the column flotation process. *Int J Miner Process.* 2009. doi:10.1016/j.minpro.2009.05.004.
 75. Benker B, Wollmann A, Sievers M. Centrifugal Flotation Applied to the Separation of Oil and Fat from Wastewater. *Eng Life Sci.* 2003. doi:10.1002/elsc.200390008.
 76. Puget FP, Melo M V., Massarani G. Comparative study of flotation techniques for the treatment of liquid effluents. *Environ Technol (United Kingdom).* 2004. doi:10.1080/09593330409355440.
 77. Melo M V., Sant'Anna GL, Massarani G. Flotation techniques for oily water treatment. *Environ Technol (United Kingdom).* 2003. doi:10.1080/09593330309385623.
 78. Ju DJ, Hu FP, Wang LY. Study on the dewatering characteristics and efficiency of thickening low concentration excess sludge by Cavitation Air Flotation (CAF). In: *Proceedings - 3rd International Conference on Measuring Technology and Mechatronics Automation, ICMTMA 2011.* ; 2011. doi:10.1109/ICMTMA.2011.705.
 79. Bahadori A. *Waste Management in the Chemical and Petroleum Industries.*; 2013. doi:10.1002/9781118731741.
 80. US EPA O. Effluent Guidelines. Environmental Protection Agency.
 81. Santiago O, Walsh K, Kele B, Gardner E, Chapman J. Novel pre-treatment of zeolite materials for the removal of sodium ions: potential materials for coal seam

- gas co-produced wastewater. *Springerplus*. 2016. doi:10.1186/s40064-016-2174-9.
82. Jeffrey G. Skousen AS and PFZ. ACID MINE DRAINAGE CONTROL AND TREATMENT. *Am Soc Agron*. 2008. doi:10.1016/j.crma.2008.09.014.
 83. Ginzburg B, Cansino R. Water Reuse in an Oil Refinery: An Innovative Solution Using Membrane Technology. *Proc Water Environ Fed*. 2012. doi:10.2175/193864709802770054.
 84. Dąbrowski A, Hubicki Z, Podkościelny P, Robens E. Selective removal of the heavy metal ions from waters and industrial wastewaters by ion-exchange method. *Chemosphere*. 2004. doi:10.1016/j.chemosphere.2004.03.006.
 85. RENIX. <https://www.renix.ca/>. Accessed August 5, 2019.
 86. Smith RW. Liquid and solid wastes from mineral processing plants. *Miner Process Extr Metall Rev*. 1996. doi:10.1080/08827509608914127.
 87. Crini G, Lichtfouse E. Advantages and disadvantages of techniques used for wastewater treatment. *Environ Chem Lett*. 2019. doi:10.1007/s10311-018-0785-9.
 88. Hayes M, Sherwood N. Removal of Selenium in Refinery Effluent with Adsorption Media. *Proc Water Environ Fed*. 2014. doi:10.2175/193864712811740701.
 89. Hashemi W Al, Maraqa MA, Rao M V, Hossain M. Characterization and removal of phenolic compounds from condensate-oil refinery wastewater. *Desalin Water Treat*. 2015;54:1-12. doi:10.1080/19443994.2014.884472.
 90. Misiti T, Tezel U, Pavlostathis SG. Fate and effect of naphthenic acids on oil refinery activated sludge wastewater treatment systems. *Water Res*. 2012;47(1):449-460. doi:10.1016/j.watres.2012.10.036.
 91. Chuah TG, Jumasiah A, Azni I, Katayon S, Thomas Choong SY. Rice husk as a potentially low-cost biosorbent for heavy metal and dye removal: An overview.

- Desalination*. 2005. doi:10.1016/j.desal.2004.10.014.
92. Bellanca KS, Marrs DR. Characterization and Treatability of Mercury in a Petroleum Refinery Wastewater Discharge. *Proc Water Environ Fed*. 2016. doi:10.2175/193864715819539902.
 93. Kuljian A, Brazier R, Arntsen B, Shamitko G. Immersed membrane biological reactor (MBR) with hollow fiber ultrafiltration technology for coke oven wastewater treatment. *AISTech - Iron Steel Technol Conf Proc*. 2014.
 94. Zouboulis A, Peleka E, Ntolia A. Treatment of Tannery Wastewater with Vibratory Shear-Enhanced Processing Membrane Filtration. *Separations*. 2019. doi:10.3390/separations6020020.
 95. Ayangbenro AS, Olanrewaju OS, Babalola OO. Sulfate-reducing bacteria as an effective tool for sustainable acid mine bioremediation. *Front Microbiol*. 2018. doi:10.3389/fmicb.2018.01986.
 96. Lu Z, Jiang J, Ren M, Xu J, Da J, Cao F. The study on removing the salts in crude oil via ethylene glycol extraction. *Energy and Fuels*. 2015. doi:10.1021/ef502453j.
 97. Qdais HA, Moussa H. Removal of heavy metals from wastewater by membrane processes: A comparative study. *Desalination*. 2004. doi:10.1016/S0011-9164(04)00169-9.
 98. Madwar K, Tarazi H. Desalination techniques for industrial wastewater reuse. *Desalination*. 2003;152(1-3):325-332. doi:10.1016/S0011-9164(02)01080-9.
 99. Basics CO. Using V ⇄ SEP to Treat Desalter Effluent. 2003.
 100. Jaffrin MY. Dynamic shear-enhanced membrane filtration: A review of rotating disks, rotating membranes and vibrating systems. *J Memb Sci*. 2008. doi:10.1016/j.memsci.2008.06.050.
 101. Kentish SE, Stevens GW. Innovations in separations technology for the recycling

- and re-use of liquid waste streams. *Chem Eng J*. 2001. doi:10.1016/S1385-8947(01)00199-1.
102. Patnaik PR. Liquid emulsion membranes: Principles, problems and applications in fermentation processes. *Biotechnol Adv*. 1995. doi:10.1016/0734-9750(95)00001-7.
 103. Kumar A, Thakur A, Panesar PS. A review on emulsion liquid membrane (ELM) for the treatment of various industrial effluent streams. *Rev Environ Sci Biotechnol*. 2019. doi:10.1007/s11157-019-09492-2.
 104. Brunori C, Cremisini C, Massanisso P, Pinto V, Torricelli L. Reuse of a treated red mud bauxite waste: Studies on environmental compatibility. *J Hazard Mater*. 2005. doi:10.1016/j.jhazmat.2004.09.010.
 105. Mamindy-Pajany Y, Hurel C, Marmier N, Roméo M. Arsenic (V) adsorption from aqueous solution onto goethite, hematite, magnetite and zero-valent iron: Effects of pH, concentration and reversibility. *Desalination*. 2011. doi:10.1016/j.desal.2011.07.046.
 106. Darwish M, Mohtar R, Elgendy Y, Chmeissani M. Desalting seawater in Qatar by renewable energy: A feasibility study. *Desalin Water Treat*. 2012;47(1-3):279-294. doi:10.1080/19443994.2012.696409.
 107. Sungpet A, Jiraratananon R, Luangsowan P. Treatment of effluents from textile-rinsing operations by thermally stable nanofiltration membranes. *Desalination*. 2004. doi:10.1016/S0011-9164(04)90019-7.
 108. Sattler C, Funken KH, Jung C, Monnerie N, De Oliveira L, Schäfer T. Demonstration of photocatalytic waste water detoxification in textile industry. In: *REWAS'04 - Global Symposium on Recycling, Waste Treatment and Clean Technology*. ; 2005.
 109. Shahrezaei F, Mansouri Y, Zinatizadeh AAL, Akhbari A. Process modeling and kinetic evaluation of petroleum refinery wastewater treatment in a photocatalytic

- reactor using TiO₂ nanoparticles. *Powder Technol.* 2012;221:203-212.
doi:10.1016/j.powtec.2012.01.003.
110. Saien J, Nejati H. Enhanced photocatalytic degradation of pollutants in petroleum refinery wastewater under mild conditions. *J Hazard Mater.* 2007.
doi:10.1016/j.jhazmat.2007.03.001.
 111. Diya'uddeen BH, Daud WMAW, Abdul Aziz AR. Treatment technologies for petroleum refinery effluents: A review. *Process Saf Environ Prot.* 2011;89(2):95-105. doi:10.1016/j.psep.2010.11.003.
 112. Jones E, Qadir M, van Vliet MTH, Smakhtin V, Kang S mu. The state of desalination and brine production: A global outlook. *Sci Total Environ.* 2019.
doi:10.1016/j.scitotenv.2018.12.076.
 113. Eltawil MA, Zhengming Z, Yuan L. A review of renewable energy technologies integrated with desalination systems. *Renew Sustain Energy Rev.* 2009.
doi:10.1016/j.rser.2009.06.011.
 114. Koroneos C, Nanaki E, Moustakas K, Malamis D. Renewable Energy Desalination. *Renew Energy Desalin.* 2012. doi:10.1596/978-0-8213-8838-9.
 115. MILLER JE. *Review of Water Resources and Desalination Technologies.*; 2003.
doi:10.2172/809106.
 116. Koroneos C, Dompros A, Roubas G. Renewable energy driven desalination systems modelling. *J Clean Prod.* 2007. doi:10.1016/j.jclepro.2005.07.017.
 117. Cohen AJ, Siu R. Sustainable Growth : Taking a Deep Dive into Water. *Goldman Sachs Gr Inc Glob Mark Inst.* 2013;(May 8):26.
<http://www.goldmansachs.com/our-thinking/clean-technology-and-renewables/cohen/report.pdf>.
 118. Gude VG. Desalination and sustainability - An appraisal and current perspective. *Water Res.* 2016. doi:10.1016/j.watres.2015.11.012.

119. Bednorz E. Global Water Prices Outstrip Inflation as Scarcity, Neglect and Public Finances Catch up with Customers.
<http://www.prweb.com/releases/2014/10/prweb12216091.htm>. Published 2019.
120. Zhou Y, Tol RSJ. Evaluating the costs of desalination and water transport. *Water Resour Res.* 2005. doi:10.1029/2004WR003749.
121. Karagiannis IC, Soldatos PG. Water desalination cost literature: review and assessment. *Desalination.* 2008. doi:10.1016/j.desal.2007.02.071.
122. Ayoub J, Alward R. Water requirements and remote arid areas: the need for small-scale desalination. *Desalination.* 1996. doi:10.1016/S0011-9164(96)00158-0.
123. Turek M, Dydo P. Hybrid membrane - Thermal versus simple membrane systems. *Desalination.* 2003. doi:10.1016/S0011-9164(03)00382-5.
124. Hafez A, El-Manharawy S. Economics of seawater RO desalination in the Red Sea region, Egypt. Part 1. A case study. *Desalination.* 2003. doi:10.1016/S0011-9164(02)01122-0.
125. Lamei A, van der Zaag P, von Münch E. Impact of solar energy cost on water production cost of seawater desalination plants in Egypt. *Energy Policy.* 2008. doi:10.1016/j.enpol.2007.12.026.
126. Rayan MA, Djebedjian B, Khaled I. Water supply and demand and a desalination option for Sinai, Egypt. *Desalination.* 2001. doi:10.1016/S0011-9164(01)00167-9.
127. Matz R, Fisher U. A comparison of the relative economics of sea water desalination by vapour compression and reverse osmosis for small to medium capacity plants. *Desalination.* 1981. doi:10.1016/S0011-9164(00)88637-3.
128. Ettouney H. Visual basic computer package for thermal and membrane desalination processes. *Desalination.* 2004. doi:10.1016/j.desal.2004.06.045.
129. Banat F, Jwaied N. Economic evaluation of desalination by small-scale

- autonomous solar-powered membrane distillation units. *Desalination*. 2008. doi:10.1016/j.desal.2007.01.057.
130. National Research Council of the National Academies; *Desalination: A National Perspective.*; 2008.
 131. Adler L, Gustafsson L. Polyhydric alcohol production and intracellular amino acid pool in relation to halotolerance of the yeast *Debaryomyces hansenii*. *Arch Microbiol*. 1980. doi:10.1007/BF00427716.
 132. Gadd GM, Edwards SW. Heavy-metal-induced flavin production by *Debaryomyces hansenii* and possible connexions with iron metabolism. *Trans Br Mycol Soc*. 1986. doi:10.1016/s0007-1536(86)80094-8.
 133. Berrocal CA, Rivera-Vicens RE, Nadathur GS. Draft genome sequence of the heavy-metal-tolerant marine yeast *Debaryomyces hansenii* J6. *Genome Announc*. 2016. doi:10.1128/genomeA.00983-16.
 134. Norkrans B. Studies on marine occurring yeasts: Growth related to pH, NaCl concentration and temperature. *Arch Mikrobiol*. 1966. doi:10.1007/BF00406719.
 135. Norkrans B, Kylin A. Regulation of the potassium to sodium ratio and of the osmotic potential in relation to salt tolerance in yeasts. *J Bacteriol*. 1969.
 136. Cavaliere AR, Moss ST. The Biology of Marine Fungi. *Mycologia*. 1987. doi:10.2307/3807837.
 137. Breuer U, Harms H. *Debaryomyces hansenii* - An extremophilic yeast with biotechnological potential. *Yeast*. 2006;23(6):415-437. doi:10.1002/yea.1374.
 138. Al-Qaysi SAS, Al-Haideri H, Thabit ZA, Al-Kubaisy WHAAR, Ibrahim JAAR. Production, Characterization, and Antimicrobial Activity of Mycocin Produced by *Debaryomyces hansenii* DSMZ70238. *Int J Microbiol*. 2017. doi:10.1155/2017/2605382.

139. Banjara N, Suhr MJ, Hallen-Adams HE. Diversity of Yeast and Mold Species from a Variety of Cheese Types. *Curr Microbiol.* 2015. doi:10.1007/s00284-015-0790-1.
140. Banjara N, Nickerson KW, Suhr MJ, Hallen-Adams HE. Killer toxin from several food-derived *Debaryomyces hansenii* strains effective against pathogenic *Candida* yeasts. *Int J Food Microbiol.* 2016. doi:10.1016/j.ijfoodmicro.2016.01.016.
141. Capece A, Romano P. "Pecorino di Filiano" cheese as a selective habitat for the yeast species, *Debaryomyces hansenii*. *Int J Food Microbiol.* 2009. doi:10.1016/j.ijfoodmicro.2009.04.007.
142. Desnos-Ollivier M, Ragon M, Robert V, Raoux D, Gantier JC, Dromer F. *Debaryomyces hansenii* (*Candida famata*), a rare human fungal pathogen often misidentified as *Pichia guilliermondii* (*Candida guilliermondii*). *J Clin Microbiol.* 2008. doi:10.1128/JCM.01451-08.
143. Yadav JS, Loper JC. Multiple P450alk (cytochrome P450 alkane hydroxylase) genes from the halotolerant yeast *Debaryomyces hansenii*. *Gene.* 1999. doi:10.1016/S0378-1119(98)00579-4.
144. Neves ML, Oliveira RP, Lucas CM. Metabolic flux response to salt-induced stress in the halotolerant yeast *Debaryomyces hansenii*. *Microbiology.* 1997;143(4):1133-1139. doi:10.1099/00221287-143-4-1133.
145. Nakase T, Suzuki M. Taxonomic studies on *debaryomyces hansenii* (zopf) lodder et kreger-van rij and related species. I. chemotaxonomic investigations. *J Gen Appl Microbiol.* 1985. doi:10.2323/jgam.31.49.
146. Middelhoven WJ. Catabolism of benzene compounds by ascomycetous and basidiomycetous yeasts and yeastlike fungi - A literature review and an experimental approach. *Antonie Van Leeuwenhoek.* 1993. doi:10.1007/BF00872388.
147. Cerniglia CE, Crow SA. Metabolism of aromatic hydrocarbons by yeasts. *Arch*

- Microbiol.* 1981. doi:10.1007/BF00417170.
148. Hofmann KH, Schauer F. Utilization of phenol by hydrocarbon assimilating yeasts. *Antonie Van Leeuwenhoek.* 1988. doi:10.1007/BF00419204.
 149. Gustafsson L, Norkrans B. On the mechanism of salt tolerance - Production of glycerol and heat during growth of *Debaryomyces hansenii*. *Arch Microbiol.* 1976. doi:10.1007/BF00690226.
 150. Adler L, Blomberg A, Nilsson A. Glycerol metabolism and osmoregulation in the salt-tolerant yeast *Debaryomyces hansenii*. *J Bacteriol.* 1985.
 151. Ratledge C. Regulation of lipid accumulation in oleaginous micro-organisms. In: *Biochemical Society Transactions.* ; 2002. doi:10.1042/BST0301047.
 152. Champenois J, Marfaing H, Pierre R. Review of the taxonomic revision of *Chlorella* and consequences for its food uses in Europe. *J Appl Phycol.* 2015. doi:10.1007/s10811-014-0431-2.
 153. Kessler E. Physiological and biochemical contributions to the taxonomy of the genus *Prototheca* - I. Hydrogenase, acid tolerance, salt tolerance, thermophily, and liquefaction of gelatin. *Arch Microbiol.* 1977. doi:10.1007/BF00428593.
 154. Němcová Y, Kalina T. Cell wall development, microfibril and pyrenoid structure in type strains of *Chlorella vulgaris*, *C. kessleri*, *C. sorokiniana* compared with *C. luteoviridis* (Trebouxiophyceae, Chlorophyta). *Algol Stud für Hydrobiol Suppl Vol.* 2000. doi:10.1127/algol_stud/100/2000/95.
 155. Krienitz L, Hegewald EH, Hepperle D, Huss VAR, Rohr T, Wolf M. Phylogenetic relationship of *Chlorella* and *Parachlorella* gen. nov. (Chlorophyta, Trebouxiophyceae). *Phycologia.* 2004. doi:10.2216/i0031-8884-43-5-529.1.
 156. Simmons DBD, Wallschläger D. Release of reduced inorganic selenium species into waters by the green fresh water algae *Chlorella vulgaris*. *Environ Sci Technol.* 2011. doi:10.1021/es103337p.

157. Slaveykova VI, Parthasarathy N, Buffle J, Wilkinson KJ. Permeation liquid membrane as a tool for monitoring bioavailable Pb in natural waters. *Sci Total Environ.* 2004. doi:10.1016/j.scitotenv.2003.10.007.
158. Slaveykova VI, Wilkinson KJ, Ceresa A, Pretsch E. Role of fulvic acid on lead bioaccumulation by *Chlorella kesslerii*. *Environ Sci Technol.* 2003. doi:10.1021/es025993a.
159. Science and Technology Branch, Environment Canada, Ottawa O. Biological test method: growth inhibition test using a freshwater alga - Canada.ca. Environment Canada. <https://www.canada.ca/en/environment-climate-change/services/wildlife-research-landscape-science/biological-test-method-publications/growth-inhibition-test-freshwater-alga.html#loa>. Published 2007. Accessed August 25, 2019.
160. Huss VAR, Frank C, Hartmann EC, et al. BIOCHEMICAL TAXONOMY AND MOLECULAR PHYLOGENY OF THE GENUS CHLORELLA SENSU LATO (CHLOROPHYTA). *J Phycol.* 1999. doi:10.1046/j.1529-8817.1999.3530587.x.
161. Ota S, Oshima K, Yamazaki T, et al. Highly efficient lipid production in the green alga *Parachlorella kesslerii*: Draft genome and transcriptome endorsed by whole-cell 3D ultrastructure. *Biotechnol Biofuels.* 2016. doi:10.1186/s13068-016-0424-2.
162. Slaveykova VI, Wilkinson KJ. Effect of pH on Pb biouptake by the freshwater alga *Chlorella kesslerii*. *Environ Chem Lett.* 2003. doi:10.1007/s10311-003-0041-8.
163. Leblanc KL, Wallschläger D. Production and Release of Selenomethionine and Related Organic Selenium Species by Microorganisms in Natural and Industrial Waters. *Environ Sci Technol.* 2016. doi:10.1021/acs.est.5b05315.
164. Assessing the effect of selenium on the life-cycle of two aquatic invertebrates: 2013.
165. Hassler CS, Behra R, Wilkinson KJ. Impact of zinc acclimation on bioaccumulation and homeostasis in *Chlorella kesslerii*. *Aquat Toxicol.* 2005.

doi:10.1016/j.aquatox.2005.02.008.

166. Slaveykova VI. Predicting Pb bioavailability to freshwater microalgae in the presence of fulvic acid: Algal cell density as a variable. *Chemosphere*. 2007. doi:10.1016/j.chemosphere.2007.04.065.
167. Lamelas C, Wilkinson KJ, Slaveykova VI. Influence of the composition of natural organic matter on Pb bioavailability to microalgae. *Environ Sci Technol*. 2005. doi:10.1021/es050445t.
168. Spierings J, Worms IAM, Miéville P, Slaveykova VI. Effect of humic substance photoalteration on lead bioavailability to freshwater microalgae. *Environ Sci Technol*. 2011. doi:10.1021/es104288y.
169. Lamelas C, Slaveykova VI. Pb uptake by the freshwater alga *Chlorella kesslerii* in the presence of dissolved organic matter of variable composition. *Environ Chem*. 2008. doi:10.1071/EN08043.
170. Hassler CS, Slaveykova VI, Wilkinson KJ. Some fundamental (and often overlooked) considerations underlying the free ion activity and biotic ligand models. *Environ Toxicol Chem*. 2004. doi:10.1897/03-149.
171. Worms IAM, Traber J, Kistler D, Sigg L, Slaveykova VI. Uptake of Cd(II) and Pb(II) by microalgae in presence of colloidal organic matter from wastewater treatment plant effluents. *Environ Pollut*. 2010. doi:10.1016/j.envpol.2009.09.007.
172. Lamelas C, Pinheiro JP, Slaveykova VI. Effect of humic acid on Cd(II), Cu(II), and Pb(II) uptake by freshwater algae: Kinetic and cell wall speciation considerations. *Environ Sci Technol*. 2009. doi:10.1021/es802557r.
173. Lamelas C, Slaveykova VI. Comparison of Cd(II), Cu(II), and Pb(II) biouptake by green algae in the presence of humic acid. *Environ Sci Technol*. 2007. doi:10.1021/es063102j.
174. Worms IAM, Parthasarathy N, Wilkinson KJ. Ni uptake by a green alga. 1.

- Validation of equilibrium models for complexation effects. *Environ Sci Technol*. 2007. doi:10.1021/es0630339.
175. Hassler CS, Wilkinson KJ. Failure of the biotic ligand and free-ion activity models to explain zinc bioaccumulation by *Chlorella kesslerii*. *Environ Toxicol Chem*. 2003. doi:10.1897/1551-5028(2003)022<0620:FOTBLA>2.0.CO;2.
176. Li Y, Han D, Hu G, et al. *Chlamydomonas* starchless mutant defective in ADP-glucose pyrophosphorylase hyper-accumulates triacylglycerol. *Metab Eng*. 2010. doi:10.1016/j.ymben.2010.02.002.
177. Li X, Příbyl P, Bišová K, et al. The microalga *Parachlorella kessleri*--A novel highly efficient lipid producer. *Biotechnol Bioeng*. 2013. doi:10.1002/bit.24595.
178. Brányiková I, Maršálková B, Doucha J, et al. Microalgae--novel highly efficient starch producers. *Biotechnol Bioeng*. 2011. doi:10.1002/bit.23016.
179. Bachmann, David. System and method for reducing hydrocarbons in wastewater. December 1992.
180. Codification C. Pulp and Paper Effluent Regulations Règlement sur les effluents des fabriques de pâtes et papiers. *ReVision*. 2012.
181. Ranade V V., Bhandari VM. Industrial Wastewater Treatment, Recycling, and Reuse: An Overview. In: *Industrial Wastewater Treatment, Recycling and Reuse*. ; 2014:1-80. doi:10.1016/B978-0-08-099968-5.00001-5.
182. El-Naas MH, Surkatti R, Al-Zuhair S. Petroleum refinery wastewater treatment: A pilot scale study. *J Water Process Eng*. 2016;14:6-11. doi:10.1016/j.jwpe.2016.10.005.
183. Sassi B, Mohamed A, Saad B, et al. Suitability of Yeasts for the Treatment of Olive Mill Wastewater. 2010;(2001):1-5.
184. Jiang Y, Wen J, Lan L, Hu Z. Biodegradation of phenol and 4-chlorophenol by the

- yeast *Candida tropicalis*. *Biodegradation*. 2007;18(6):719-729.
doi:10.1007/s10532-007-9100-3.
185. Komarkova E, Paca J, Klapkova E, Stiborova M, Soccol CR, Sobotka M. Physiological changes of *Candida tropicalis* population degrading phenol in fed batch reactor. *Brazilian Arch Biol Technol*. 2003;46(4):537-543.
186. Navarrete C, Siles A, Martínez JL, Calero F, Ramos J. Oxidative stress sensitivity in *Debaryomyces hansenii*. *FEMS Yeast Res*. 2009;9(4):582-590.
doi:10.1111/j.1567-1364.2009.00500.x.
187. Koganti S, Ju LK. *Debaryomyces hansenii* fermentation for arabitol production. *Biochem Eng J*. 2013;79:112-119. doi:10.1016/j.bej.2013.07.014.
188. Cano-García L, Belloch C, Flores M. Impact of *Debaryomyces hansenii* strains inoculation on the quality of slow dry-cured fermented sausages. *Meat Sci*. 2014;96(4):1469-1477. doi:10.1016/j.meatsci.2013.12.011.
189. Anagnostopoulos VA, Symeopoulos BD. Significance of age , temperature , and aeration of yeast cell culture for the biosorption of europium from aquatic systems. *Desalin Water Treat*. 2016;57:1-7. doi:10.1080/19443994.2014.987177.
190. Pinteus S, Alves C, Rodrigues A, Mouga T, Pedrosa R. Algae from the Peniche coast (Portugal) exhibit new promising antibacterial activities against fish pathogenic bacteria. *Curr Opin Biotechnol*. 2011;22(2011):S33-S34.
doi:10.1016/j.copbio.2011.05.074.
191. Mulchandani A, Luong JHT. Microbial inhibition kinetics revisited. *Enzyme Microb Technol*. 1989;11(2):66-73. doi:10.1016/0141-0229(89)90062-8.
192. Tazda??t D, Abdi N, Grib H, Lounici H, Pauss A, Mameri N. Comparison of different models of substrate inhibition in aerobic batch biodegradation of malathion. *Turkish J Eng Environ Sci*. 2013;37(3):221-230. doi:10.3906/muh-1211-7.

193. Prista C, Almagro A, Loureiro-Dias MC, Ramos J. Physiological basis for the high salt tolerance of *Debaryomyces hansenii*. *Appl Environ Microbiol*. 1997;63(10):4005-4009.
194. Aiba S, Shoda M, Nagatani M. Kinetics of product inhibition in alcohol fermentation. *Biotechnol Bioeng*. 2000;67(6):671-690. doi:10.1002/(SICI)1097-0290(20000320)67:6<671::AID-BIT6>3.0.CO;2-W.
195. Edwards VH. The influence of high substrate concentrations on microbial kinetics. *Biotechnol Bioeng*. 1970;12(5):679-712. doi:10.1002/bit.260120504.
196. Hill GA, Robinson CW. Substrate inhibition kinetics: phenol degradation by *Pseudomonas putida*. *Biotechnol Bioeng*. 1975;XVII:1599-1615.
197. Yan J, Jianping W, Hongmei L, Suliang Y, Zongding H. The biodegradation of phenol at high initial concentration by the yeast *Candida tropicalis*. *Biochem Eng J*. 2005;24(3):243-247. doi:10.1016/j.bej.2005.02.016.
198. Zhang L, Ying H, Yan S, Zhan N, Guo Y, Fang W. Hyperbranched poly(amido amine) demulsifiers with ethylenediamine/1,3-propanediamine as an initiator for oil-in-water emulsions with microdroplets. *Fuel*. 2018. doi:10.1016/j.fuel.2018.03.196.
199. Zolfaghari R, Fakhru'l-Razi A, Abdullah LC, Elnashaie SSEH, Pendashteh A. Demulsification techniques of water-in-oil and oil-in-water emulsions in petroleum industry. *Sep Purif Technol*. 2016. doi:10.1016/j.seppur.2016.06.026.
200. Zhou JF, Gao PK, Dai XH, et al. Heavy hydrocarbon degradation of crude oil by a novel thermophilic *Geobacillus stearothermophilus* strain A-2. *Int Biodeterior Biodegrad*. 2018;126:224-230. doi:10.1016/j.ibiod.2016.09.031.
201. De Carvalho CCCR, Da Fonseca MMR. Degradation of hydrocarbons and alcohols at different temperatures and salinities by *Rhodococcus erythropolis* DCL14. *FEMS Microbiol Ecol*. 2005. doi:10.1016/j.femsec.2004.09.010.

202. Gargouri B, Mhiri N, Karray F, Aloui F, Sayadi S. Isolation and Characterization of Hydrocarbon-Degrading Yeast Strains from Petroleum Contaminated Industrial Wastewater. *Biomed Res Int*. 2015. doi:10.1155/2015/929424.
203. Kebabci Ö, Cihangir N. Comparison of three *Yarrowia lipolytica* strains for lipase production: Nbrc 1658, ifo 1195, and a local strain. *Turkish J Biol*. 2012. doi:10.3906/biy-1102-10.
204. Andreishcheva EN, Isakova EP, Sidorov NN, et al. Adaptation to salt stress in a salt-tolerant strain of the yeast *Yarrowia lipolytica*. *Biochemistry (Mosc)*. 1999.
205. Hassanshahian M, Tebyanian H, Cappello S. Isolation and characterization of two crude oil-degrading yeast strains, *Yarrowia lipolytica* PG-20 and PG-32, from the Persian Gulf. *Mar Pollut Bull*. 2012. doi:10.1016/j.marpolbul.2012.04.020.
206. Fukumaki T, Inoue A, Moriya K, Horikoshi K. Isolation of a marine yeast that degrades hydrocarbon in the presence of organic solvent. *Biosci Biotechnol Biochem*. 1994. doi:10.1080/bbb.58.1784.
207. Sørensen BB, Jakobsen M. The combined effects of temperature, pH and NaCl on growth of *Debaryomyces hansenii* analyzed by flow cytometry and predictive microbiology. *Int J Food Microbiol*. 1997;34(3):209-220. doi:10.1016/S0168-1605(96)01192-0.
208. Al-Qaysi SAS, Al-Haideri H, Thabit ZA, Al-Kubaisy WHAAR, Ibrahim JAAR. Production, Characterization, and Antimicrobial Activity of Mycocin Produced by *Debaryomyces hansenii* DSMZ70238. *Int J Microbiol*. 2017. doi:10.1155/2017/2605382.
209. KOCKOVA-KRATOCHVILOVA A, SLAVIKOVA E, JENSEN V. Numerical Taxonomy of the Yeast Genus *Debaryomyces* Lodder & Kreger-van Rij. *J Gen Microbiol*. 2009. doi:10.1099/00221287-104-2-257.
210. Van Dijken JP, Oostra-Demkes GJ, Otto R, Harder W. S-formylglutathione: The substrate for formate dehydrogenase in methanol-utilizing yeasts. *Arch Microbiol*.

1976. doi:10.1007/BF00446552.
211. P. Barthe, M. Chaugny et al. *Best Available Techniques (BAT) Reference Document for the Refining of Mineral Oil and Gas.*; 2015. doi:10.2791/010758.
212. Dubber D, Gray NF. Replacement of chemical oxygen demand (COD) with total organic carbon (TOC) for monitoring wastewater treatment performance to minimize disposal of toxic analytical waste. *J Environ Sci Heal - Part A Toxic/Hazardous Subst Environ Eng.* 2010. doi:10.1080/10934529.2010.506116.
213. Lan Y, Coetsier C, Causserand C, Groenen Serrano K. On the role of salts for the treatment of wastewaters containing pharmaceuticals by electrochemical oxidation using a boron doped diamond anode. *Electrochim Acta.* 2017. doi:10.1016/j.electacta.2017.01.160.
214. Rojo F. Enzymes for Aerobic Degradation of Alkanes. In: *Handbook of Hydrocarbon and Lipid Microbiology.* ; 2009. doi:10.1007/978-3-540-77587-4_59.
215. Kaczorek E, Chrzanowski, Pijanowska A, Olszanowski A. Yeast and bacteria cell hydrophobicity and hydrocarbon biodegradation in the presence of natural surfactants: Rhamnolipides and saponins. *Bioresour Technol.* 2008;99(10):4285-4291. doi:10.1016/j.biortech.2007.08.049.
216. Peña AA, Miller CA. Solubilization rates of oils in surfactant solutions and their relationship to mass transport in emulsions. *Adv Colloid Interface Sci.* 2006. doi:10.1016/j.cis.2006.05.005.
217. Tehrani-Bagha AR, Holmberg K. Solubilization of hydrophobic dyes in surfactant solutions. *Materials (Basel).* 2013. doi:10.3390/ma6020580.
218. Helenius A, McCaslin DR, Fries E, Tanford C. Properties of Detergents. *Methods Enzymol.* 1979. doi:10.1016/0076-6879(79)56066-2.
219. Aiba S, Shoda M, Nagatani M. Kinetics of product inhibition in alcohol

- fermentation. Reprinted from *Biotechnology and Bioengineering*, Vol. X, Issue 6, Pages 845-864 (1968). *Biotechnol Bioeng*. 2000.
220. Sáez-Navarrete C, Gelmi CA, Reyes-Bozo L, Godoy-Faúndez A. An exploratory study of peat and sawdust as enhancers in the (bio)degradation of n-dodecane. *Biodegradation*. 2008. doi:10.1007/s10532-007-9158-y.
221. Jemli M, Zaghden H, Rezgi F, Sayadi S, Kchaou S, Aloui F. Biotreatment of Petrochemical Wastewater: A Case Study from Northern Tunisia. *Water Environ Res*. 2016. doi:10.2175/106143016x14609975746082.
222. Bogan BW, Lahner LM, Sullivan WR, Paterek JR. Degradation of straight-chain aliphatic and high-molecular-weight polycyclic aromatic hydrocarbons by a strain of *Mycobacterium austroafricanum*. *J Appl Microbiol*. 2003. doi:10.1046/j.1365-2672.2003.01824.x.
223. Miranda RDC, De Souza CS, Gomes EDB, Lovaglio RB, Lopes CE, Sousa MDFVDQ. Biodegradation of diesel oil by yeasts isolated from the vicinity of Suape Port in the State of Pernambuco -Brazil. *Brazilian Arch Biol Technol*. 2007;50(1):147-152. doi:10.1590/S1516-89132007000100018.
224. Binazadeh M, Karimi IA, Li Z. Fast biodegradation of long chain n-alkanes and crude oil at high concentrations with *Rhodococcus* sp. Moj-3449. *Enzyme Microb Technol*. 2009;45(3):195-202. doi:10.1016/j.enzmictec.2009.06.001.
225. Zhang J, Zhang X, Liu J, Li R, Shen B. Isolation of a thermophilic bacterium, *Geobacillus* sp. SH-1, capable of degrading aliphatic hydrocarbons and naphthalene simultaneously, and identification of its naphthalene degrading pathway. *Bioresour Technol*. 2012;124:83-89. doi:10.1016/j.biortech.2012.08.044.
226. Wang XB, Chi CQ, Nie Y, et al. Degradation of petroleum hydrocarbons (C6-C40) and crude oil by a novel *Dietzia* strain. *Bioresour Technol*. 2011;102(17):7755-7761. doi:10.1016/j.biortech.2011.06.009.
227. Sponza DT, Gök O. Effect of rhamnolipid on the aerobic removal of polyaromatic

- hydrocarbons (PAHs) and COD components from petrochemical wastewater. *Bioresour Technol.* 2010. doi:10.1016/j.biortech.2009.09.022.
228. Calahorra M, Sánchez NS, Peña A. Activation of fermentation by salts in *Debaryomyces hansenii*. *FEMS Yeast Res.* 2009. doi:10.1111/j.1567-1364.2009.00556.x.
229. Masoud W, Jakobsen M. The combined effects of pH, NaCl and temperature on growth of cheese ripening cultures of *Debaryomyces hansenii* and coryneform bacteria. *Int Dairy J.* 2005. doi:10.1016/j.idairyj.2004.05.008.
230. Prista C, Almagro A, Loureiro-Dias MC, Ramos J. Physiological basis for the high salt tolerance of *Debaryomyces hansenii*. *Appl Environ Microbiol.* 1997.
231. Sánchez NS, Arreguín R, Calahorra M, Peña A. Effects of salts on aerobic metabolism of *Debaryomyces hansenii*. *FEMS Yeast Res.* 2008;8(8):1303-1312. doi:10.1111/j.1567-1364.2008.00426.x.
232. Almagro A, Prista C, Castro S, et al. Effects of salts on *Debaryomyces hansenii* and *Saccharomyces cerevisiae* under stress conditions. *Int J Food Microbiol.* 2000. doi:10.1016/S0168-1605(00)00220-8.
233. Praphailong W, Fleet GH. The effect of pH, sodium chloride, sucrose, sorbate and benzoate on the growth of food spoilage yeasts. *Food Microbiol.* 1997. doi:10.1006/fmic.1997.0106.
234. Sánchez NS, Calahorra M, Ramírez J, Peña A. Salinity and high pH affect energy pathways and growth in *Debaryomyces hansenii*. *Fungal Biol.* 2018. doi:10.1016/j.funbio.2018.07.002.
235. Hobot JA, Jennings DH. Growth of *Debaryomyces hansenii* and *Saccharomyces cerevisiae* in relation to pH and salinity. *Exp Mycol.* 1981. doi:10.1016/0147-5975(81)90025-6.
236. Merritt NR. THE INFLUENCE OF TEMPERATURE ON SOME PROPERTIES

- OF YEAST. *J Inst Brew.* 1966. doi:10.1002/j.2050-0416.1966.tb02977.x.
237. Mohajeri E, Noudeh GD. Effect of temperature on the critical micelle concentration and micellization thermodynamic of nonionic surfactants: Polyoxyethylene sorbitan fatty acid esters. *E-Journal Chem.* 2012. doi:10.1155/2012/961739.
238. Cormack WP Mac, Fraile ER. Characterization of a hydrocarbon degrading psychrotrophic Antarctic bacterium. *Antarct Sci.* 2004. doi:10.1017/S0954102097000199.
239. Al-Hawash AB, Alkooranee JT, Abbood HA, et al. Isolation and characterization of two crude oil-degrading fungi strains from Rumaila oil field, Iraq. *Biotechnol Reports.* 2018;17:104-109. doi:10.1016/j.btre.2017.12.006.
240. Parthipan P, Elumalai P, Sathishkumar K, et al. Biosurfactant and enzyme mediated crude oil degradation by *Pseudomonas stutzeri* NA3 and *Acinetobacter baumannii* MN3. *3 Biotech.* 2017;7(5). doi:10.1007/s13205-017-0902-7.
241. Varjani SJ, Upasani VN. Biodegradation of petroleum hydrocarbons by oleophilic strain of *Pseudomonas aeruginosa* NCIM 5514. *Bioresour Technol.* 2016;222:195-201. doi:10.1016/j.biortech.2016.10.006.
242. Vuppaladadiyam AK, Prinsen P, Raheem A, Luque R, Zhao M. Sustainability Analysis of Microalgae Production Systems: A Review on Resource with Unexploited High-Value Reserves. *Environ Sci Technol.* 2018. doi:10.1021/acs.est.8b02876.
243. Bohutskyi P, Liu K, Nasr LK, et al. Bioprospecting of microalgae for integrated biomass production and phytoremediation of unsterilized wastewater and anaerobic digestion centrate. *Appl Microbiol Biotechnol.* 2015. doi:10.1007/s00253-015-6603-4.
244. Kang R, Wang J, Shi D, Cong W, Cai Z, Ouyang F. Interactions between organic and inorganic carbon sources during mixotrophic cultivation of *Synechococcus* sp.

- Biotechnol Lett.* 2004. doi:10.1023/B:BILE.0000045646.23832.a5.
245. Clavijo Rivera E, Montalescot V, Viau M, et al. Mechanical cell disruption of *Parachlorella kessleri* microalgae: Impact on lipid fraction composition. *Bioresour Technol.* 2018. doi:10.1016/j.biortech.2018.01.148.
246. Takáčová A, Smolinská M, Semerád M, Matúš P. Degradation of btex by microalgae *Parachlorella kessleri*. *Pet Coal.* 2015.
247. You Z, Zhang Q, Miao X. Increasing DNA content for cost-effective oil production in *Parachlorella kessleri*. *Bioresour Technol.* 2019;285(March):121332. doi:10.1016/j.biortech.2019.121332.
248. O'Rourke R, Gaffney M, Murphy R. The effects of *Parachlorella kessleri* cultivation on brewery wastewater. *Water Sci Technol.* 2016. doi:10.2166/wst.2015.618.
249. Zonouzi A, Auli M, Dakheli MJ, Hejazi MA. Oil Extraction from Microalgae *Dunalliella sp.* by Polar and Non-Polar Solvents. *Int J Biol Biomol Agric Food Biotechnol Eng.* 2016.
250. Gao Y, Feng J, Lv J, et al. Physiological Changes of *Parachlorella Kessleri* TY02 in Lipid Accumulation under Nitrogen Stress. *Int J Environ Res Public Health.* 2019;16(7):1188. doi:10.3390/ijerph16071188.
251. FOLCH J, LEES M, SLOANE STANLEY GH. A simple method for the isolation and purification of total lipides from animal tissues. *J Biol Chem.* 1957.
252. Bligh EG, Dyer WJ. A RAPID METHOD OF TOTAL LIPID EXTRACTION AND PURIFICATION. *Can J Biochem Physiol.* 2010. doi:10.1139/y59-099.
253. Gallego-Díez ML, Correa-Ochoa MA, Saldarriaga-Molina JC. Validation of a methodology to determine Benzene, Toluene, Ethylbenzene, and Xylenes concentration present in the air and adsorbed in activated charcoal passive samplers by GC/FID chromatography. *Rev Fac Ing Univ Antioquia.* 2016.

doi:10.17533/udea.redin.n79a13.

254. Boczkaj G, Makoś P, Przyjazny A. Application of dispersive liquid–liquid microextraction and gas chromatography with mass spectrometry for the determination of oxygenated volatile organic compounds in effluents from the production of petroleum bitumen. *J Sep Sci*. 2016. doi:10.1002/jssc.201501355.
255. Sharma AK, Parul, General T. Variation of both chemical composition and antioxidant properties of newly isolated *Parachlorella kessleri* GB1, by growing in different culture conditions. *LWT*. 2019. doi:10.1016/j.lwt.2019.05.103.
256. Piasecka A, Krzemińska I, Tys J. Enrichment of *Parachlorella kessleri* biomass with bioproducts: oil and protein by utilization of beet molasses. *J Appl Phycol*. 2017. doi:10.1007/s10811-017-1081-y.
257. THE CHARACTERISTICS OF BIOMASS PRODUCTION AND LIPID ACCUMULATION OF *CHLORELLA KESSLERI* GROWTH UNDER MIXOTROPHIC AND HETEROTROPHIC CONDITIONS. 2013;9(1):19-26.
258. Liu Y, Lv J, Feng J, Liu Q, Nan F, Xie S. Treatment of real aquaculture wastewater from a fishery utilizing phytoremediation with microalgae. *J Chem Technol Biotechnol*. 2019. doi:10.1002/jctb.5837.
259. De Morais MG, Costa JA V. Carbon dioxide fixation by *Chlorella kessleri*, *C. vulgaris*, *Scenedesmus obliquus* and *Spirulina* sp. cultivated in flasks and vertical tubular photobioreactors. *Biotechnol Lett*. 2007. doi:10.1007/s10529-007-9394-6.
260. Perez-Garcia O, Bashan Y, Bashan Y, Bashan Y. Microalgal heterotrophic and mixotrophic culturing for bio-refining: From metabolic routes to techno-economics. In: *Algal Biorefineries: Volume 2: Products and Refinery Design*. ; 2015. doi:10.1007/978-3-319-20200-6_3.
261. Bates SS. Effects of light and ammonium on nitrate uptake by two species of estuarine phytoplankton. *Limnol Oceanogr*. 1976. doi:10.4319/lo.1976.21.2.0212.

262. Ohmori M, Ohmori K, Strotmann H. *Microbiology*. 1977;229:225-226.
263. Bingham DR, Lin C, Hoag RS, Bingham DR, Lin C, Hoag RS. Nitrogen cycle and algal growth modeling. 2019;56(10):1118-1122.
264. Dortch Q. The interaction between ammonium and nitrate uptake in phytoplankton. *Mar Ecol Prog Ser*. 1990. doi:10.3354/meps061183.
265. Chen SY, Pan LY, Hong MJ, Lee AC. The effects of temperature on the growth of and ammonia uptake by marine microalgae. *Bot Stud*. 2012.
266. Tilak KS, Lakshmi SJ, Susan TA. The toxicity of ammonia, nitrite and nitrate to the fish, *Catla catla* (Hamilton). *J Environ Biol*. 2002.
267. Camargo JA, Alonso A, Salamanca A. Nitrate toxicity to aquatic animals: a review with new data for freshwater invertebrates. *Chemosphere*. 2005. doi:10.1016/j.chemosphere.2004.10.044.
268. Dugdale R, Wilkerson F, Parker AE, Marchi A, Taberski K. River flow and ammonium discharge determine spring phytoplankton blooms in an urbanized estuary. *Estuar Coast Shelf Sci*. 2012. doi:10.1016/j.ecss.2012.08.025.
269. Erratt KJ, Creed IF, Trick CG. Comparative effects of ammonium, nitrate and urea on growth and photosynthetic efficiency of three bloom-forming cyanobacteria. *Freshw Biol*. 2018. doi:10.1111/fwb.13099.
270. Dassanayake M. Corrigendum: Making Plants Break a Sweat: the Structure, Function, and Evolution of Plant Salt Glands. *Front Plant Sci*. 2017;8. doi:10.3389/fpls.2017.00724.
271. Sample KT, Cain RB, Schmidt S. Biodegradation of aromatic compounds by microalgae. *FEMS Microbiol Lett*. 1999;170(2):291-300. doi:10.1016/S0378-1097(98)00544-8.
272. Fernandes B, Teixeira J, Dragone G, et al. Relationship between starch and lipid

- accumulation induced by nutrient depletion and replenishment in the microalga *Parachlorella kessleri*. *Bioresour Technol*. 2013.
doi:10.1016/j.biortech.2013.06.096.
273. Kato Y, Ho SH, Vavricka CJ, Chang JS, Hasunuma T, Kondo A. Evolutionary engineering of salt-resistant *Chlamydomonas* sp. strains reveals salinity stress-activated starch-to-lipid biosynthesis switching. *Bioresour Technol*. 2017.
doi:10.1016/j.biortech.2017.06.035.
274. Arora N, Patel A, Sharma M, et al. Insights into the Enhanced Lipid Production Characteristics of a Fresh Water Microalga under High Salinity Conditions. *Ind Eng Chem Res*. 2017;56(25):7413-7421. doi:10.1021/acs.iecr.7b00841.
275. Barkla BJ, Rhodes T, Tran K-NT, Wijesinghege C, Larkin JC, Dassanayake M. Making Epidermal Bladder Cells Bigger: Developmental- and Salinity-Induced Endopolyploidy in a Model Halophyte. *Plant Physiol*. 2018;177(2):615-632.
doi:10.1104/pp.18.00033.
276. Khan MI, Shin JH, Kim JD. The promising future of microalgae: Current status, challenges, and optimization of a sustainable and renewable industry for biofuels, feed, and other products. *Microb Cell Fact*. 2018. doi:10.1186/s12934-018-0879-x.
277. Zhang L, Pei H, Chen S, et al. Salinity-induced cellular cross-talk in carbon partitioning reveals starch-to-lipid biosynthesis switching in low-starch freshwater algae. *Bioresour Technol*. 2018. doi:10.1016/j.biortech.2017.11.067.
278. Yan N, Fan C, Chen Y, Hu Z. The potential for microalgae as bioreactors to produce pharmaceuticals. *Int J Mol Sci*. 2016. doi:10.3390/ijms17060962.
279. Zhu LD, Li ZH, Hiltunen E. Strategies for Lipid Production Improvement in Microalgae as a Biodiesel Feedstock. *Biomed Res Int*. 2016.
doi:10.1155/2016/8792548.
280. Minhas AK, Hodgson P, Barrow CJ, Adholeya A. A review on the assessment of stress conditions for simultaneous production of microalgal lipids and carotenoids.

- Front Microbiol.* 2016. doi:10.3389/fmicb.2016.00546.
281. Wang Y, Chen T, Qin S. Differential fatty acid profiles of *Chlorella kessleri* grown with organic materials. *J Chem Technol Biotechnol.* 2013. doi:10.1002/jctb.3881.
282. Wang Y, Chen T, Qin S. Heterotrophic cultivation of *Chlorella kessleri* for fatty acids production by carbon and nitrogen supplements. *Biomass and Bioenergy.* 2014. doi:10.1016/j.biombioe.2012.09.018.
283. Piasecka A, Krzemińska I, Tys J. Enrichment of *Parachlorella kessleri* biomass with bioproducts: oil and protein by utilization of beet molasses. *J Appl Phycol.* 2017. doi:10.1007/s10811-017-1081-y.
284. Li XJ, Zheng K, Wang LD, Li YT, Wu ZY, Yan CW. Syntheses and crystal structures of tetracopper(II) complexes bridged by asymmetric N,N'-bis(substituted)oxamides: Molecular docking, DNA-binding and in vitro anticancer activity. *J Inorg Biochem.* 2013. doi:10.1016/j.jinorgbio.2013.07.027.
285. Mallick N, Bagchi SK, Koley S, Singh AK. Progress and challenges in microalgal biodiesel production. *Front Microbiol.* 2016. doi:10.3389/fmicb.2016.01019.
286. Şahin E. *Debaryomyces hansenii* as a new biocatalyst in the asymmetric reduction of substituted acetophenones. *Biocatal Biotransformation.* 2017. doi:10.1080/10242422.2017.1348500.
287. Pugazhendi A, Qari H, Al-Badry Basahi JM, Godon JJ, Dhavamani J. Role of a halothermophilic bacterial consortium for the biodegradation of PAHs and the treatment of petroleum wastewater at extreme conditions. *Int Biodeterior Biodegrad.* 2017. doi:10.1016/j.ibiod.2017.03.015.
288. Jamal MT, Pugazhendi A. Degradation of petroleum hydrocarbons and treatment of refinery wastewater under saline condition by a halophilic bacterial consortium enriched from marine environment (Red Sea), Jeddah, Saudi Arabia. *3 Biotech.* 2018. doi:10.1007/s13205-018-1296-x.

289. Patel BP, Kumar A. Biodegradation of 4-chlorophenol in an airlift inner loop bioreactor with mixed consortium: effect of HRT, loading rate and biogenic substrate. *3 Biotech*. 2016. doi:10.1007/s13205-016-0435-5.
290. Gargouri B, Karray F, Mhiri N, Aloui F, Sayadi S. Application of a continuously stirred tank bioreactor (CSTR) for bioremediation of hydrocarbon-rich industrial wastewater effluents. *J Hazard Mater*. 2011. doi:10.1016/j.jhazmat.2011.02.057.
291. Pugazhendi A, Abbad Wazin H, Qari H, Basahi JMAB, Godon JJ, Dhavamani J. Biodegradation of low and high molecular weight hydrocarbons in petroleum refinery wastewater by a thermophilic bacterial consortium. *Environ Technol (United Kingdom)*. 2017. doi:10.1080/09593330.2016.1262460.
292. Gargouri B, Karray F, Mhiri N, Aloui F, Sayadi S. Bioremediation of petroleum hydrocarbons-contaminated soil by bacterial consortium isolated from an industrial wastewater treatment plant. *J Chem Technol Biotechnol*. 2014. doi:10.1002/jctb.4188.
293. Mizzouri NS, Shaaban MG. Kinetic and hydrodynamic assessment of an aerobic purification system for petroleum refinery wastewater treatment in a continuous regime. *Int Biodeterior Biodegrad*. 2013. doi:10.1016/j.ibiod.2013.03.026.
294. Monod J. a Certain Number. *Annu Rev M*. 1949;3(XI):371-394.
295. Harvey W. Blanch DSC. Biochemical Engineering, Second Edition - Douglas S. Clark, Harvey W. Blanch - Google Books. CRC Press, - Science .
https://books.google.ca/books?id=ST_p2AOApZsC&printsec=frontcover&redir_esc=y#v=onepage&q&f=false. Published 1997. Accessed August 13, 2019.
296. Liu S. *Bioprocess Engineering: Kinetics, Biosystems, Sustainability, and Reactor Design.*; 2012. doi:10.1016/C2012-0-00326-2.
297. Salleh SF, Kamaruddin A, Uzir MH, Mohamed AR, Shamsuddin AH. Modeling the light attenuation phenomenon during photoautotrophic growth of *A. variabilis* ATCC 29413 in a batch photobioreactor. *J Chem Technol Biotechnol*. 2017.

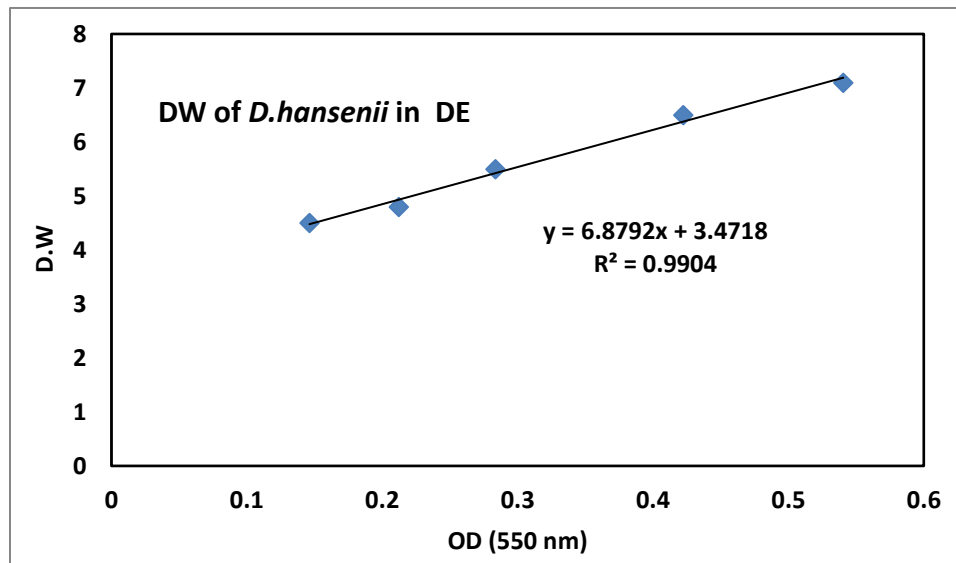
doi:10.1002/jctb.5013.

298. Hibbett DS. 21st Century Guidebook to Fungi . By David Moore, Geoffrey D. Robson, and Anthony P. J. Trinci. Cambridge and New York: Cambridge University Press. \$135.00 (hardcover); \$65.00 (paper). xii + 627 p. + 64 pl.; ill.; index. ISBN: 978-1-107-00676-8 (hc); 978-. The Quarterly Review of Biology. doi:10.1086/668171.
299. Sigeo DC. *Freshwater Microbiology: Biodiversity and Dynamic Interactions of Microorganisms in the Aquatic Environment.*; 2005. doi:10.1002/9780470011256.
300. Engelking LR. *96-Textbook of Veterinary Physiological Chemistry.*; 2015. doi:10.1016/B978-0-12-391909-0.50062-1.
301. Roskoski R. Michaelis-menten kinetics. In: *XPharm: The Comprehensive Pharmacology Reference.* ; 2011. doi:10.1016/B978-008055232-3.60041-8.
302. Gargouri B, Aloui F, Sayadi S. Reduction of petroleum hydrocarbons content from an engine oil refinery wastewater using a continuous stirred tank reactor monitored by spectrometry tools. *J Chem Technol Biotechnol.* 2012. doi:10.1002/jctb.2705.
303. Imperial Oil C. Sarnia | Imperial. Imperial Oil. <https://www.imperialoil.ca/en-ca/company/operations/refining-and-supply/sarnia>. Published 2019. Accessed August 8, 2019.

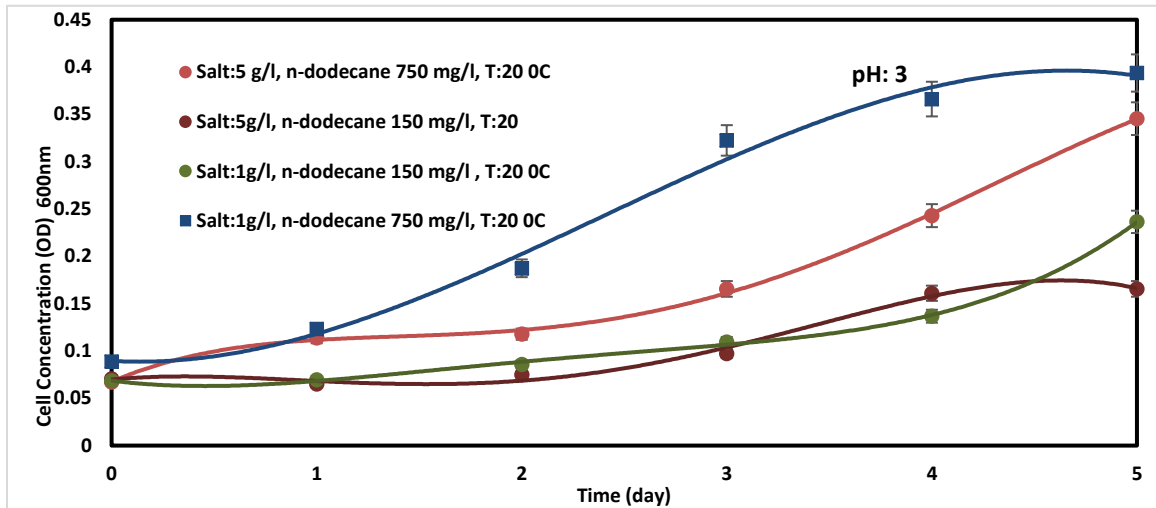
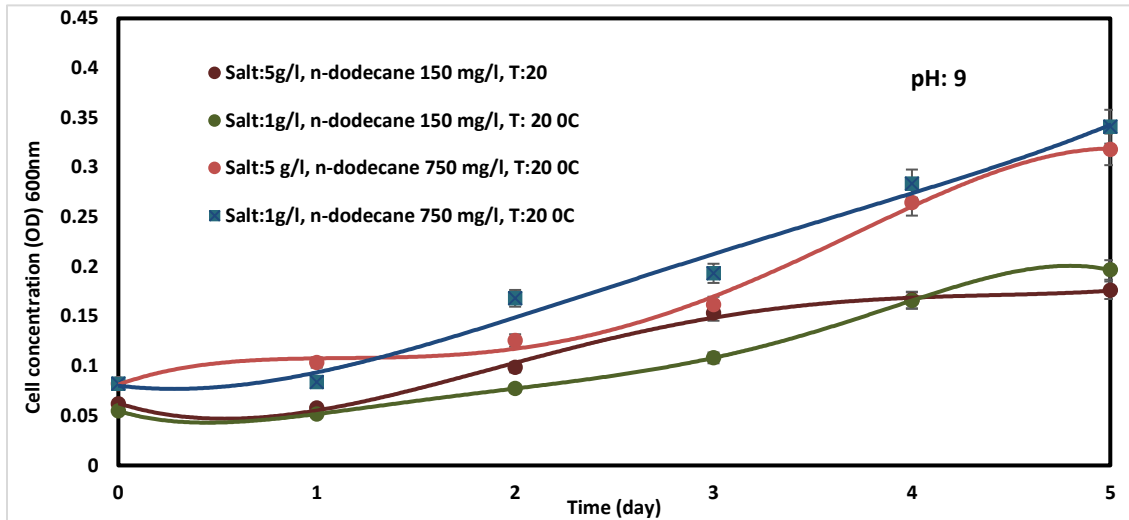
Appendices

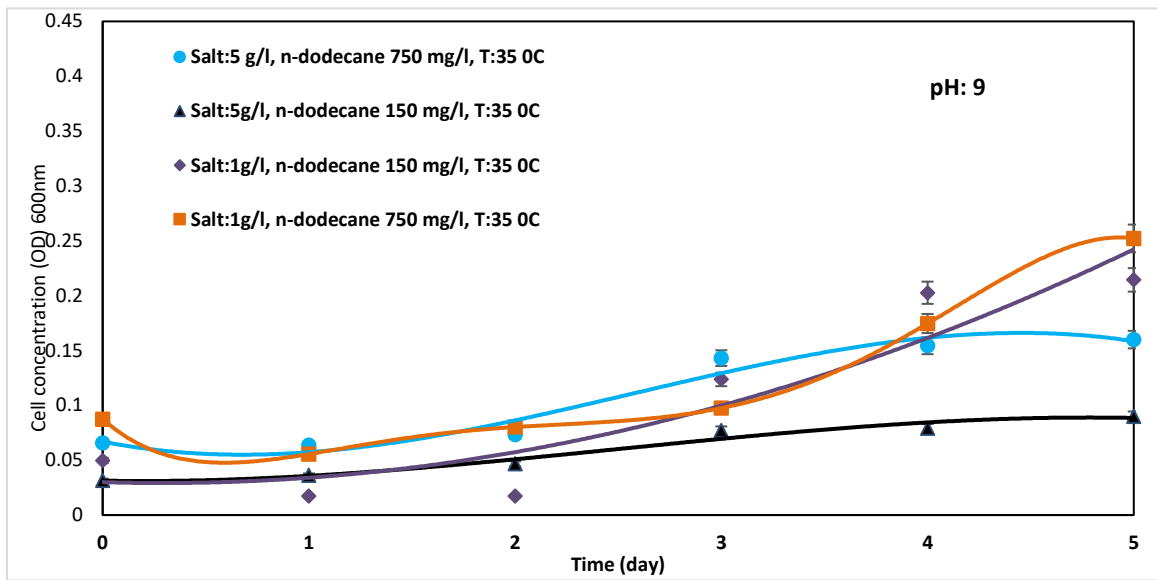
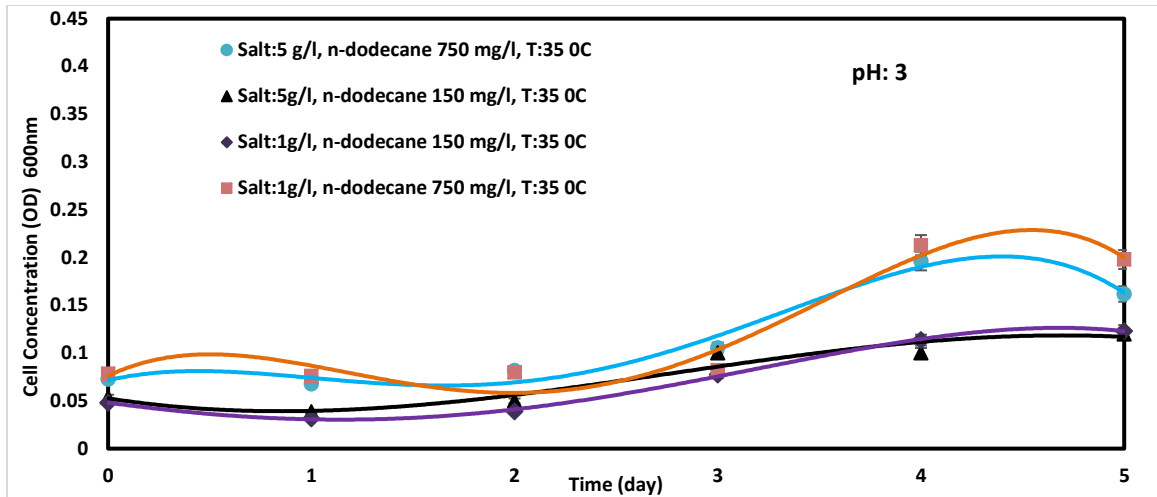
Optical density and dry weight of *D.hansenii* in desalter effluent

Dry weight of *D.hansenii* in actual Desalter Effluent (Figure and Data)



Design of experiment at different range of Salt, Temperature, and Dodecane. To investigate yield, dodecane removal (COD)





Biodegradation of dodecane using *D.hansenii* in SDE in CSRT



Experimental methods

Lipid Extraction measurement

- Lipid content Folch method (Folch et al, 1957)
- Weighted Dry microalgae
- Add bead (Silica)
- Disrupt cells: Bead beater 8 min
- Chloroform- methanol: 1-0.5 ml
- Hold in ultrasonic (2 hours)
- 0.2 *(1.5 ml) Chloroform- methanol add in samples
- Centrifuge 1000 rpm 10 min
- Transfer lower layer (Chloroform) to pre-weighted pan
- Dry in open air
- 30 min in oven (105 °C)
- Total lipid% = $\frac{W_3 - W_2}{W_2} \times 100$

Water Quality - COD

DOC316.53.01099- Hach Method 8000

USEPA Reactor Digestion Method (Oxygen Demand, Chemical, Dichromate method)

- Reactor Digestion Method
- Use a clean pipet to add 2.00 mL of sample to the vial.
- For 250–15,000 mg/L vials: add 0.20 mL of sample to the vial.
- Blank: add 2.00 mL of deionized water. For 250–15,000 mgL⁻¹ vials: add 0.20 mL of deionized water to the vial.
- Heat the vials for 2 hours in DRB200 reactor
- Insert the blank into the cell holder. Push zero
- Insert the prepared sample into the cell holder
- Nutrient removal efficiency (RE, %) $\mathcal{R} = \frac{C_i - C_f}{C_i} \times 100$

Water Quality- Ammonia

Ammonia, High Range Test'N Tube™, Hach Method 10031

- Blank: Add 0.1 DI water the high range N tube vial
- Add 0.1 ml of sample to the other
- Add Ammonia Salicylate Reagent Powder Pillow to each vials
- Add Ammonia Cyanurate Reagent Powder Pillow to each vials
- Shake and Waite 20 minutes
- Place into the cell holder of spectrophotometer DR2800
- Blank press Zero
- Samples and read Ammonia concentration mgL⁻¹
- Nutrient removal efficiency (RE, %) $\mathcal{R} = \frac{C_i - C_f}{C_i} \times 100$

Water Quality- Phosphorus, Total

Phosphorous, Total, HR, Hach Method 10127

Molybdovanadate Method with Acid Persulfate Digestion

- Molybdovanadate with Acid Persulfate Digestion Method
- 5.0 mL of deionized water to a Total Phosphorus Test Vial
- Add 5.0 mL of sample to a Total Phosphorus Test Vial.
- Add the contents of one Potassium Persulfate Powder Pillow to each vial.
- Shake to dissolve the powder.
- A 30-minute reaction time in the reactor
- Add 2 mL of 1.54 N Sodium Hydroxide Standard Solution to each vial.
- add 0.5 mL of Molybdovanadate Reagent.
- A 7-minute reaction time starts
- Using and comparing to the blank, PO_4^{3-} mgl⁻¹ is measured

Monitoring algal populations - Cell Counting- Haemocytometer

Document: http://site.iugaza.edu.ps/aajrami/files/5_Monitoring-algal-populations.pdf

The volume of central large square= length * width*depth

$$= 1\text{mm} * 1\text{mm} * 0.1\text{mm} = 0.1\text{mm}^3$$

Multiplication by 10 will give the number of cells in 1mm^3

Since there are $1000\text{mm}^3 (=1\text{cm}^3)$ in 1 ml, so multiplication by 1000 will give the number of cells per ml

The number of cells per ml= average cell count * 10^4

Which is called chamber conversion factor Neubauer ($X * 10^4$)

Curriculum Vitae

Name: Leila Azimian

Post-secondary Iran University of Science and Technology (IUST)

Education and Tehran, Iran

Degrees: BSc.

B.Sc. final project; design of a biogas reactor for refinement of residential complexes wastewater

The University of Tehran

Tehran, Iran

2009-2011 MBA

The University of Western Ontario

London, Ontario, Canada

2014-2015 MEng.

MEng final project; preparation of advanced membranes for water purification and recycling

The University of Western Ontario

London, Ontario, Canada

2015-2019 Ph.D.

PhD thesis: Bioremediation of Refinery Desalter Effluent using *Debaryomyces hansenii* and *Parachlorella kessleri*

Honors and Awards:	E.G.D. Murray scholarship 2015-2016, 2018-2019
	Queen Elizabeth II Graduate Scholarship Doctoral Fellowship 2017-2018
	Winner of Industrial Problem Solving of Western University 2014-2015
	Selected Engineering Management's Employee 2009-2010
	Best Chemical Engineering Thesis Project Award" at IUST 2000-2001
Related Work Experience	Teaching Assistant University of Western Ontario 2015-2019
	Lead Process Improvement Engineer Renault & Peugeot 2003-2013
	Rapid Prototyping Engineering R&D Renault & Peugeot 2001-2002

Publications & Conferences:

Azimian, L., Bassi, A.S., 2019, Investigation of Growth Kinetics of *Debaryomyces Hansenii* in Petroleum Refinery Desalter Effluent, Canadian Journal of Chemical Engineering 97 (1), 27-31, <https://doi.org/10.1002/cjce.23297>

Azimian, L., (2018), Investigation of Growth Kinetics of *Debaryomyces Hansenii* in Petroleum Refinery Desalter Effluent, CSChE2018 Annual Meeting, Toronto, ON

Azimian, L., (2019), Investigation of Hydrocarbon Utilization by *Debaryomyces Hansenii* (LAF-3 10 u) in Desalter Effluent, 2019 AIChE Spring Meeting, New Orleans, LA, US